



CryOcean-QCV - quality control/validation for CryoSat-2

Monthly Data Quality report for May 2023

| DOCUMENT INFORMATION | | | |
|----------------------|----------|-------------------|----------|
| Document history | | | |
| Version | Issued | Reason for change | Author |
| 2.0 | 27/01/24 | Creation | C. Banks |

| This Version | | |
|--|---------------|--|
| Version 2.0 – issued by National Oceanography Centre on 27/01/24 | | |
| Written by: | C. Banks | |
| Checked by: | F. M. Calafat | |
| Approved by: | | |
| Distribution List | | |
| Company | Delivered via | Names |
| ESA | ftp | Jerome Bouffard Alessandro Di Bella |
| NOC | ftp | C. Banks F.M. Calafat |

MONTHLY QUALITY ASSESSMENT FOR May 2023

Report issued on 27/01/24

Contents

1. Summary of results for NOP

- 1.1. Data used
- 1.2. Data flow
- 1.3. Data coverage and completeness
- 1.4. SSH anomaly coverage and completeness
- 1.5. Crossover analysis
- 1.6. SWH coverage and validity
- 1.7. Sigma0 coverage and validity
- 1.8. Wind speed coverage and validity
- 1.9. Mispointing coverage and validity

2. Summary of results for IOP

- 2.1. Data used
- 2.2. Data flow
- 2.3. Data coverage and completeness
- 2.4. SSH anomaly coverage and completeness
- 2.5. Crossover analysis
- 2.6. SWH coverage and validity
- 2.7. Sigma0 coverage and validity
- 2.8. Wind speed coverage and validity
- 2.9. Mispointing coverage and validity

3. Summary of results for GOP

- 3.1. Data used
- 3.2. Data flow
- 3.3. Data coverage and completeness
- 3.4. SSH anomaly coverage and completeness
- 3.5. Crossover analysis
- 3.6. SWH coverage and validity

- 3.7. Sigma0 coverage and validity**
- 3.8. Wind speed coverage and validity**
- 3.9. Mispointing coverage and validity**

4. GOP validation

- 4.1. Validation against in situ measurements and models**
 - 4.1.1. Absolute validation of GOP SSH against selected tide gauges**
 - 4.1.2. Validation of GOP SSH anomaly against tide gauges**
 - 4.1.3. Validation of GOP SWH and wind speed against buoy data**
 - 4.1.4. Validation of GOP SWH against Wavewatch III model data**
 - 4.1.5. Validation of GOP derived geostrophic velocities**
 - 4.1.6. Comparison of GOP SSH anomaly with the steric heights derived from temperature and salinity ARGO profiles**
- 4.2. Validation against reference mission (Jason/Sentinel-6a)**
- 4.3. Global mean sea level time series**

Annex. Geographical distribution of corrections

1 Summary of results for NOP

Note 1.1: unless otherwise stated, measurements taken over polar polygons have been excluded from the computation of all statistics shown in this section.

Note 1.2: most statistics shown in this section have been computed separately for the low resolution mode (LRM) and the pseudo low resolution mode (SAR).

Note 1.3: “flag-valid” refers to those records that have not been flagged as bad by either the average status flag or the measurement confidence flag.

Note 1.4: “science-valid” refers to flag-valid records (over oceans and lakes and excluding polar regions) that meet the editing criteria described in the Tables 2, 3, 4, 5.

1.1. Data used

Product: **NOP**

Date and time of the first record: **01 05 2023 00:00:00.189**

Date and time of the last record: **31 05 2023 23:59:59.906**

Range of complete orbits in present month: **69228 to 69676**

1.2. Data flow

Median latency [min max]: 2.1 days [0.2 - 15.0]

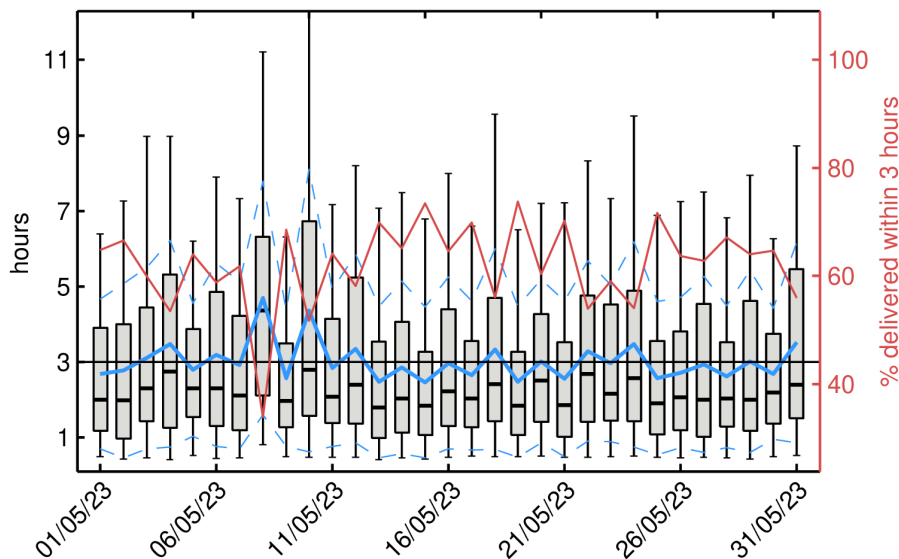


Figure 1. Box-and-whiskers plot for the NOP latency showing for each day in May 2023 the first and third quartiles (bottom and top of the box), the median (thick black), the 5%

and 95% percentiles (lower and upper whiskers), the mean (blue) and the mean ± 1 standard deviation (blue dashed line). The percentage of records delivered within 3 hours is also shown (red, right y-axis). The horizontal black line denotes the 3 hours threshold.

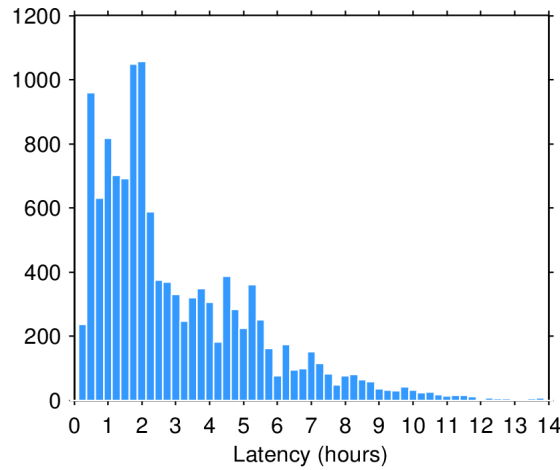


Figure 2. Histogram of the NOP data latency for May 2023. The y-axis denotes the number of files that are made available with a delay of x-hours with respect to the mean time of the records stored in the file.

1.3. Data coverage and completeness

| | Present in month | Theoretical max. | Percentage (%) |
|-------------------------|------------------|------------------|----------------|
| Total | 2167419 | 2295830 | 94.4 |
| Oceans and lakes | 1708998 | 1797486 | 95.1 |

Table 1. Number of total (land and ocean/lake) and only ocean/lake records (based on the surface_type flag) together with their percentage relative to the theoretically expected number of measurements from the orbits ground tracks for May 2023. Theoretical values are also shown.

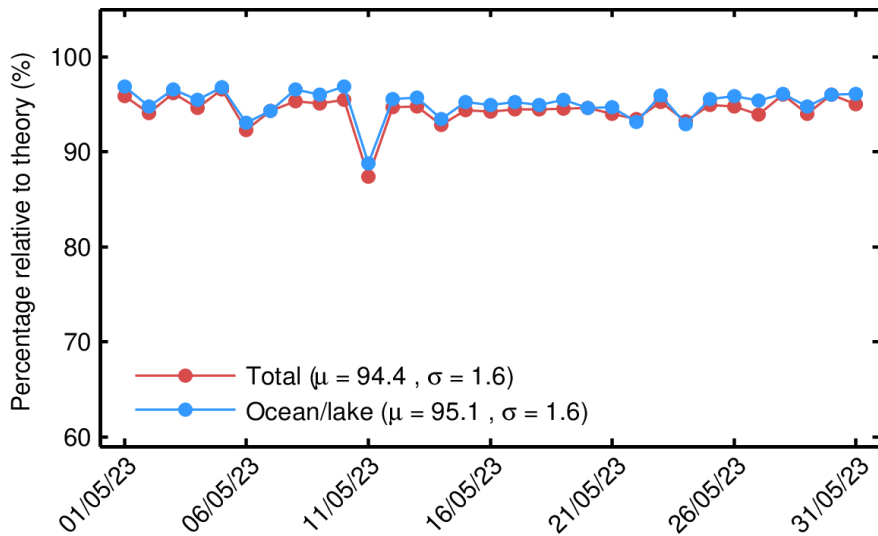


Figure 3. Percentage of NOP 1-Hz records over land and ocean/lake (red) and only over ocean/lake (blue) relative to the theoretically expected number from the orbits ground tracks for each day in May 2023.

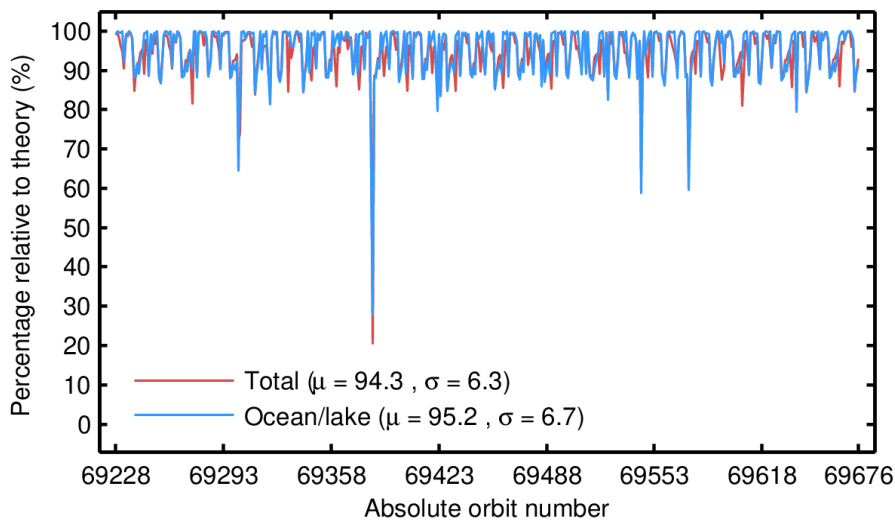


Figure 4. Percentage of NOP 1-Hz records over land and ocean/lake (red) and only over ocean/lake (blue) relative to the theoretically expected number from the orbits ground tracks for each orbit in May 2023. The mean (μ) and standard deviation (σ) are also shown.

1.4. SSH anomaly coverage and validity

| Parameter | Min threshold | Max threshold | Percentage edited |
|-----------------------------------|---------------|---------------|-------------------|
| Flagged as bad | - | - | 1.1% |
| Biased orbit | - | - | 1.6% |
| SSH anomaly | -3 m | 3 m | 0.1% |
| Standard deviation of SSH anomaly | 0 m | 0.20 m | 1.0% |
| Inverse barometer correction | -2 m | 2 m | 0.0% |
| Wet tropospheric correction | -0.5 m | -0.001 m | 0.0% |
| Dry tropospheric correction | -2.5 m | -1.9 m | 0.0% |
| Ionospheric correction | -0.4 m | 0.04 m | 0.0% |
| Sea state bias | -0.5 m | 0 m | 0.2% |
| Sigma0 | 7 dB | 30 dB | 0.2% |
| Standard deviation of sigma0 | 0 dB | 0.23 dB | 4.0% |
| All together | - | - | 6.1% |

Table 2. Editing criteria. The percentage of “flagged as bad” refers to records that have been flagged as bad by either the average status flag or the measurement confidence flag. Such percentage is computed only for records over oceans/lakes and outside polar regions. All other percentages refer to the percentage of flag-valid records that have been rejected by the corresponding criteria or by all criteria (“All together”). The biased orbit criteria in the table refers to the orbits highlighted in the 'Warnings' table at the beginning of this report as being suspicious of suffering from a significant orbit bias. For such orbits, all records are rejected.

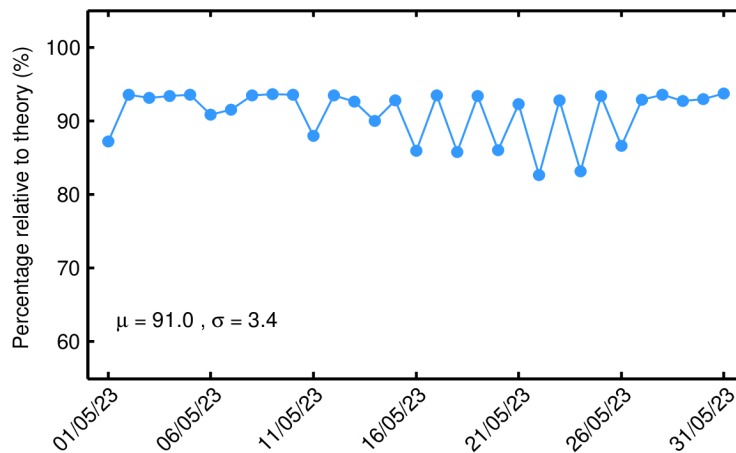


Figure 5. Percentage of science-valid NOP 1-Hz SSH records over ocean and lakes relative to theory for each day in May 2023. The mean (μ) and standard deviation (σ) are also shown.

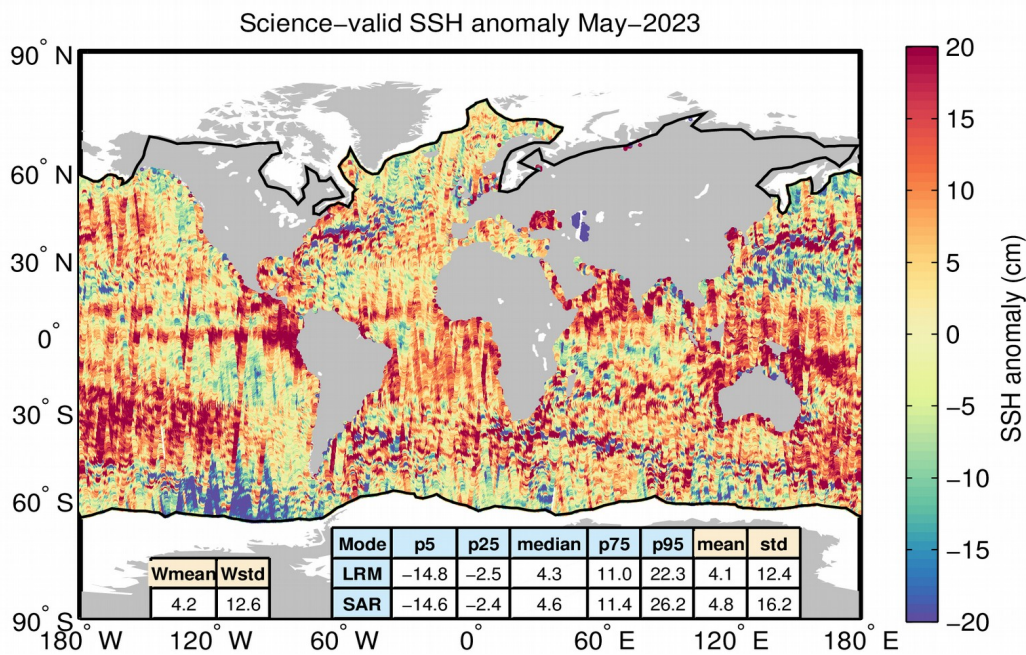


Figure 6. Geographical distribution of science-valid NOP 1-Hz SSH anomaly data over oceans and lakes for May 2023. The statistical values shown in the table refer to the SSH anomaly in cm and are calculated separately for LRM and SAR regions. Wmean and Wstd denote the spatial area-weighted average and its standard deviation. Measurements taken over polar polygons have been excluded from the computation of the statistical values. The black lines mark the outer limit of the Arctic and Antarctic polar polygons.

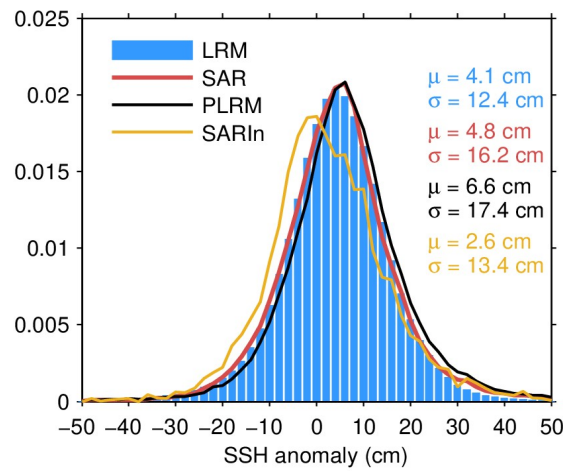


Figure 7. Histogram of science-valid NOP SSH anomaly over oceans and lakes for LRM (blue), SAR (red), PLRM (black) and SARIn (orange) for May 2023. The mean (μ) and standard deviation (σ) are also shown. Values outside $[-50\ 50]$ cm are excluded from the histogram for the sake of readability but not from the computation of μ and σ .

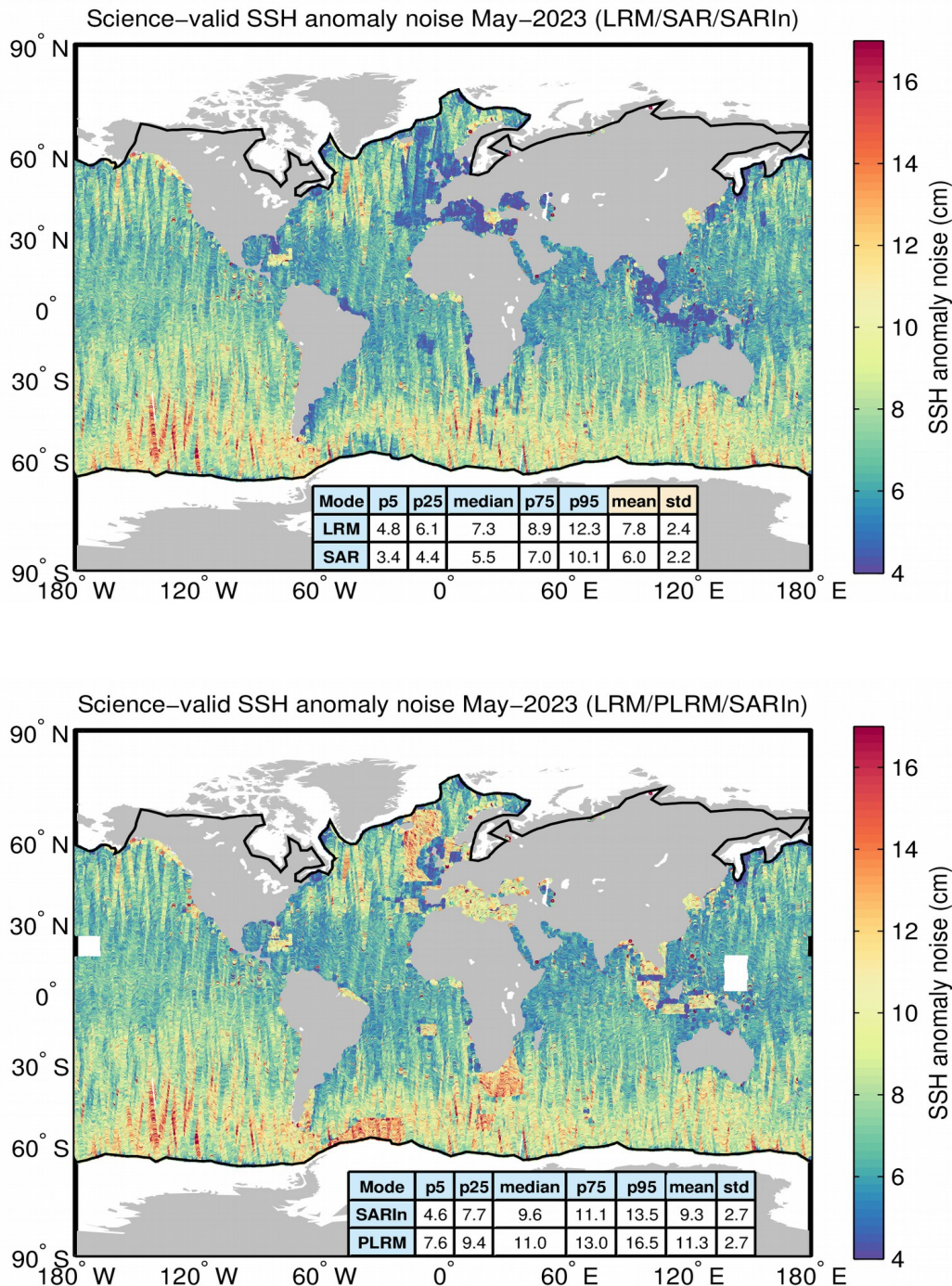


Figure 8. Geographical distribution of flag-valid 20-Hz SSH anomaly measurement noise over oceans and lakes for LRM/SAR/SARIn (top) and LRM/PLRM/SARIn (bottom) and for May 2023. The statistical values shown in the tables refer to the SSH anomaly noise and are calculated separately for LRM, SAR/PLRM, and SARIn regions. Measurements taken

over polar polygons have been excluded from the computation of the statistical values. The black lines mark the outer limit of the Arctic and Antarctic polar polygons.

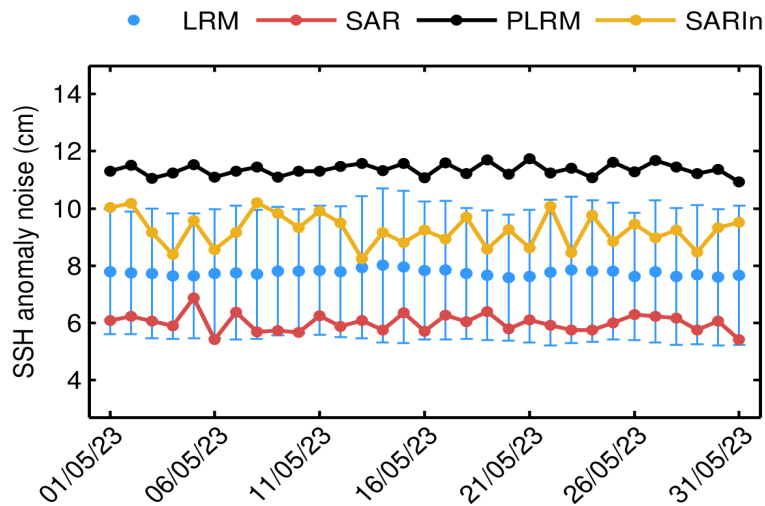
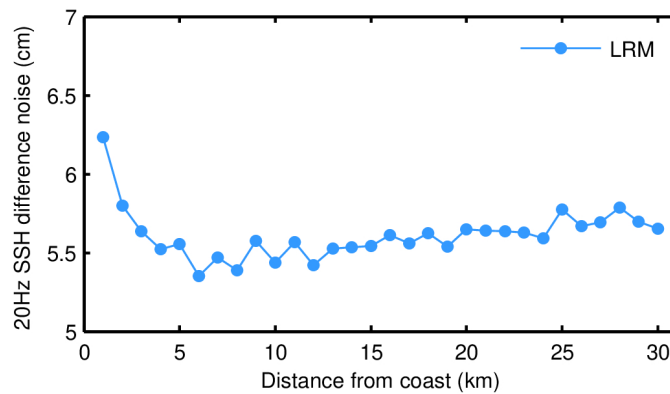
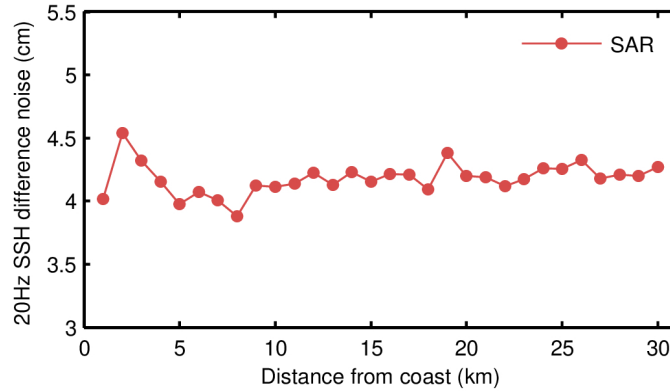


Figure 9. Mean science-valid NOP SSH anomaly noise for LRM (blue dot), SAR (red dot), PLRM (black dot) and SARIn (orange dot) for each day in May 2023. The corresponding standard deviation for LRM (blue error bar) is also shown.



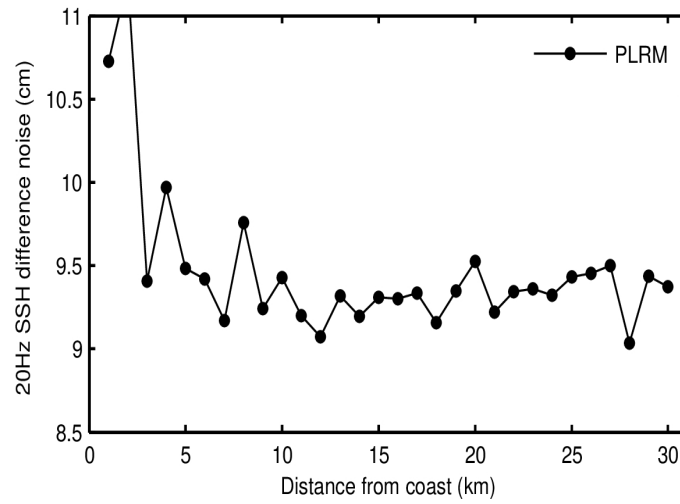
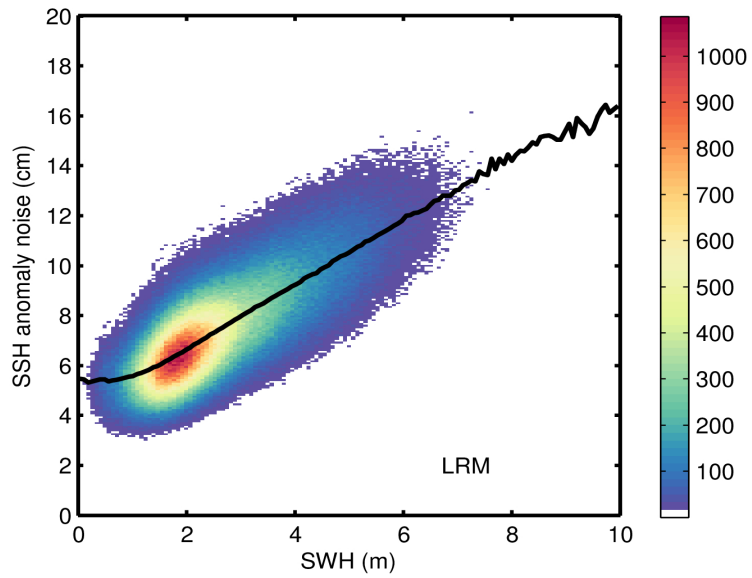
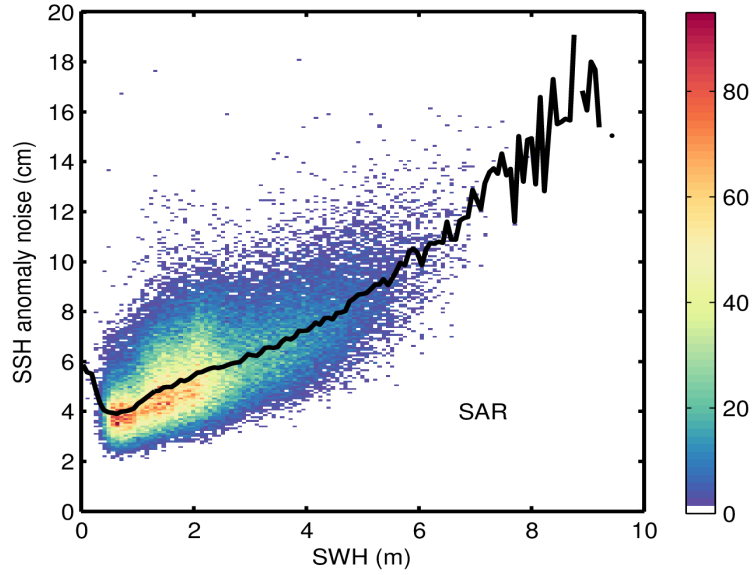


Figure 10. Science-valid NOP 20-Hz SSH anomaly noise as a function of distance from the coast for SAR (top panel), LRM (middle panel), and PLRM (bottom panel) for May 2023. Noise values have been calculated as the median of the absolute value of the difference between consecutive 20-Hz records.



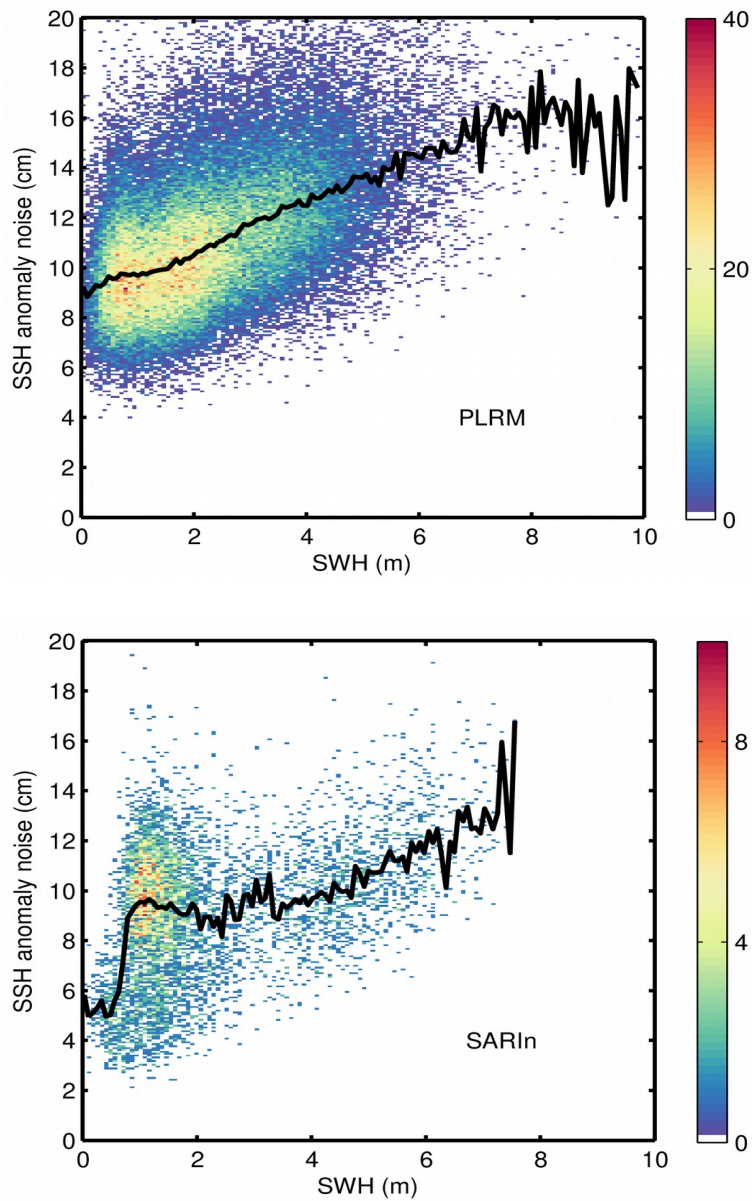


Figure 11. 2D histogram showing science-valid NOP SSH anomaly noise as a function of SWH for SAR, LRM, PLRM, and SARIn (from top to bottom) for May 2023. The black line denotes the median SSH anomaly noise as a function of SWH.

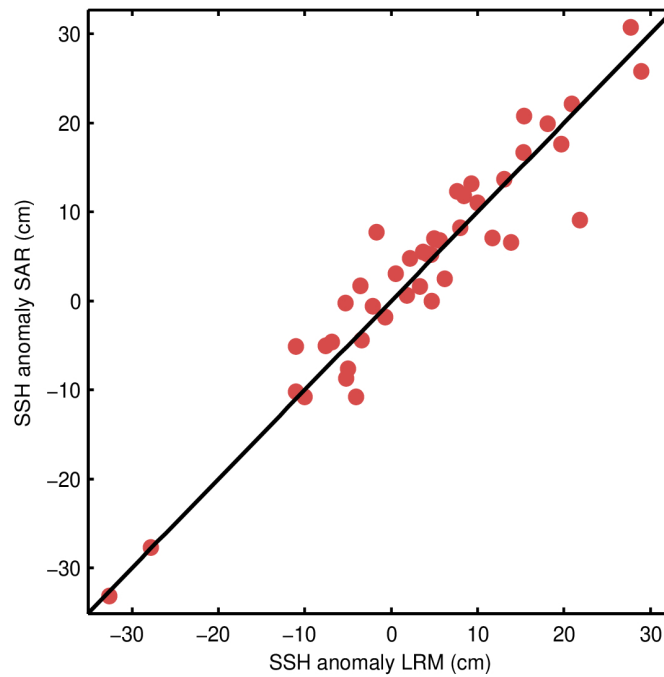


Figure 12. Scatter plot of the science-valid NOP SSH anomaly at the two nearest points outside (LRM, x-axis) and inside (SAR, y-axis) the Pacific SAR mode box for each pass. The RMS of the differences is 3.5 cm for the pairs shown in the figure as compared to a RMS of 3.8 cm for the differences between such outside points and their respective nearest neighbour also outside the box in the LRM region.

1.5. Crossover analysis

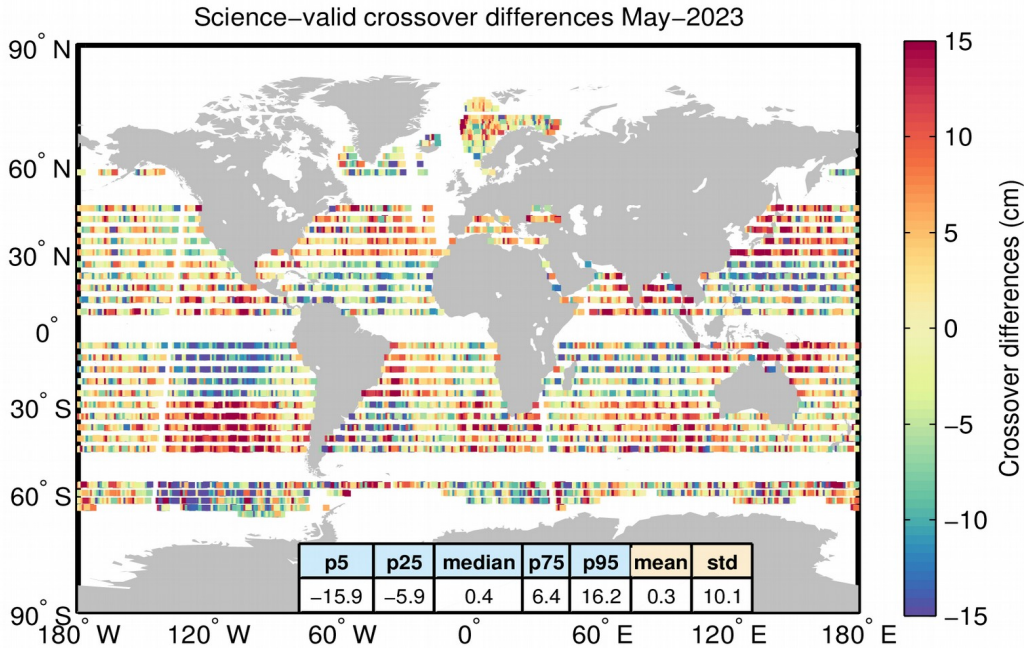


Figure 13. Crossover differences (absolute values) for the science-valid NOP SSH anomaly for May 2023. The difference at each crossover is computed as the difference between median values over 2-second windows centered about the crossover.

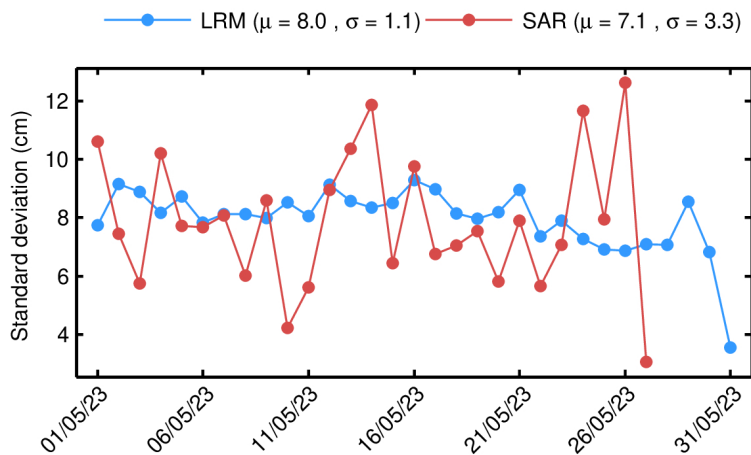


Figure 14. Standard deviation of differences at crossovers for NOP SSH anomaly for each day in May 2023. The values shown in this figure have been computed for the science-valid data further edited according to the following two additional criteria: 1) rejecting crossover differences larger than 20 cm; and 2) rejecting shallow waters (1000 m). The mean (μ) and standard deviation (σ) are also shown.



Monthly Quality Report for
May 2023
Version 2.0 - 27/01/24

CryoOcean-QCV



1.6. SWH coverage and validity

| Parameter | Min threshold | Max threshold | Percentage edited |
|--|---------------|---------------|-------------------|
| Flagged as bad | - | - | 1.1% |
| SWH | 0 m | 15 m | 0.0% |
| Standard deviation of SWH (1-Hz block) | 0 m | 1 m | 1.4% |
| All together | - | - | 1.4% |

Table 3. Editing criteria. The percentage of “flagged as bad” refers to records that have been flagged as bad by either the average status flag or the measurement confidence flag. Such percentage is computed only for records over oceans/lakes and outside polar regions. All other percentages refer to the percentage of flag-valid records that have been rejected by the corresponding criteria or by all criteria (“All together”).

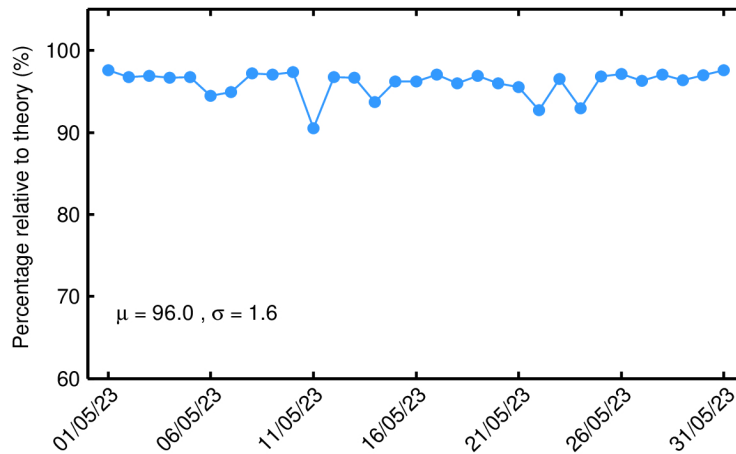


Figure 15. Percentage of science-valid NOP 1-Hz SWH records over ocean and lakes relative to theory for each day in May 2023. The mean (μ) and standard deviation (σ) are also shown.

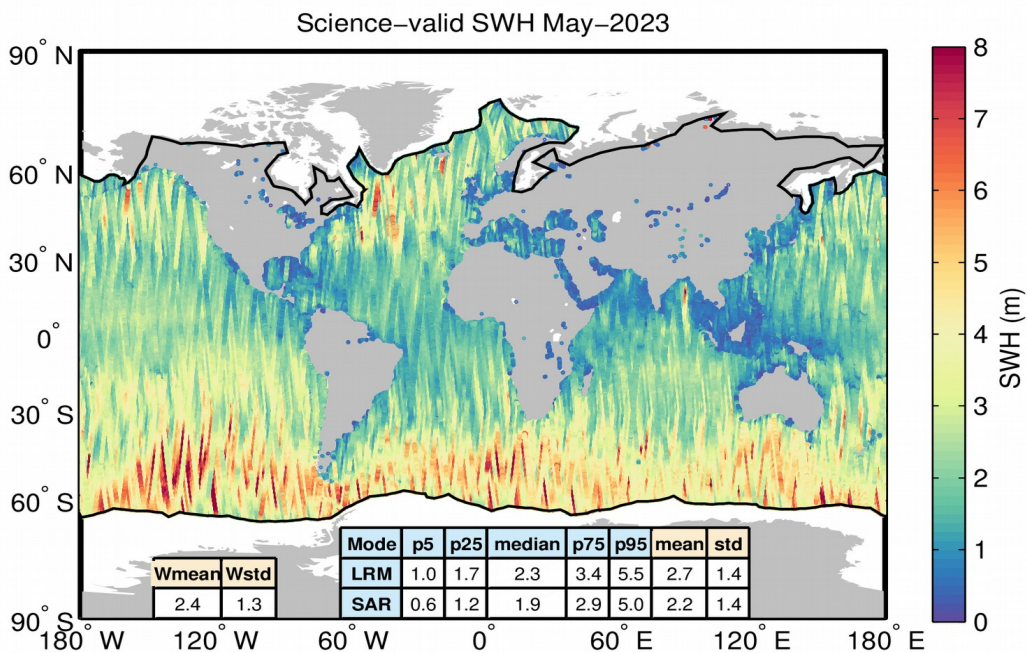


Figure 16. Geographical distribution of science-valid NOP SWH data over oceans and lakes for May 2023. The statistical values shown in the table refer to the SWH in m and are calculated separately for LRM and SAR regions. Wmean and Wstd denote the spatial area-weighted average and its standard deviation. Measurements taken over polar polygons have been excluded from the computation of the statistical values. The black lines mark the outer limit of the Arctic and Antarctic polar polygons.

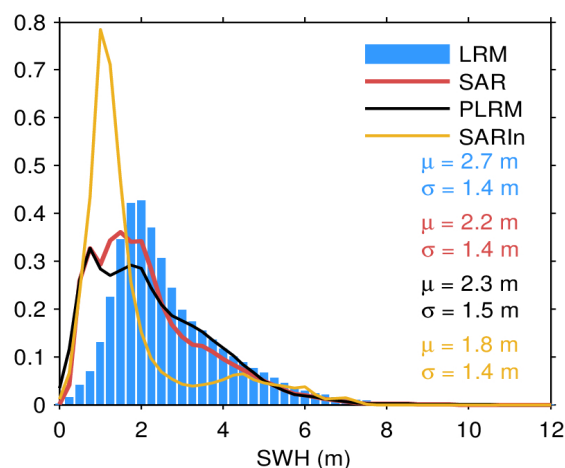


Figure 17. Histogram of science-valid NOP SWH over oceans and lakes for LRM (blue), SAR (red), PLRM (black) and SARIn (orange) for May 2023. The mean (μ) and standard deviation (σ) are also shown. Values larger than 12 m are excluded from the histogram for the sake of readability but not from the computation of μ and σ .

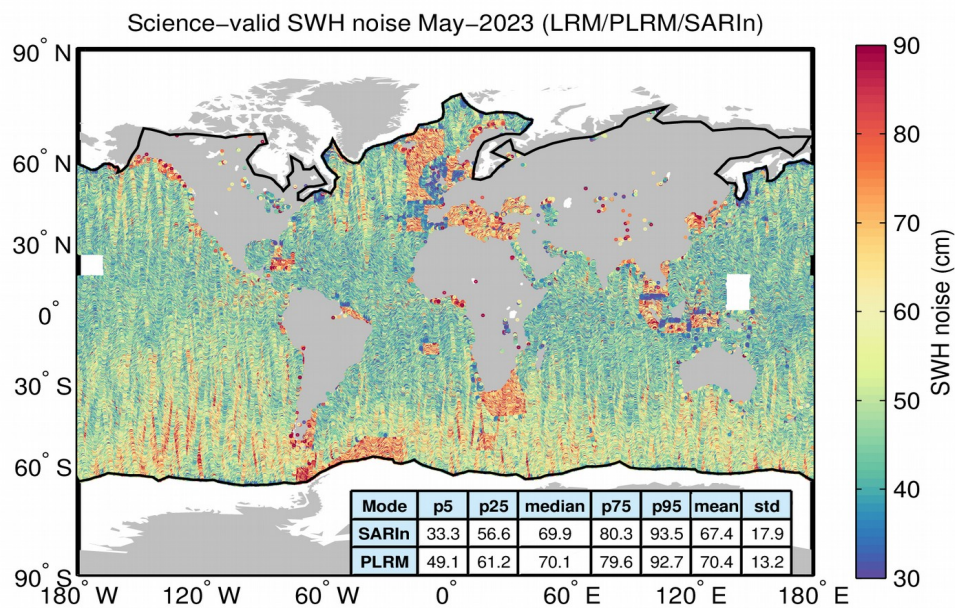
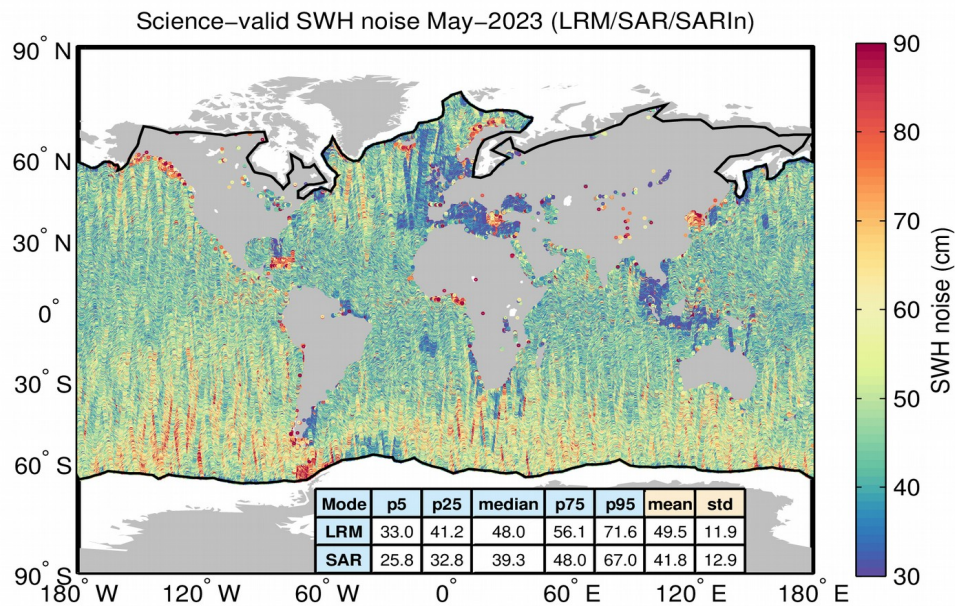


Figure 18. Geographical distribution of flag-valid 20-Hz SWH measurement noise over oceans and lakes for LRM/SAR/SARIn (top) and LRM/PLRM/SARIn (bottom) and for May 2023. The statistical values shown in the table refer to the SWH noise and are calculated separately for LRM, SAR/PLRM and SARIn regions. Measurements taken over polar polygons have been excluded from the computation of the statistical values. The black lines mark the outer limit of the Arctic and Antarctic polar polygons.

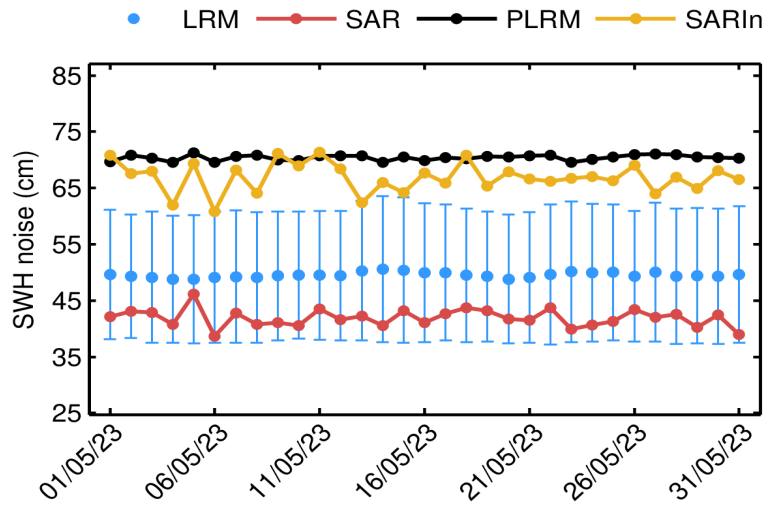
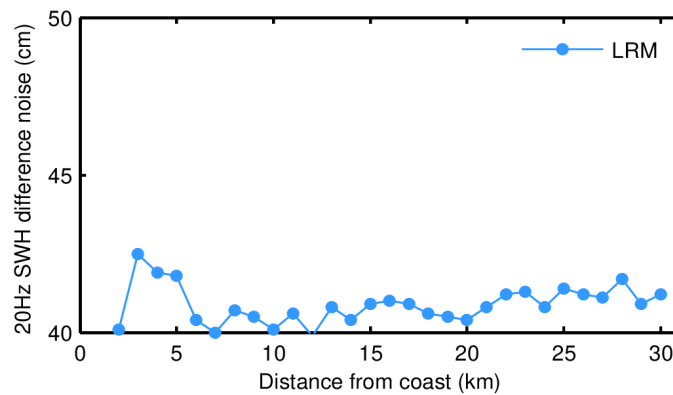
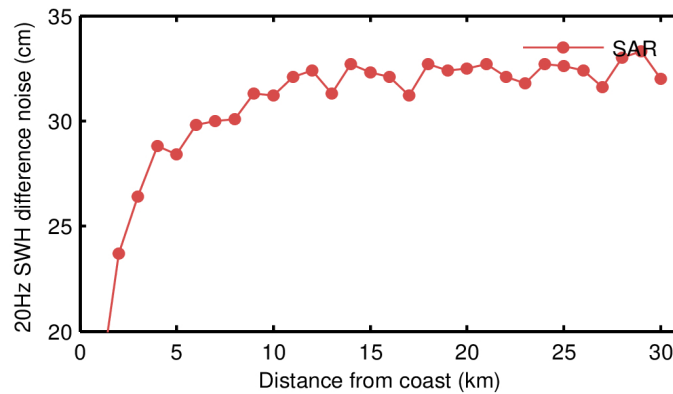


Figure 19. Mean science-valid NOP SWH noise for LRM (blue dot), SAR (red dot), PLRM (black dot) and SARIn (orange dot) for each day in May 2023. The corresponding standard deviation for LRM (blue error bar) is also shown.



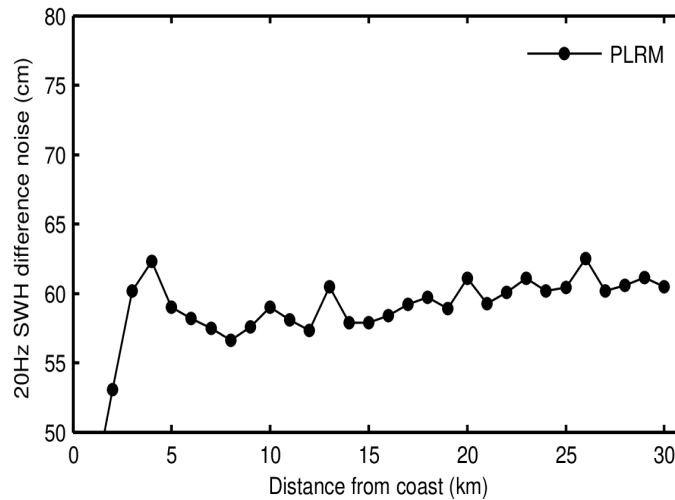


Figure 20. Science-valid NOP 20-Hz SWH noise as a function of distance from the coast for SAR (top panel), LRM (middle panel), and PLRM (bottom panel) for May 2023. Noise values have been calculated as the median of the absolute value of the difference between consecutive 20-Hz records.

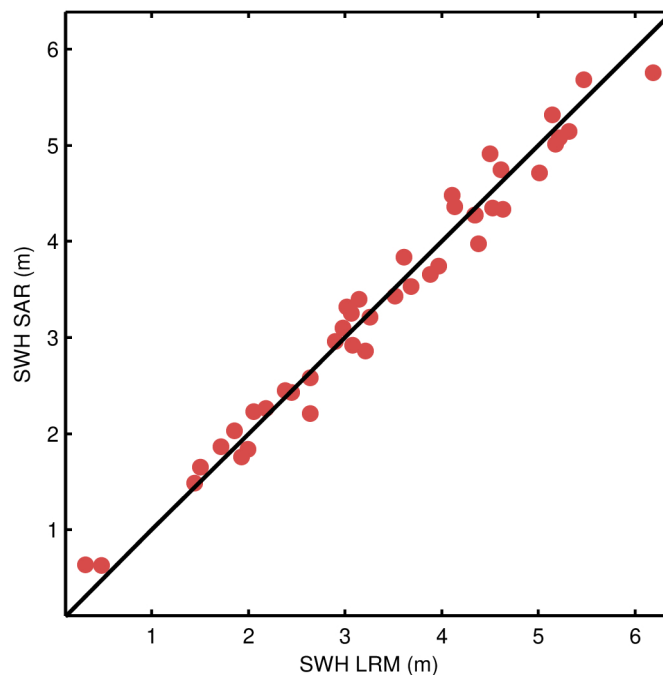


Figure 21. Scatter plot of the science-valid NOP SWH at the two nearest points outside (LRM, x-axis) and inside (SAR, y-axis) the Pacific SAR mode box for each pass. The RMS of the differences is 22.2 cm for the pairs shown in the figure as compared to a RMS of 23.3 cm for the differences between such outside points and their respective nearest neighbour also outside the box in the LRM region.

1.7. Sigma0 coverage and validity

| Parameter | Min threshold | Max threshold | Percentage edited |
|---|---------------|---------------|-------------------|
| Flagged as bad | - | - | 0.7% |
| Sigma0 | 7 dB | 30 dB | 0.2% |
| Standard deviation of Sigma0 (1-Hz block) | 0 dB | 0.23 dB | 4.3% |
| All together | - | - | 4.4% |

Table 4. Editing criteria. The percentage of “flagged as bad” refers to records that have been flagged as bad by either the average status flag or the measurement confidence flag. Such percentage is computed only for records over oceans/lakes and outside polar regions. All other percentages refer to the percentage of flag-valid records that have been rejected by the corresponding criteria or by all criteria (“All together”).

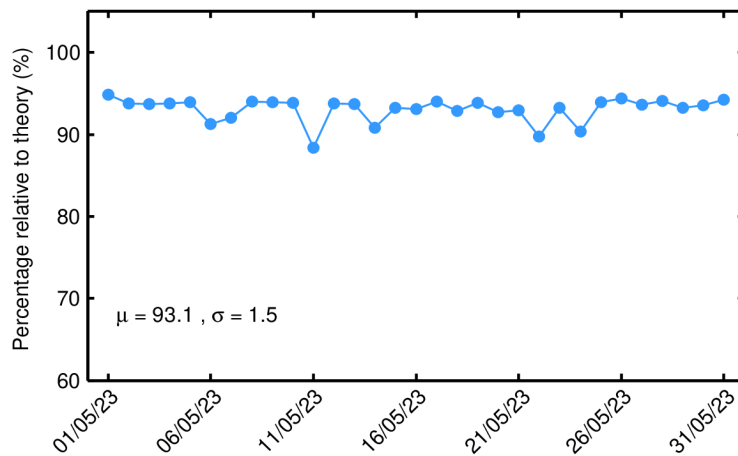


Figure 22. Percentage of science-valid NOP 1-Hz sigma0 records over ocean and lakes relative to theory for each day in May 2023. The mean (μ) and standard deviation (σ) are also shown.

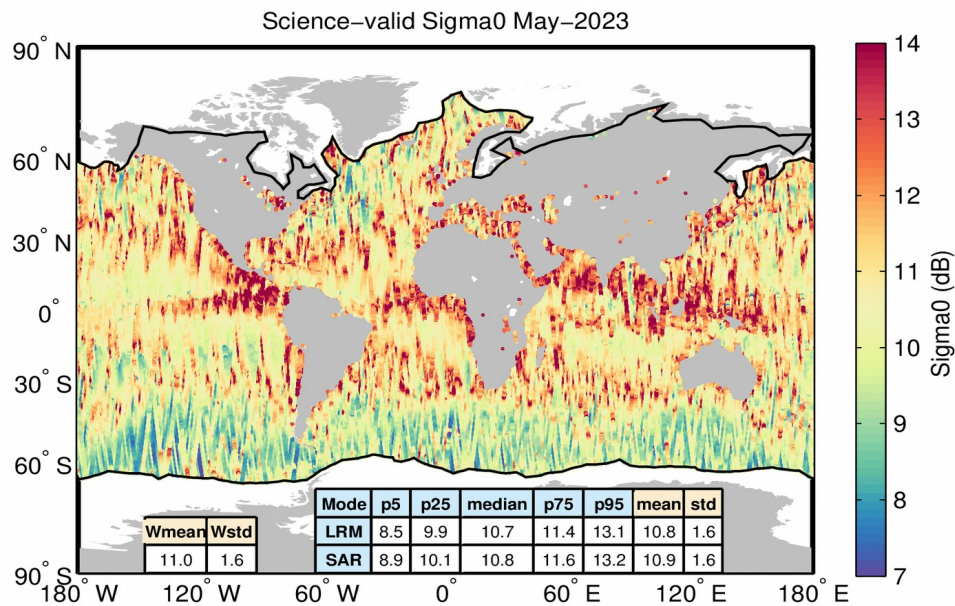


Figure 23. Geographical distribution of science-valid NOP sigma0 data over oceans and lakes for May 2023. The statistical values shown in the table refer to the sigma0 in m and are calculated separately for LRM and SAR regions. Wmean and Wstd denote the spatial area-weighted average and its standard deviation. Measurements taken over polar polygons have been excluded from the computation of the statistical values. The black lines mark the outer limit of the Arctic and Antarctic polar polygons.

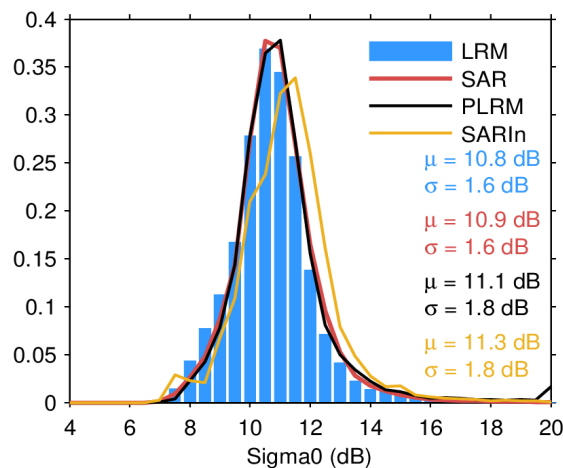


Figure 24. Histogram of science-valid NOP sigma0 over oceans and lakes for LRM (blue), SAR (red), PLRM (black) and SARIn (orange) for May 2023. The mean (μ) and standard deviation (σ) are also shown. Values larger than 12 m are excluded from the histogram for the sake of readability but not from the computation of μ and σ .

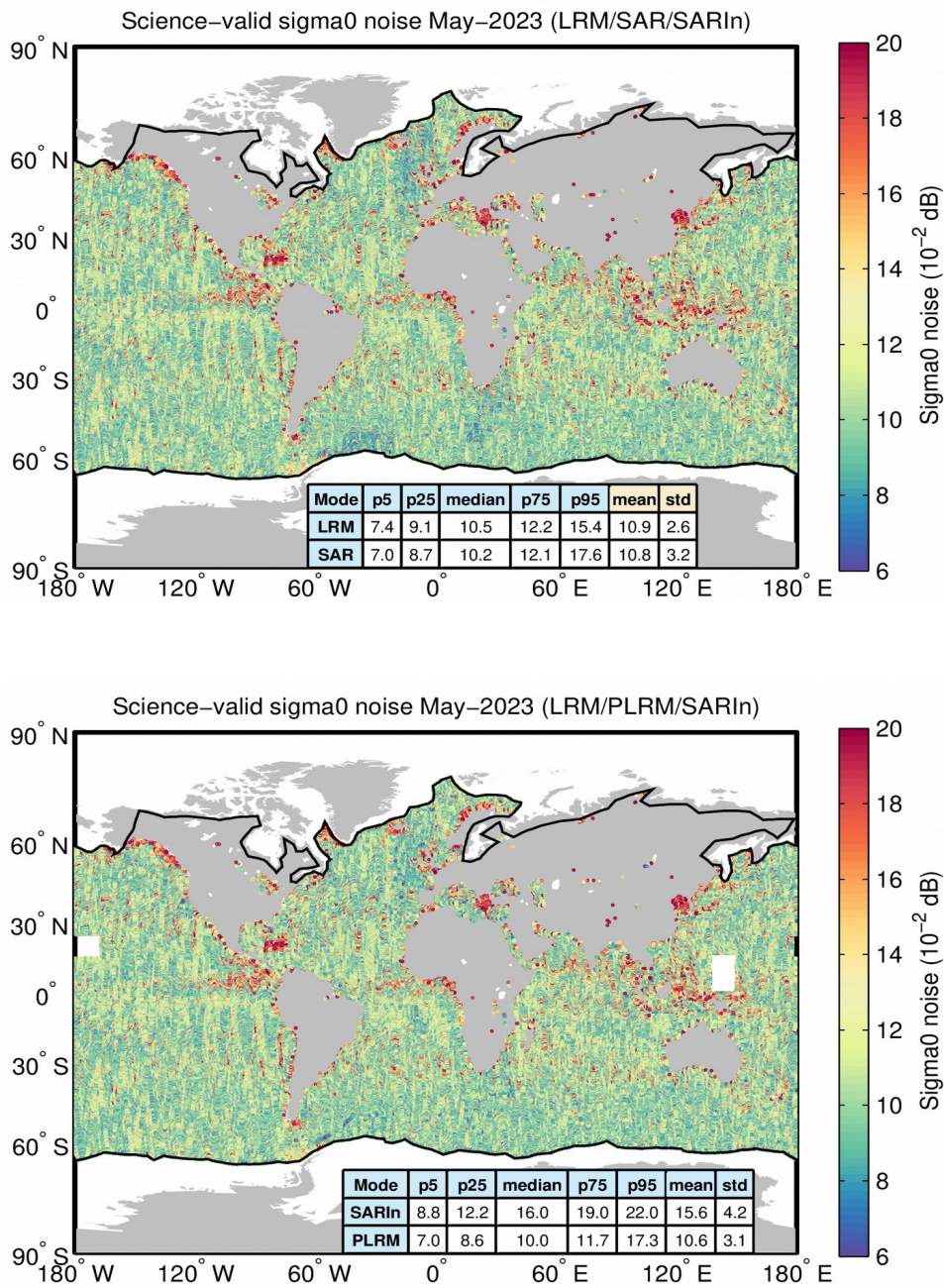


Figure 25. Geographical distribution of flag-valid 20-Hz sigma0 measurement noise over oceans and lakes for LRM/SAR/SARIn (top) and LRM/PLRM/SARIn (bottom) and for May 2023. The statistical values shown in the table refer to the sigma0 noise and are calculated separately for LRM, SAR/PLRM and SARIn regions. Measurements taken over polar polygons have been excluded from the computation of the statistical values. The black lines mark the outer limit of the Arctic and Antarctic polar polygons.

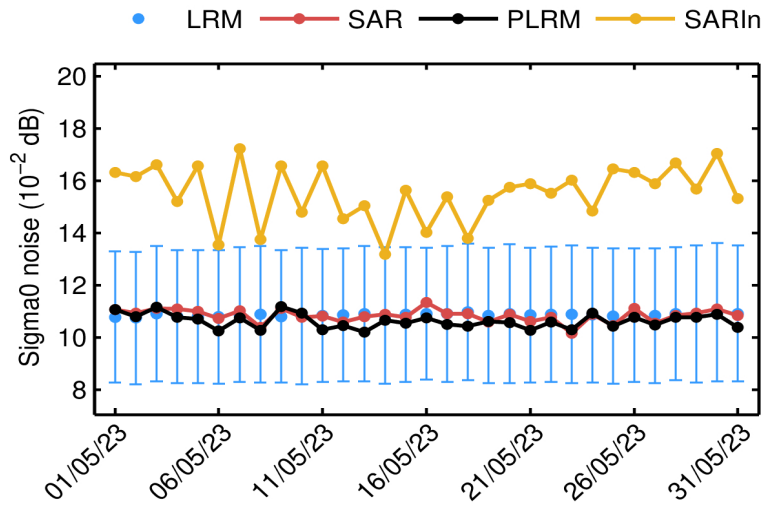
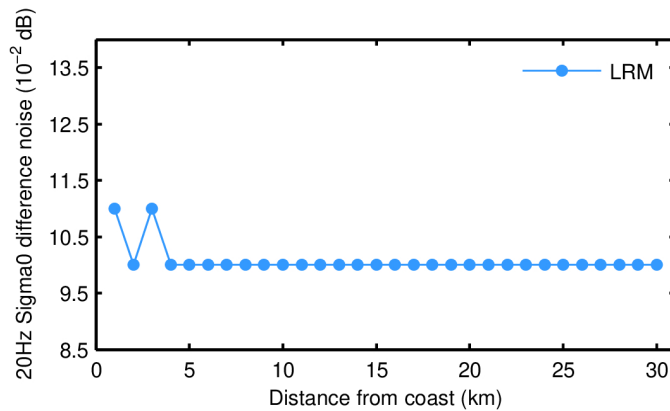
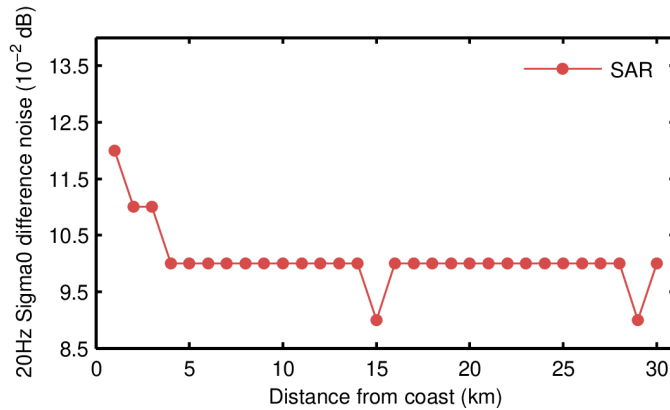


Figure 26. Mean science-valid NOP sigma0 noise for LRM (blue dot), SAR (red dot), PLRM (black dot) and SARIn (orange dot) for each day in May 2023. The corresponding standard deviation for LRM (blue error bar) is also shown.



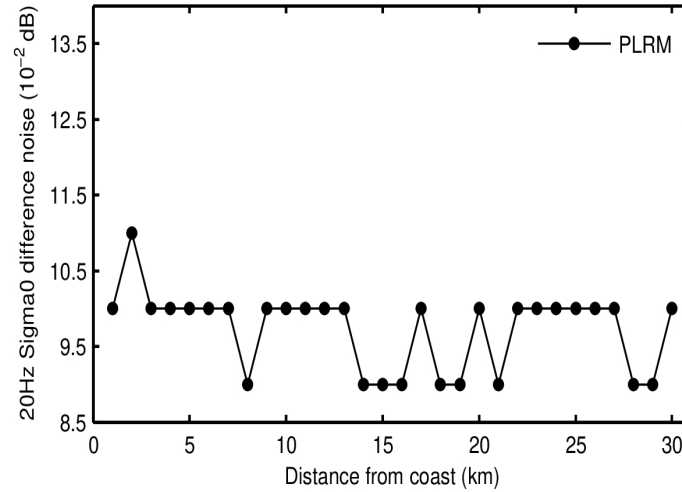


Figure 27. Science-valid NOP 20-Hz sigma0 noise as a function of distance from the coast for SAR (top panel), LRM (middle panel), and PLRM (bottom panel) for May 2023. Noise values have been calculated as the median of the absolute value of the difference between consecutive 20-Hz records.

1.8. Wind speed coverage and validity

| Parameter | Min threshold | Max threshold | Percentage edited |
|----------------------|---------------|---------------|-------------------|
| Flagged as bad | - | - | 0.7% |
| Altimeter wind speed | 0 m/s | 30 m/s | 0.0% |

Table 5. Editing criteria. The percentage of “flagged as bad” refers to records that have been flagged as bad by either the average status flag or the measurement confidence flag. Such percentage is computed only for records over oceans/lakes and outside polar regions. All other percentages refer to the percentage of flag-valid records that have been rejected by the corresponding criteria.

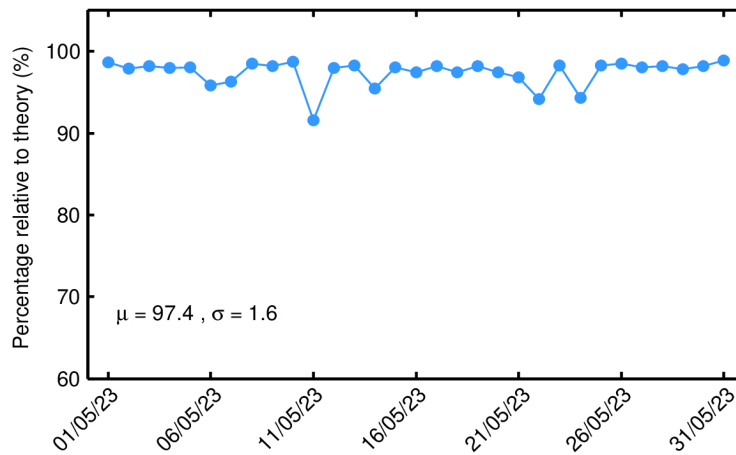


Figure 28. Percentage of science-valid NOP 1-Hz wind records over ocean and lakes relative to theory for each day in May 2023. The mean (μ) and standard deviation (σ) are also shown.

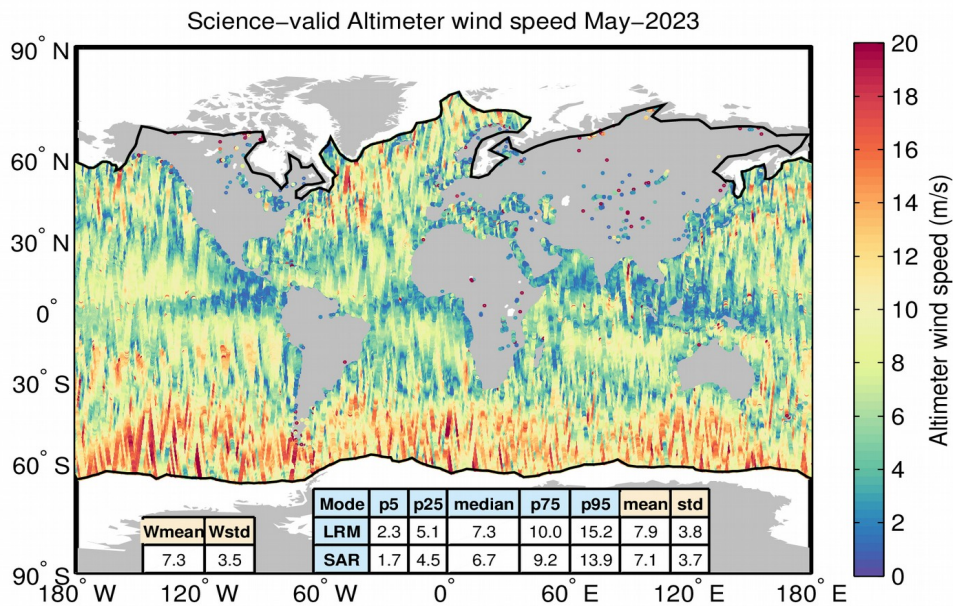


Figure 29. Geographical distribution of science-valid NOP wind data over oceans and lakes for May 2023. The statistical values shown in the table refer to the wind in m and are calculated separately for LRM and SAR regions. Wmean and Wstd denote the spatial area-weighted average and its standard deviation. Measurements taken over polar polygons have been excluded from the computation of the statistical values. The black lines mark the outer limit of the Arctic and Antarctic polar polygons.

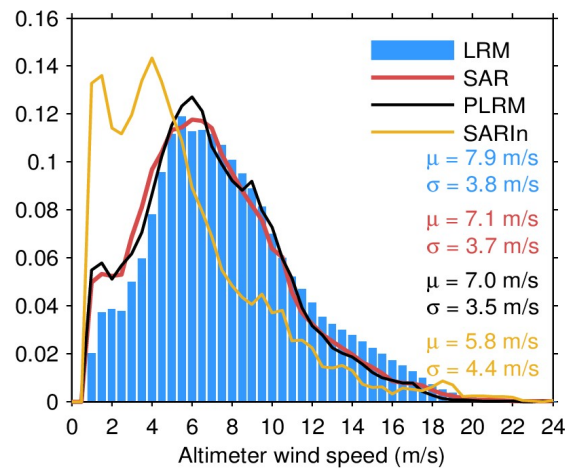


Figure 30. Histogram of science-valid NOP wind over oceans and lakes for LRM (blue), SAR (red), PLRM (black) and SARIn (orange) for May 2023. The mean (μ) and standard deviation (σ) are also shown. Values larger than 12 m are excluded from the histogram for the sake of readability but not from the computation of μ and σ .

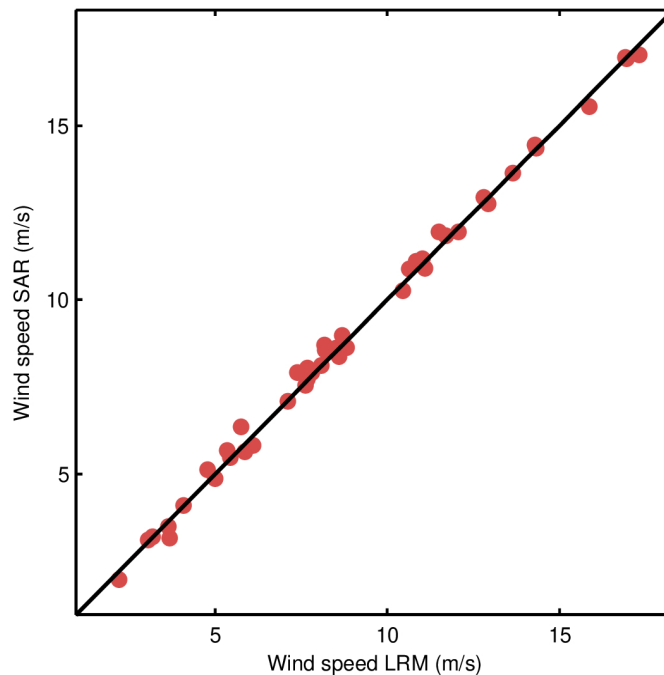


Figure 31. Scatter plot of the science-valid NOP wind speed at the two nearest points outside (LRM, x-axis) and inside (SAR, y-axis) the Pacific SAR mode box for each pass. The RMS of the differences is 25.6 cm/s for the pairs shown in the figure as compared to a RMS of 22.9 cm/s for the differences between such outside points and their respective nearest neighbour also outside the box in the LRM region.

1.9. Mispointing coverage and validity

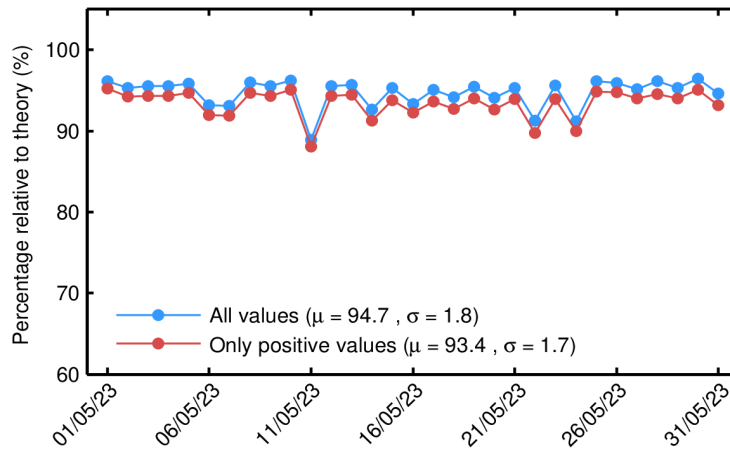
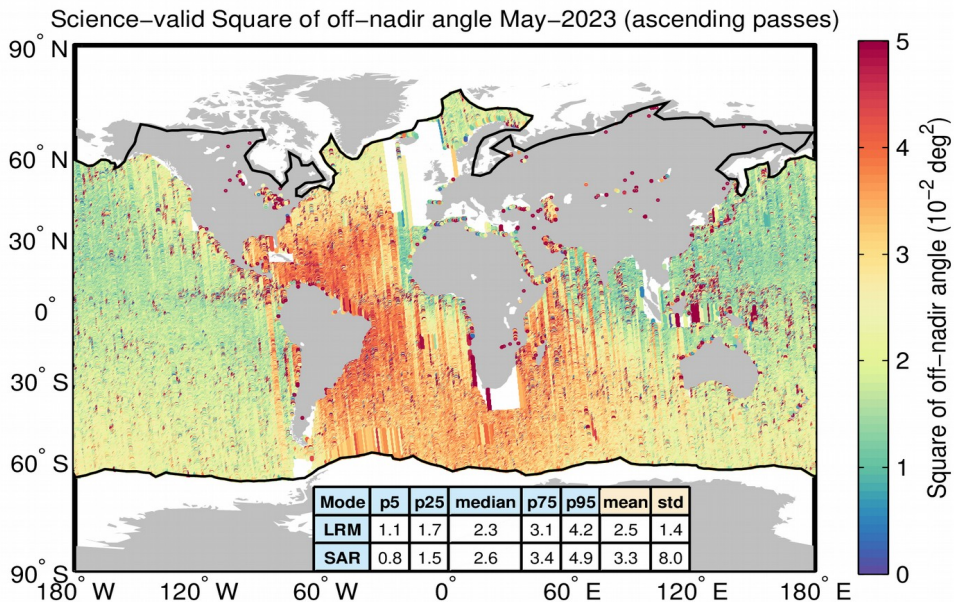


Figure 32. Percentage of science-valid NOP 1-Hz mispointing records over ocean and lakes relative to theory for each day in May 2023. The mean (μ) and standard deviation (σ) are also shown.



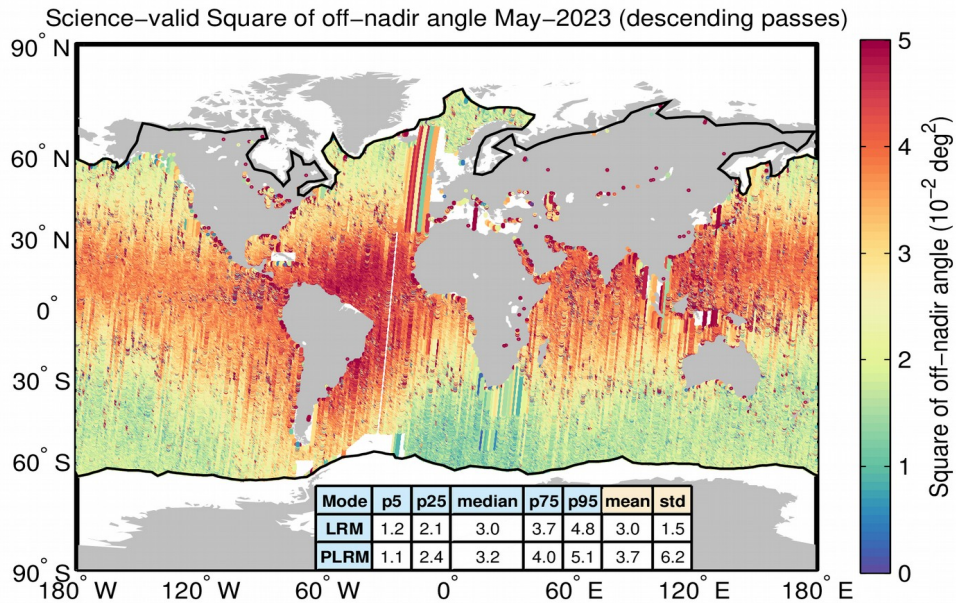


Figure 33. Geographical distribution of science-valid NOP mispointing data over oceans and lakes for ascending (top) and descending (bottom) passes for May 2023. The statistical values shown in the table refer to the wind in m and are calculated separately for LRM and SAR regions. Measurements taken over polar polygons have been excluded from the computation of the statistical values. The black lines mark the outer limit of the Arctic and Antarctic polar polygons.

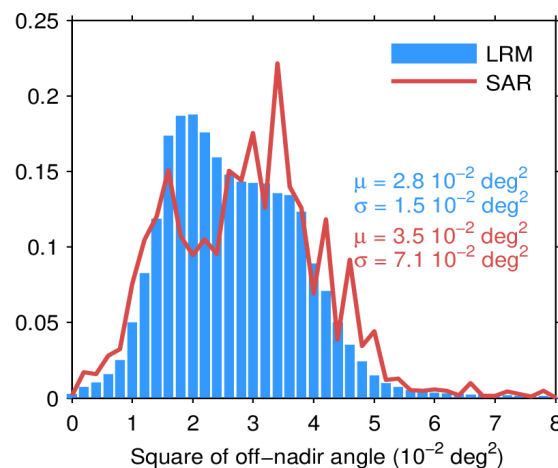


Figure 34. Histogram of science-valid NOP mispointing over oceans and lakes for LRM (blue) and SAR (red) for May 2023. The mean (μ) and standard deviation (σ) are also shown. Note that values larger than 12 m are excluded from the histogram for the sake of readability but not from the computation of μ and σ .

2 Summary of results for IOP

Note 2.1: unless otherwise stated, measurements taken over polar polygons have been excluded from the computation of all statistics shown in this section.

Note 2.2: most statistics shown in this section have been computed separately for the low resolution mode (LRM) and the pseudo low resolution mode (SAR).

Note 2.3: “flag-valid” refers to those records that have not been flagged as bad by either the average status flag or the measurement confidence flag.

Note 2.4: “science-valid” refers to flag-valid records (over oceans and lakes and excluding polar regions) that meet the editing criteria described in the Tables 7, 8, 9, 10.

2.1. Data used

Product: **IOP**

Date and time of the first record: **01 05 2023 00:00:00.189**

Date and time of the last record: **31 05 2023 23:59:59.906**

Range of complete orbits in present month: **69228 to 69676**

2.2. Data flow

Median latency [min max]: 1.4 days [0.6 - 2.0]

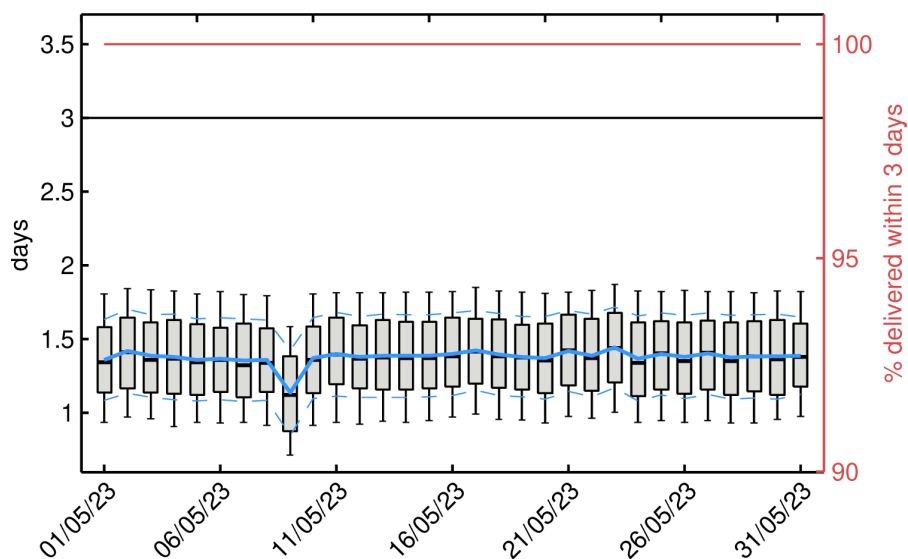


Figure 35. Box-and-whiskers plot for the IOP latency showing for each day in May 2023 the first and third quartiles (bottom and top of the box), the median (thick black), the 5% and 95% percentiles (lower and upper whiskers), the mean (blue) and the mean ± 1 standard deviation (blue dashed line). The percentage of records delivered within 3 days is also shown (red, right y-axis). The horizontal black line denotes the 3 days threshold.

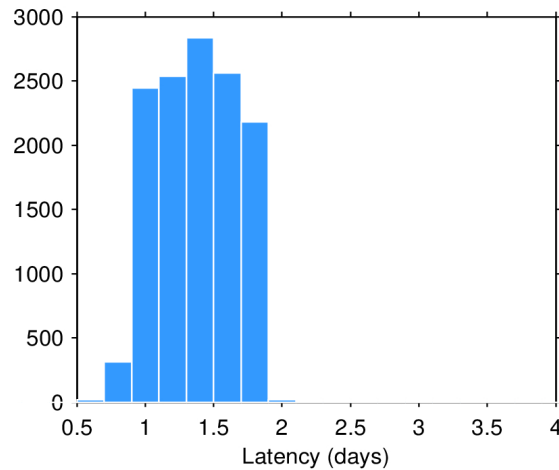


Figure 36. Histogram of the IOP data latency for May 2023. The y-axis denotes the number of files that are made available with a delay of x-hours with respect to the mean time of the records stored in the file.

2.3. Data coverage and completeness

| | Present in month | Theoretical max. | Percentage (%) |
|-------------------------|------------------|------------------|----------------|
| Total | 2675661 | 2716186 | 98.5 |
| Oceans and lakes | 1867259 | 1890524 | 98.8 |

Table 6. Number of total (land and ocean/lake) and only ocean/lake records (based on the surface_type flag) together with their percentage relative to the theoretically expected number of measurements from the orbits ground tracks for May 2023. Theoretical values are also shown.

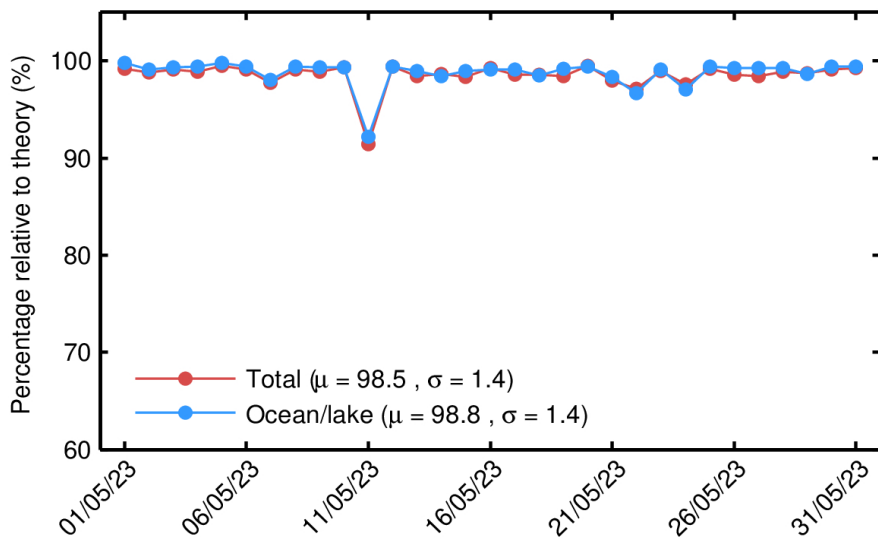


Figure 37. Percentage of IOP 1-Hz records over land and ocean/lake (red) and only over ocean/lake (blue) relative to the theoretically expected number from the orbits ground tracks for each day in May 2023.

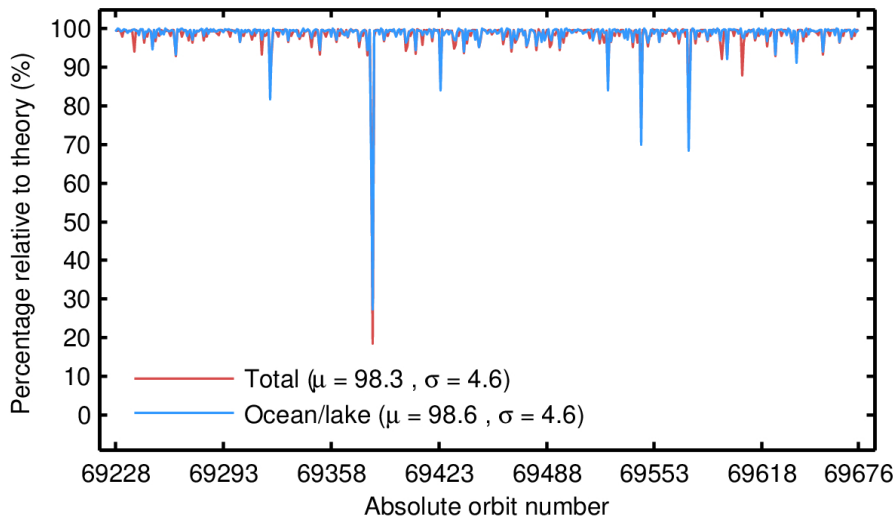


Figure 38. Percentage of IOP 1-Hz records over land and ocean/lake (red) and only over ocean/lake (blue) relative to the theoretically expected number from the orbits ground tracks for each orbit in May 2023. The mean (μ) and standard deviation (σ) are also shown.

2.4. SSH anomaly coverage and validity

| Parameter | Min threshold | Max threshold | Percentage edited |
|-----------------------------------|---------------|---------------|-------------------|
| Flagged as bad | - | - | 1.1% |
| Biased orbit | - | - | 20.4% |
| SSH anomaly | -3 m | 3 m | 0.1% |
| Standard deviation of SSH anomaly | 0 m | 0.20 m | 1.0% |
| Inverse barometer correction | -2 m | 2 m | 0.0% |
| Wet tropospheric correction | -0.5 m | -0.001 m | 0.0% |
| Dry tropospheric correction | -2.5 m | -1.9 m | 0.0% |
| Ionospheric correction | -0.4 m | 0.04 m | 0.0% |
| Sea state bias | -0.5 m | 0 m | 0.2% |
| Sigma0 | 7 dB | 30 dB | 0.2% |
| Standard deviation of sigma0 | 0 dB | 0.23 dB | 4.1% |
| All together | - | - | 24.2% |

Table 7. Editing criteria. The percentage of “flagged as bad” refers to records that have been flagged as bad by either the average status flag or the measurement confidence flag. Such percentage is computed only for records over oceans/lakes and outside polar regions. All other percentages refer to the percentage of flag-valid records that have been rejected by the corresponding criteria or by all criteria (“All together”). The biased orbit criteria in the table refers to the orbits highlighted in the 'Warnings' table at the beginning of this report as being suspicious of suffering from a significant orbit bias. For such orbits, all records are rejected.

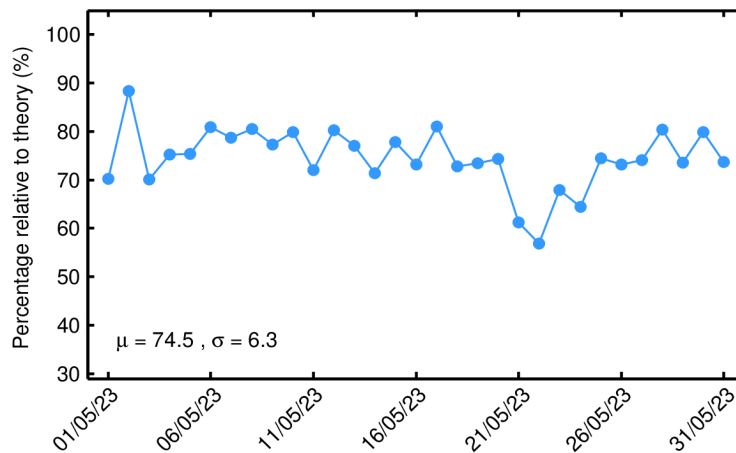


Figure 39. Percentage of science-valid IOP 1-Hz SSH records over ocean and lakes relative to theory for each day in May 2023. The mean (μ) and standard deviation (σ) are also shown.

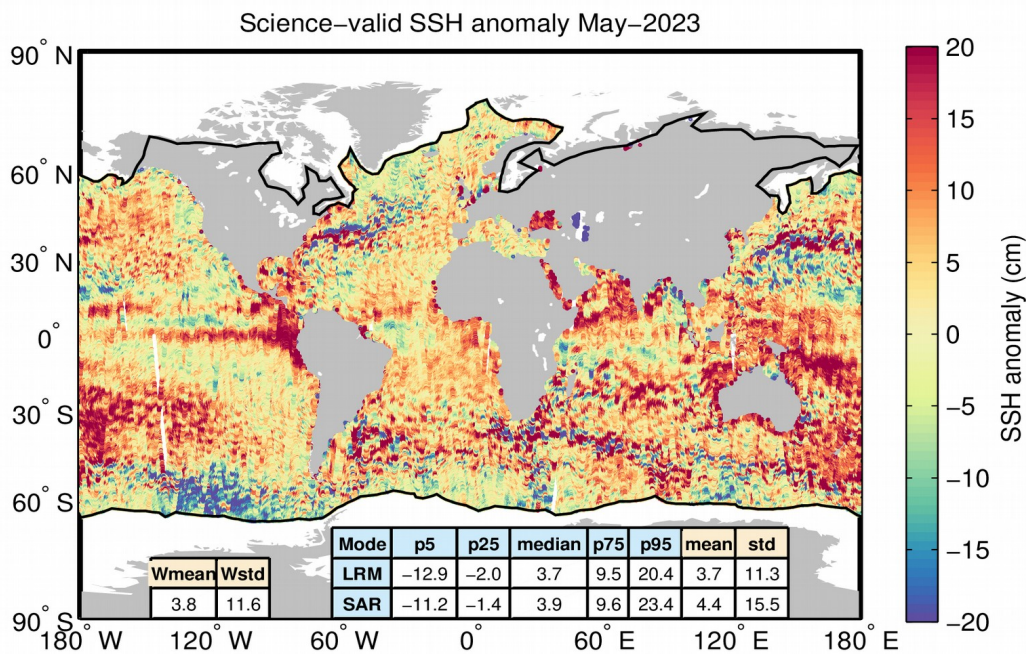


Figure 40. Geographical distribution of science-valid IOP 1-Hz SSH anomaly data over oceans and lakes for May 2023. The statistical values shown in the table refer to the SSH anomaly in cm and are calculated separately for LRM and SAR regions. Wmean and Wstd denote the spatial area-weighted average and its standard deviation. Measurements taken over polar polygons have been excluded from the computation of the statistical values. The black lines mark the outer limit of the Arctic and Antarctic polar polygons.

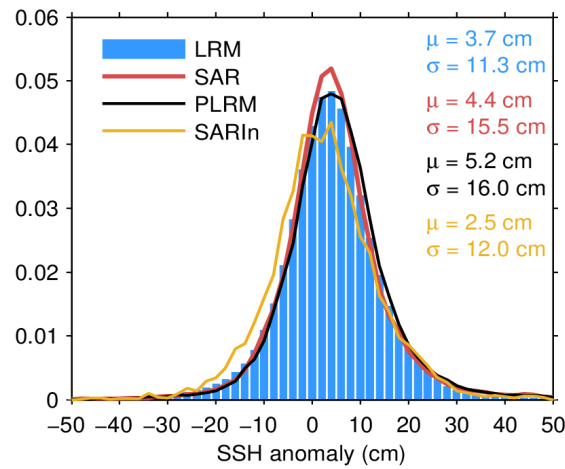
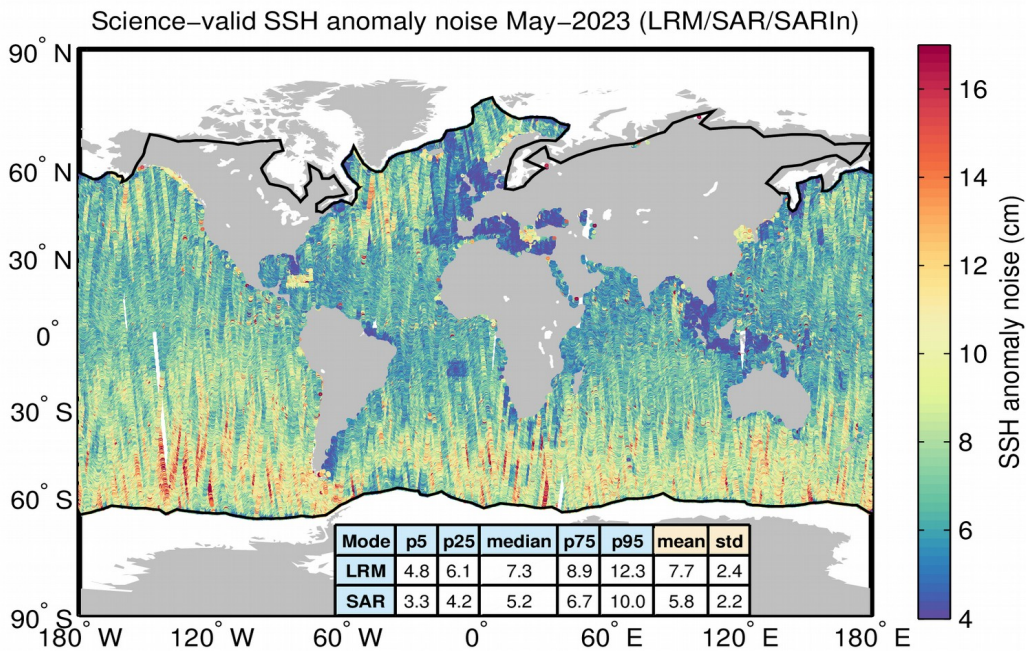


Figure 41. Histogram of science-valid IOP SSH anomaly over oceans and lakes for LRM (blue), SAR (red), PLRM (black) and SARIn (orange) for May 2023. The mean (μ) and standard deviation (σ) are also shown. Values outside [-50 50] cm are excluded from the histogram for the sake of readability but not from the computation of μ and σ .



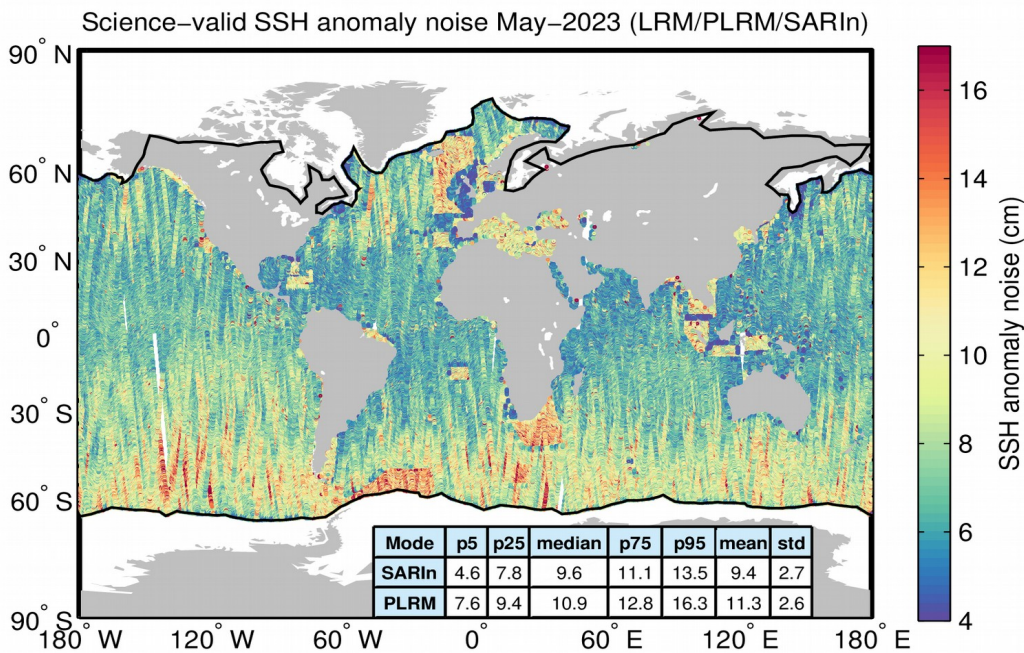


Figure 42. Geographical distribution of flag-valid 20-Hz SSH anomaly measurement noise over oceans and lakes for LRM/SAR/SARIn (top) and LRM/PLRM/SARIn (bottom) and for May 2023. The statistical values shown in the tables refer to the SSH anomaly noise and are calculated separately for LRM, SAR/PLRM and SARIn regions. Measurements taken over polar polygons have been excluded from the computation of the statistical values. The black lines mark the outer limit of the Arctic and Antarctic polar polygons.

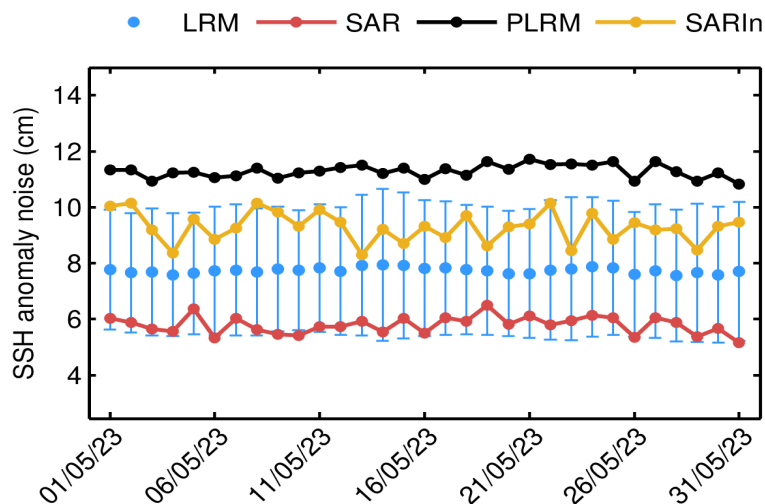


Figure 43. Mean science-valid IOP SSH anomaly noise for LRM (blue dot), SAR (red dot), PLRM (black dot) and SARIn (orange dot) for each day in May 2023. The corresponding standard deviation for LRM (blue error bar) is also shown.

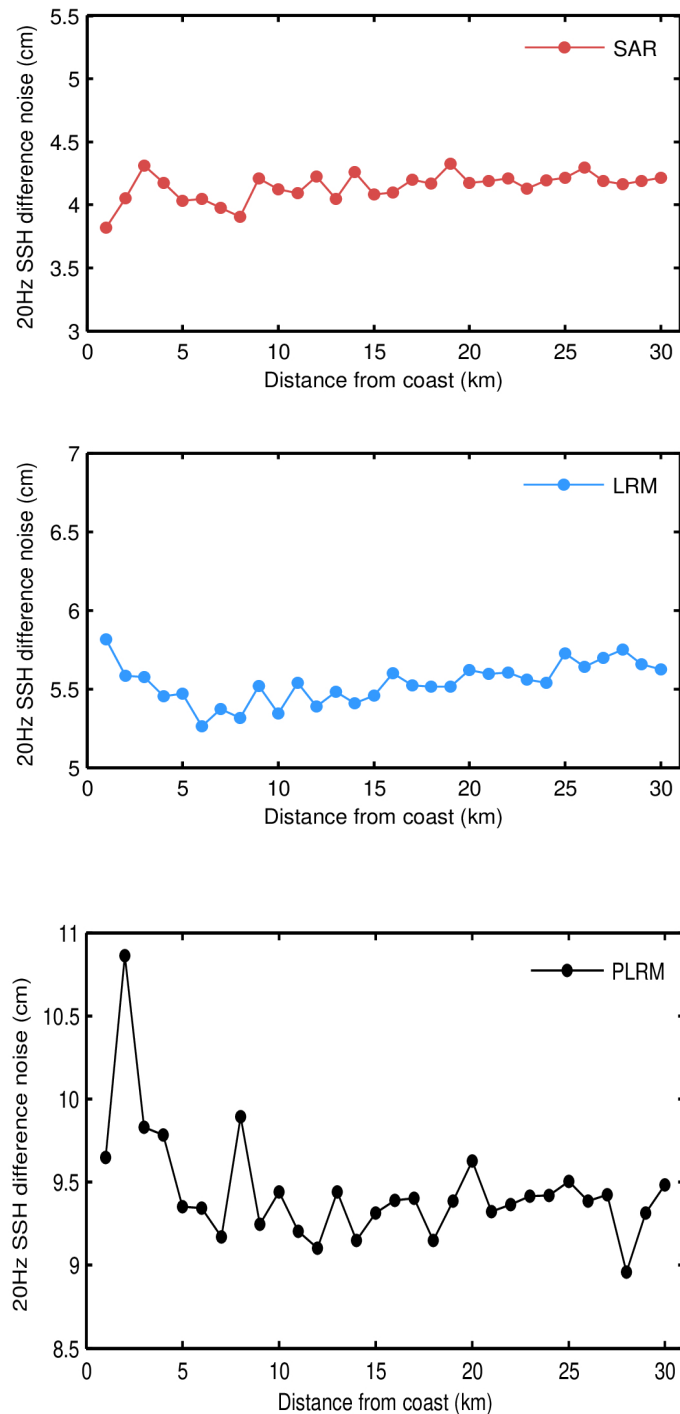
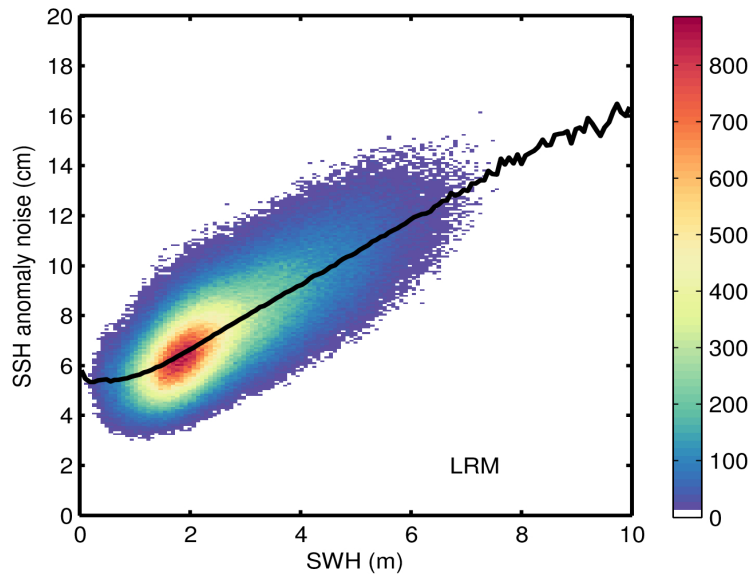
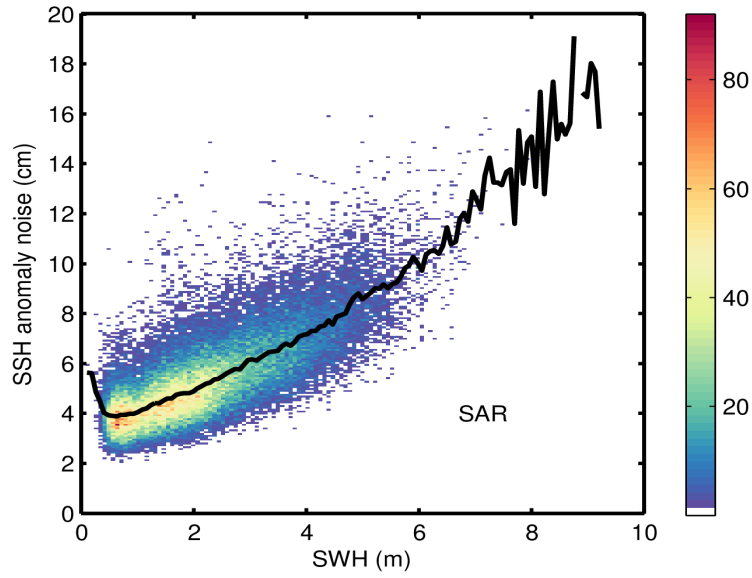


Figure 44. Science-valid IOP 20-Hz SSH anomaly noise as a function of distance from the coast for SAR (top panel), LRM (middle panel), and PLRM (bottom panel) for May 2023. Noise values have been calculated as the median of the absolute value of the difference between consecutive 20-Hz records.



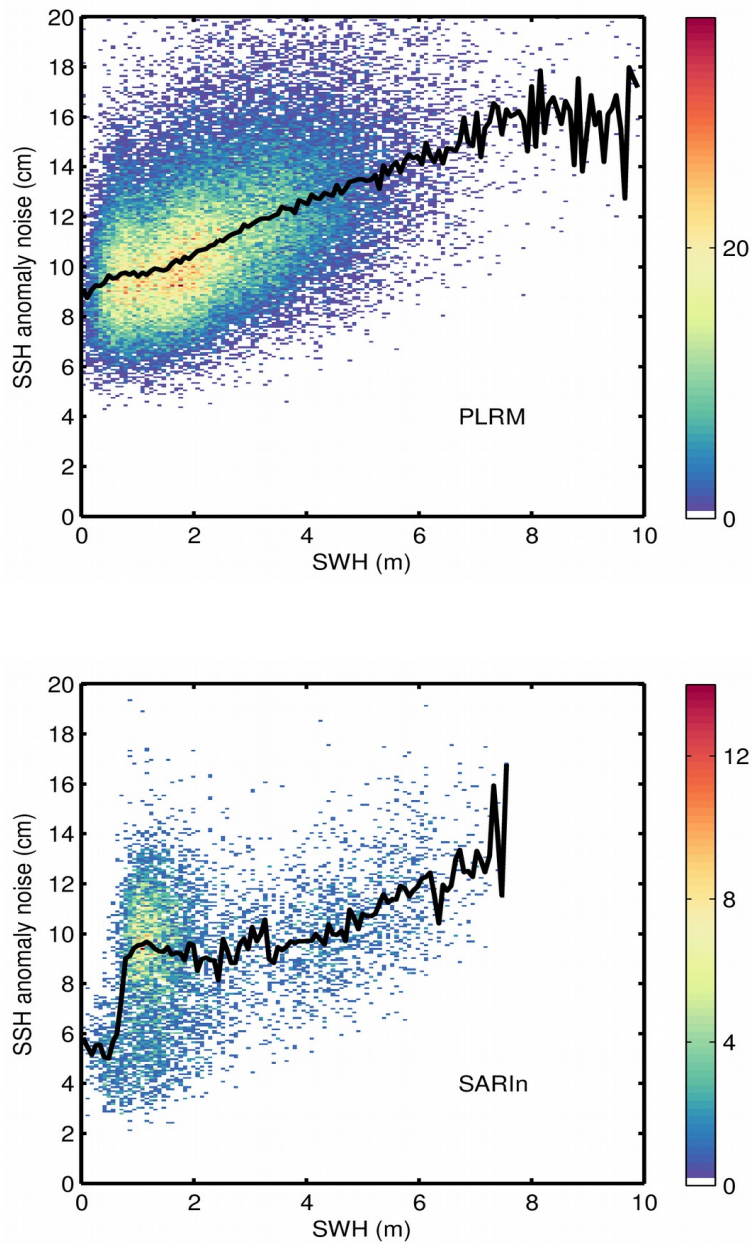


Figure 45. 2D histogram showing science-valid IOP SSH anomaly noise as a function of SWH for SAR, LRM, PLRM, and SARIn (from top to bottom) for May 2023. The black line denotes the median SSH anomaly noise as a function of SWH.

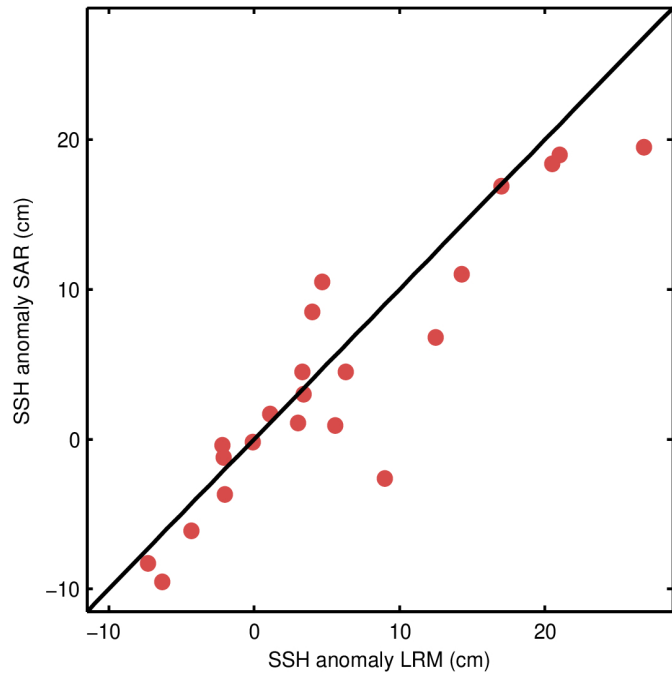


Figure 46. Scatter plot of the science-valid IOP SSH anomaly at the two nearest points outside (LRM, x-axis) and inside (SAR, y-axis) the Pacific SAR mode box for each pass. The RMS of the differences is 3.2 cm for the pairs shown in the figure as compared to a RMS of 4.5 cm for the differences between such outside points and their respective nearest neighbour also outside the box in the LRM region.

2.5. Crossover analysis

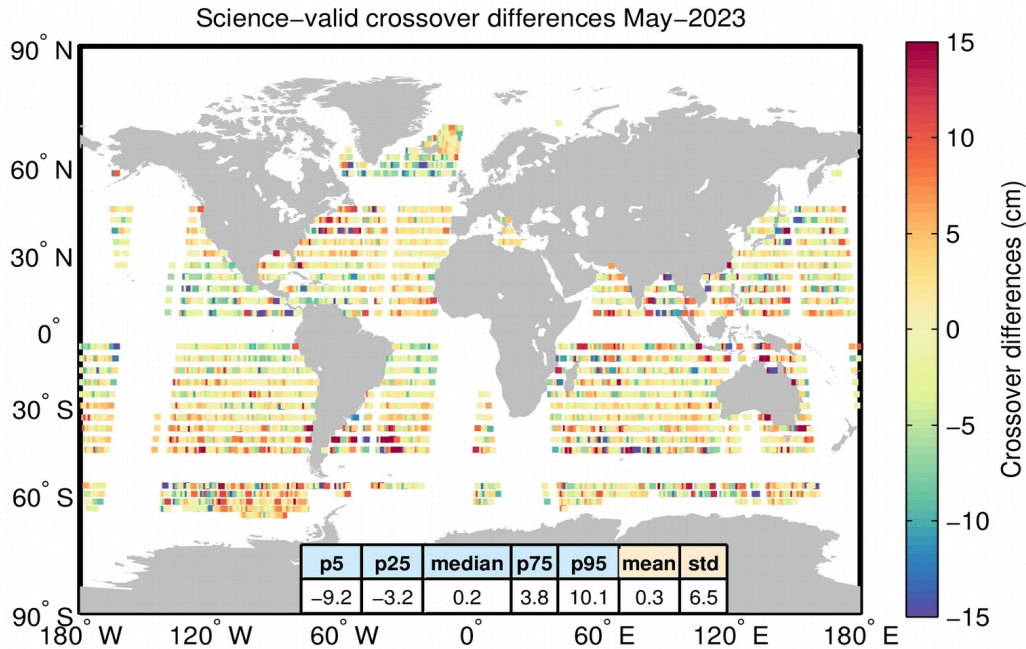


Figure 47. Crossover differences (absolute values) for the science-valid IOP SSH anomaly for May 2023. The difference at each crossover is computed as the difference between median values over 2-second windows centered about the crossover.

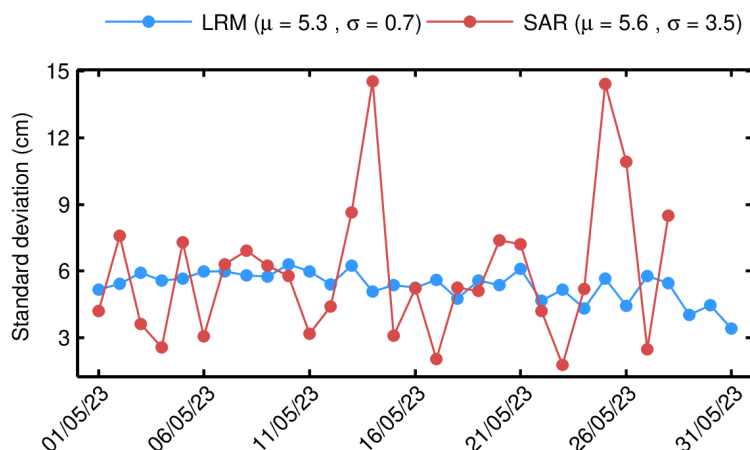


Figure 48. Standard deviation of differences at crossovers for IOP SSH anomaly for each day in May 2023. The values shown in this figure have been computed for the science-valid data further edited according to the following two additional criteria: 1) rejecting crossover differences larger than 20 cm; and 2) rejecting shallow waters (1000 m). The mean (μ) and standard deviation (σ) are also shown.

2.6. SWH coverage and validity

| Parameter | Min threshold | Max threshold | Percentage edited |
|--|---------------|---------------|-------------------|
| Flagged as bad | - | - | 1.1% |
| SWH | 0 m | 15 m | 0.0% |
| Standard deviation of SWH (1-Hz block) | 0 m | 1 m | 1.4% |
| All together | - | - | 1.4% |

Table 8. Editing criteria. The percentage of “flagged as bad” refers to records that have been flagged as bad by either the average status flag or the measurement confidence flag. Such percentage is computed only for records over oceans/lakes and outside polar regions. All other percentages refer to the percentage of flag-valid records that have been rejected by the corresponding criteria or by all criteria (“All together”).

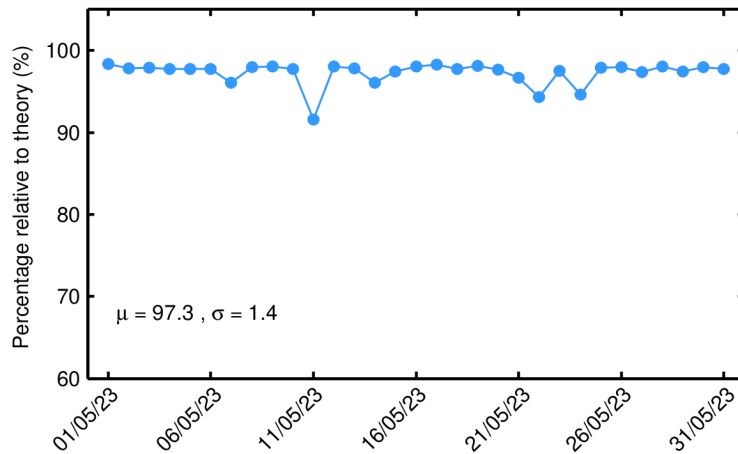


Figure 49. Percentage of science-valid IOP 1-Hz SWH records over ocean and lakes relative to theory for each day in May 2023. The mean (μ) and standard deviation (σ) are also shown.

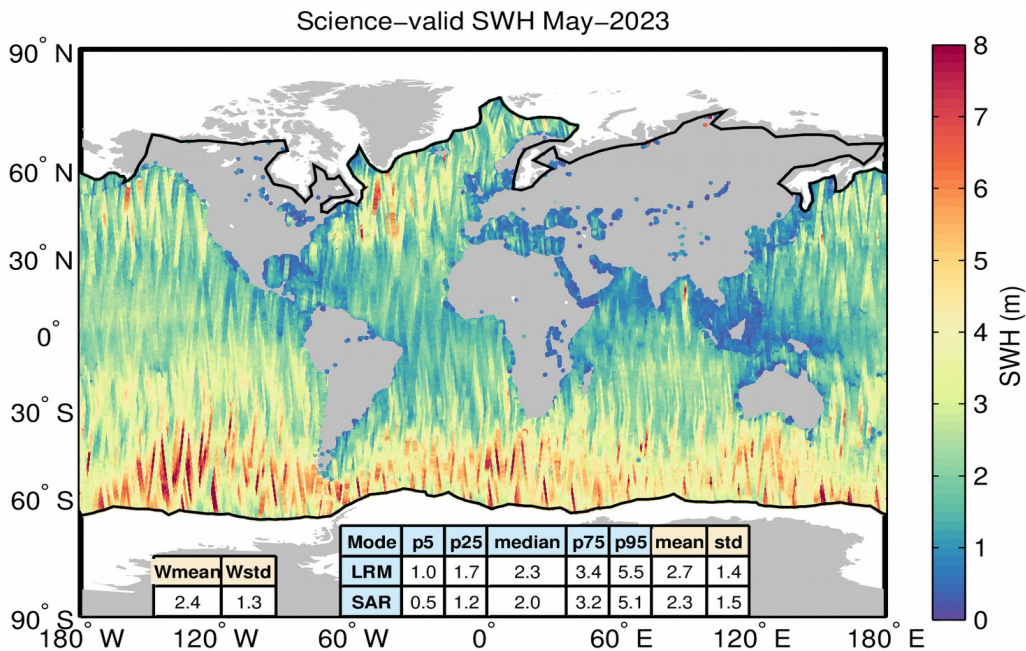


Figure 50. Geographical distribution of science-valid IOP SWH data over oceans and lakes for May 2023. The statistical values shown in the table refer to the SWH in m and are calculated separately for LRM and SAR regions. Wmean and Wstd denote the spatial area-weighted average and its standard deviation. Measurements taken over polar polygons have been excluded from the computation of the statistical values. The black lines mark the outer limit of the Arctic and Antarctic polar polygons.

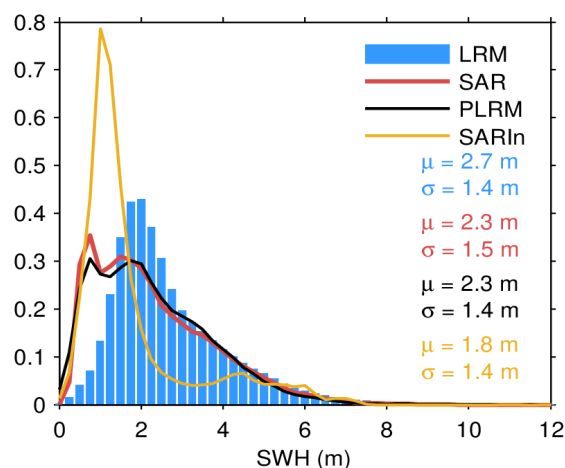


Figure 51. Histogram of science-valid IOP SWH over oceans and lakes for LRM (blue), SAR (red), PLRM (black) and SARIn (orange) for May 2023. The mean (μ) and standard deviation (σ) are also shown. Values larger than 12 m are excluded from the histogram for the sake of readability but not from the computation of μ and σ .

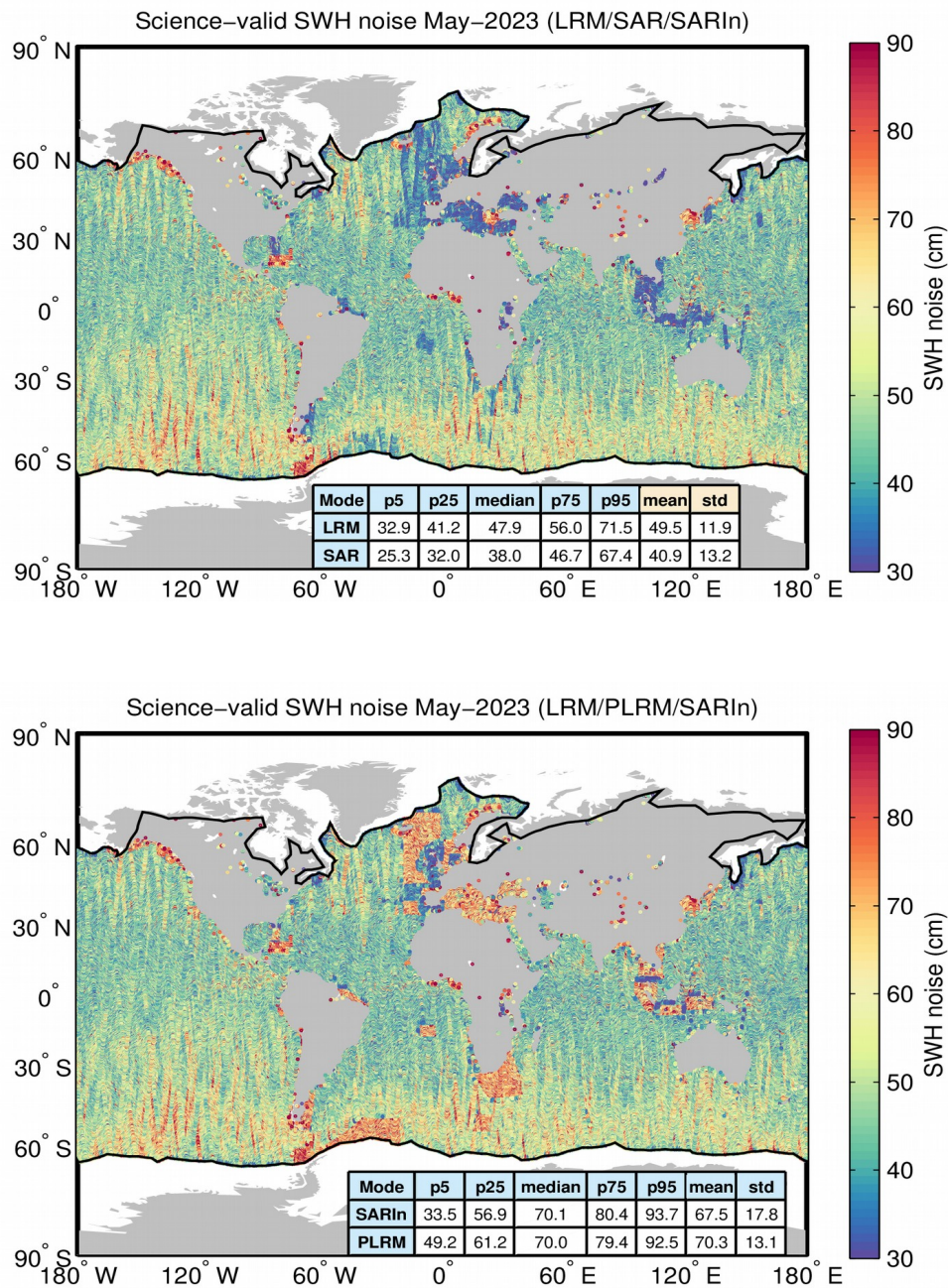


Figure 52. Geographical distribution of flag-valid 20-Hz SWH measurement noise over oceans and lakes for LRM/SAR/SARIn (top) and LRM/PLRM/SARIn (bottom) and for May 2023. The statistical values shown in the table refer to the SWH noise and are calculated separately for LRM, SAR/PLRM and SARIn regions. Measurements taken over polar polygons have been excluded from the computation of the statistical values. The black lines mark the outer limit of the Arctic and Antarctic polar polygons.

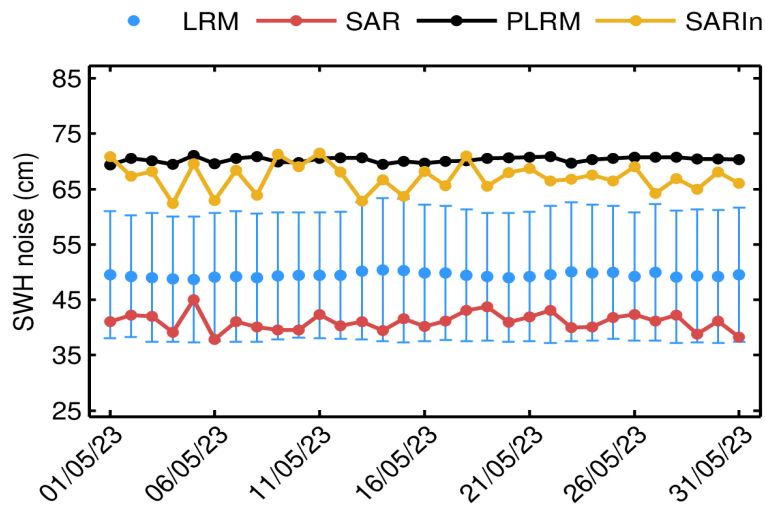
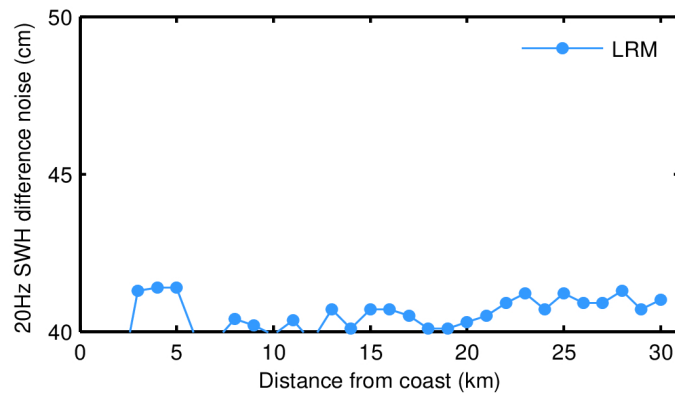
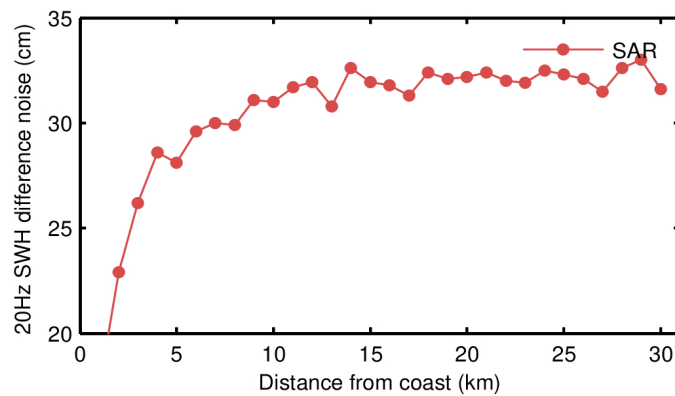


Figure 53. Mean science-valid IOP SWH noise for LRM (blue dot), SAR (red dot), PLRM (black dot) and SARIn (orange dot) for each day in May 2023. The corresponding standard deviation for LRM (blue error bar) is also shown.



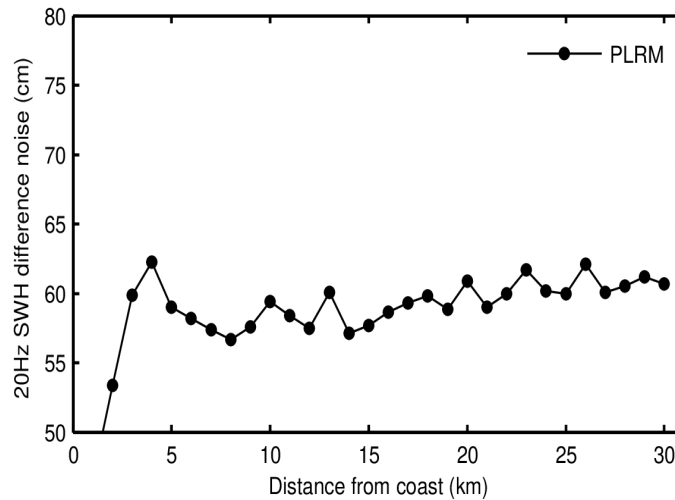


Figure 54. Science-valid IOP 20-Hz SWH noise as a function of distance from the coast for SAR (top panel), LRM (middle panel), and PLRM (bottom panel) for May 2023. Noise values have been calculated as the median of the absolute value of the difference between consecutive 20-Hz records.

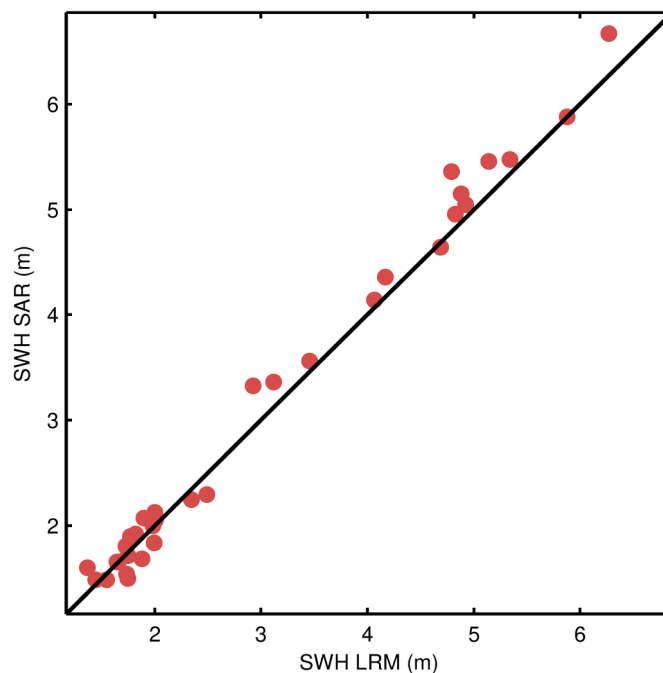


Figure 55. Scatter plot of the science-valid IOP SWH at the two nearest points outside (LRM, x-axis) and inside (SAR, y-axis) the Pacific SAR mode box for each pass. The RMS of the differences is 17.8 cm for the pairs shown in the figure as compared to a RMS of 15.8 cm for the differences between such outside points and their respective nearest neighbour also outside the box in the LRM region.

2.7. Sigma0 coverage and validity

| Parameter | Min threshold | Max threshold | Percentage edited |
|---|---------------|---------------|-------------------|
| Flagged as bad | - | - | 0.7% |
| Sigma0 | 7 dB | 30 dB | 0.2% |
| Standard deviation of Sigma0 (1-Hz block) | 0 dB | 0.23 dB | 4.4% |
| All together | - | - | 4.5% |

Table 9. Editing criteria. The percentage of “flagged as bad” refers to records that have been flagged as bad by either the average status flag or the measurement confidence flag. Such percentage is computed only for records over oceans/lakes and outside polar regions. All other percentages refer to the percentage of flag-valid records that have been rejected by the corresponding criteria or by all criteria (“All together”).

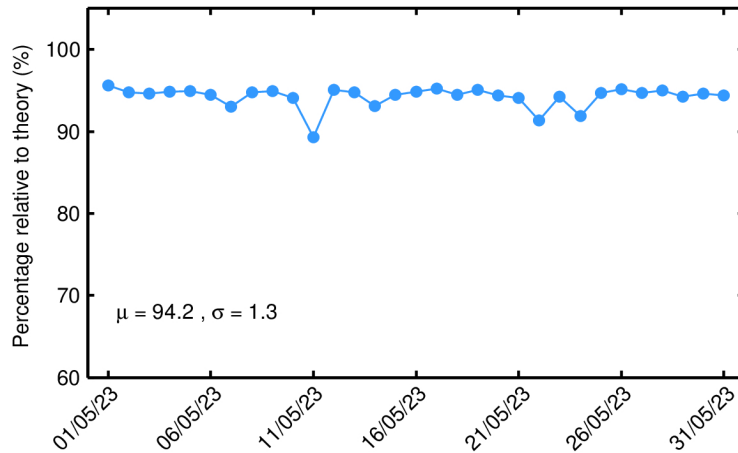


Figure 56. Percentage of science-valid IOP 1-Hz sigma0 records over ocean and lakes relative to theory for each day in May 2023. The mean (μ) and standard deviation (σ) are also shown.

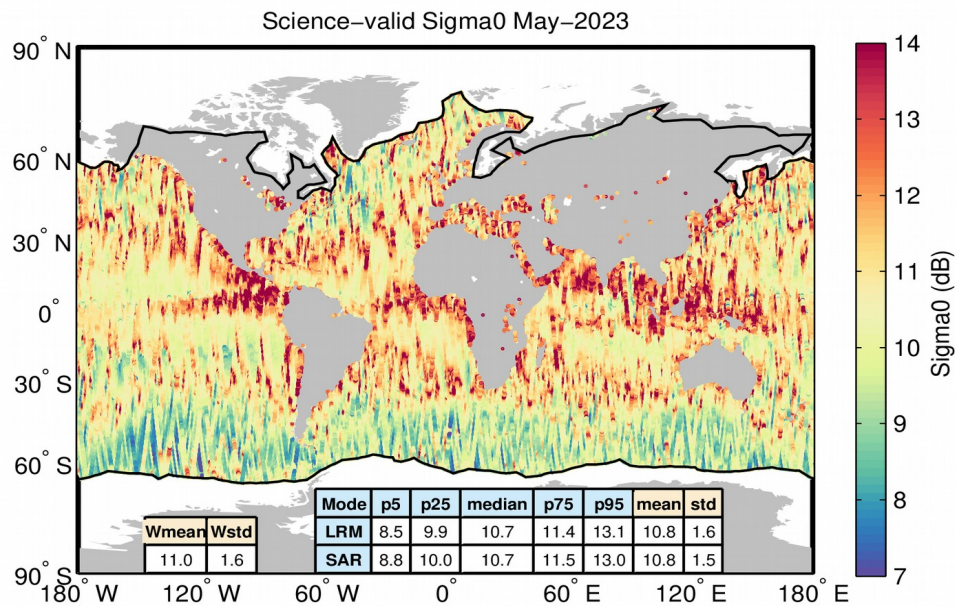


Figure 57. Geographical distribution of science-valid IOP sigma0 data over oceans and lakes for May 2023. The statistical values shown in the table refer to the sigma0 in m and are calculated separately for LRM and SAR regions. Wmean and Wstd denote the spatial area-weighted average and its standard deviation. Measurements taken over polar polygons have been excluded from the computation of the statistical values. The black lines mark the outer limit of the Arctic and Antarctic polar polygons.

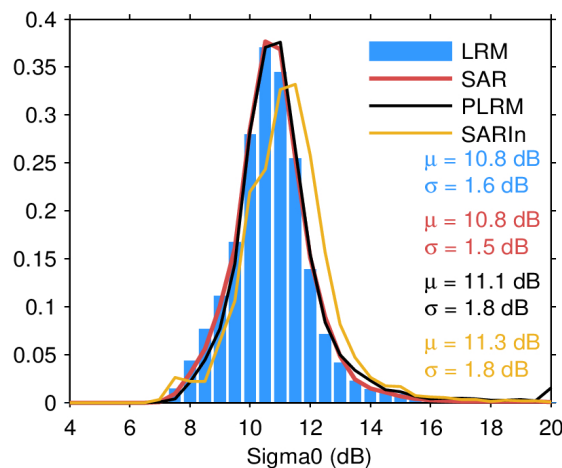


Figure 58. Histogram of science-valid IOP sigma0 over oceans and lakes for LRM (blue), SAR (red), PLRM (black) and SARIn (orange) for May 2023. The mean (μ) and standard deviation (σ) are also shown. Values larger than 12 m are excluded from the histogram for the sake of readability but not from the computation of μ and σ .

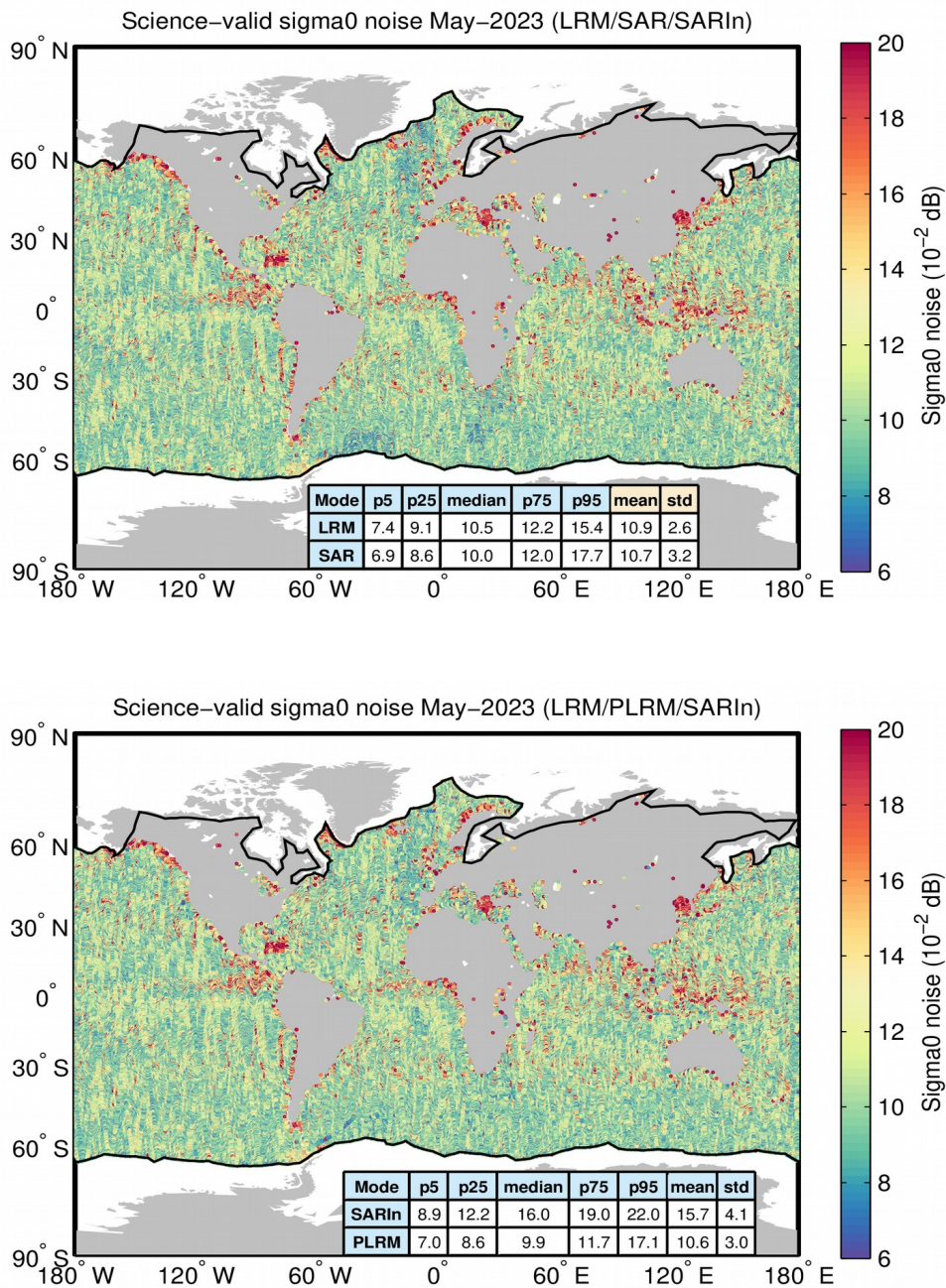


Figure 59. Geographical distribution of flag-valid 20-Hz sigma0 measurement noise over oceans and lakes for LRM/SAR/SARIn (top) and LRM/PLRM/SARIn (bottom) and for May 2023. The statistical values shown in the table refer to the sigma0 noise and are calculated separately for LRM, SAR/PLRM and SARIn regions. Measurements taken over polar polygons have been excluded from the computation of the statistical values. The black lines mark the outer limit of the Arctic and Antarctic polar polygons.

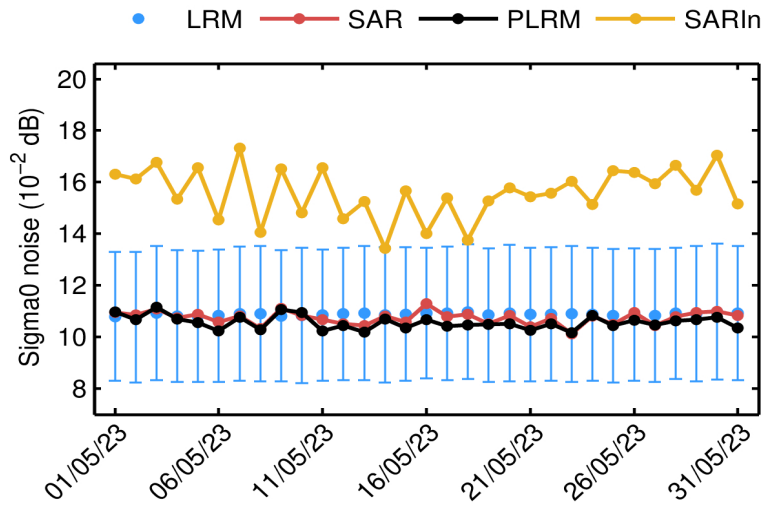
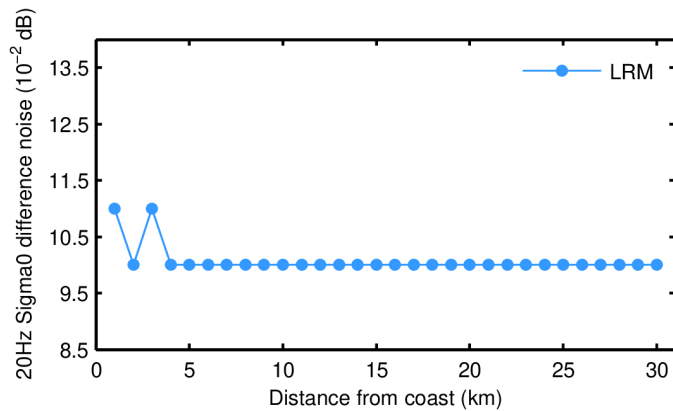
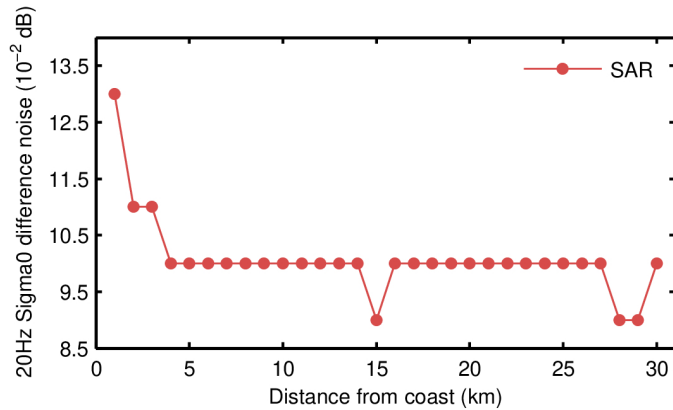


Figure 60. Mean science-valid IOP sigma0 noise for LRM (blue dot), SAR (red dot), PLRM (black dot) and SARIn (orange dot) for each day in May 2023. The corresponding standard deviation for LRM (blue error bar) is also shown.



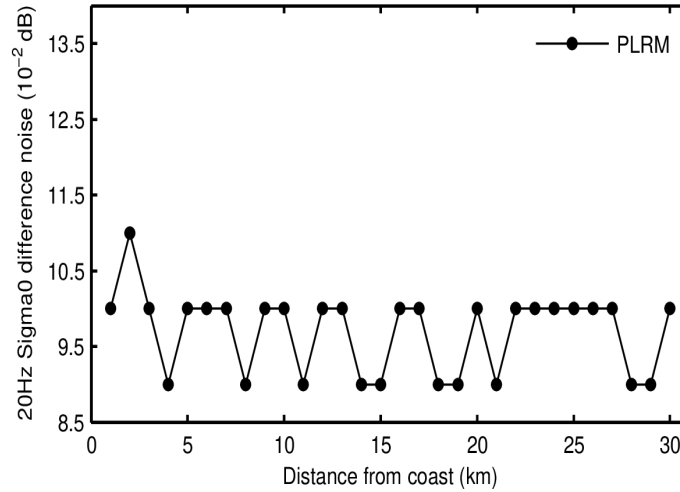


Figure 61. Science-valid IOP 20-Hz sigma0 noise as a function of distance from the coast for SAR (top panel), LRM (middle panel), and PLRM (bottom panel) for May 2023. Noise values have been calculated as the median of the absolute value of the difference between consecutive 20-Hz records.

2.8. Wind speed coverage and validity

| Parameter | Min threshold | Max threshold | Percentage edited |
|----------------------|---------------|---------------|-------------------|
| Flagged as bad | - | - | 0.7% |
| Altimeter wind speed | 0 m/s | 30 m/s | 0.0% |

Table 10. Editing criteria. The percentage of “flagged as bad” refers to records that have been flagged as bad by either the average status flag or the measurement confidence flag. Such percentage is computed only for records over oceans/lakes and outside polar regions. All other percentages refer to the percentage of flag-valid records that have been rejected by the corresponding criteria.

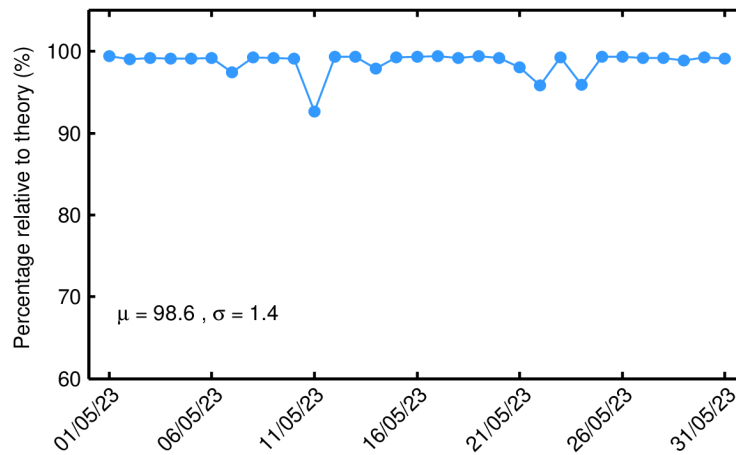


Figure 62. Percentage of science-valid IOP 1-Hz wind records over ocean and lakes relative to theory for each day in May 2023. The mean (μ) and standard deviation (σ) are also shown.

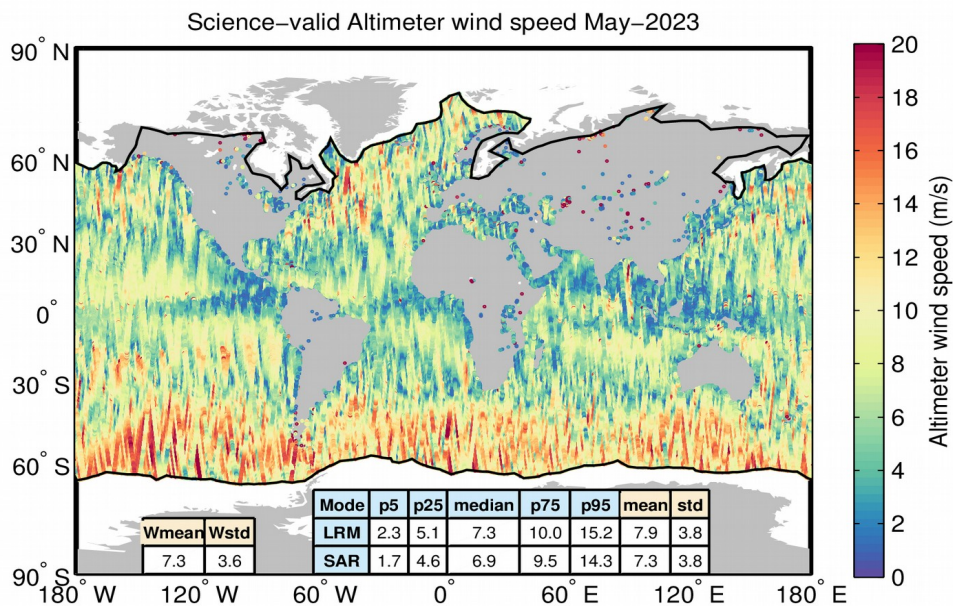


Figure 63. Geographical distribution of science-valid IOP wind data over oceans and lakes for May 2023. The statistical values shown in the table refer to the wind in m and are calculated separately for LRM and SAR regions. Wmean and Wstd denote the spatial area-weighted average and its standard deviation. Measurements taken over polar polygons have been excluded from the computation of the statistical values. The black lines mark the outer limit of the Arctic and Antarctic polar polygons.

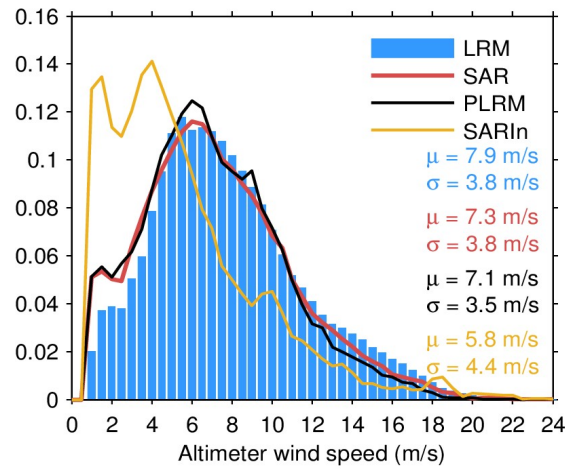


Figure 64. Histogram of science-valid IOP wind over oceans and lakes for LRM (blue), SAR (red), PLRM (black) and SARIn (orange) for May 2023. The mean (μ) and standard deviation (σ) are also shown. Values larger than 12 m are excluded from the histogram for the sake of readability but not from the computation of μ and σ .

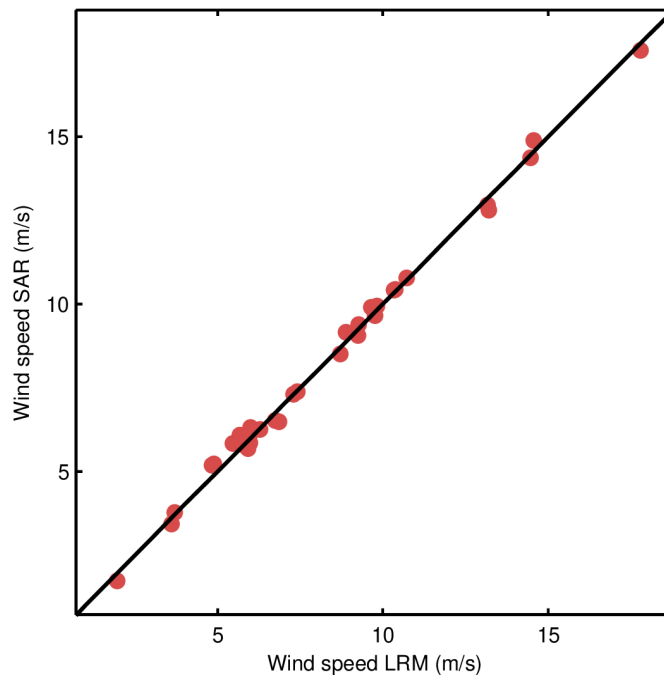


Figure 65. Scatter plot of the science-valid IOP wind speed at the two nearest points outside (LRM, x-axis) and inside (SAR, y-axis) the Pacific SAR mode box for each pass. The RMS of the differences is 22.4 cm/s for the pairs shown in the figure as compared to a RMS of 20.6 cm/s for the differences between such outside points and their respective nearest neighbour also outside the box in the LRM region.

2.9. Mispointing coverage and validity

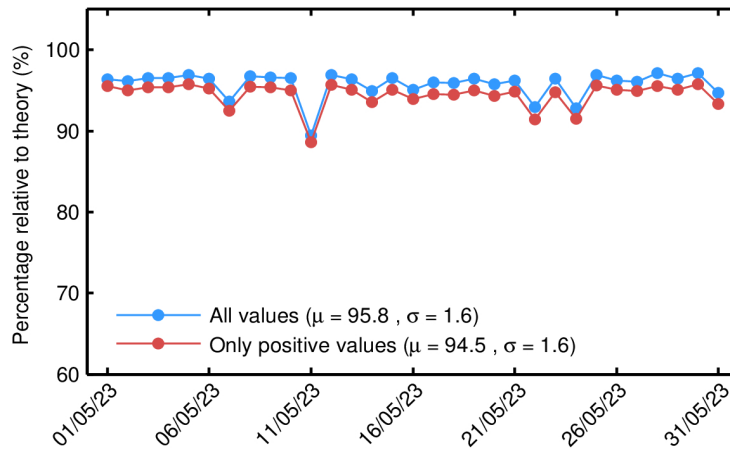
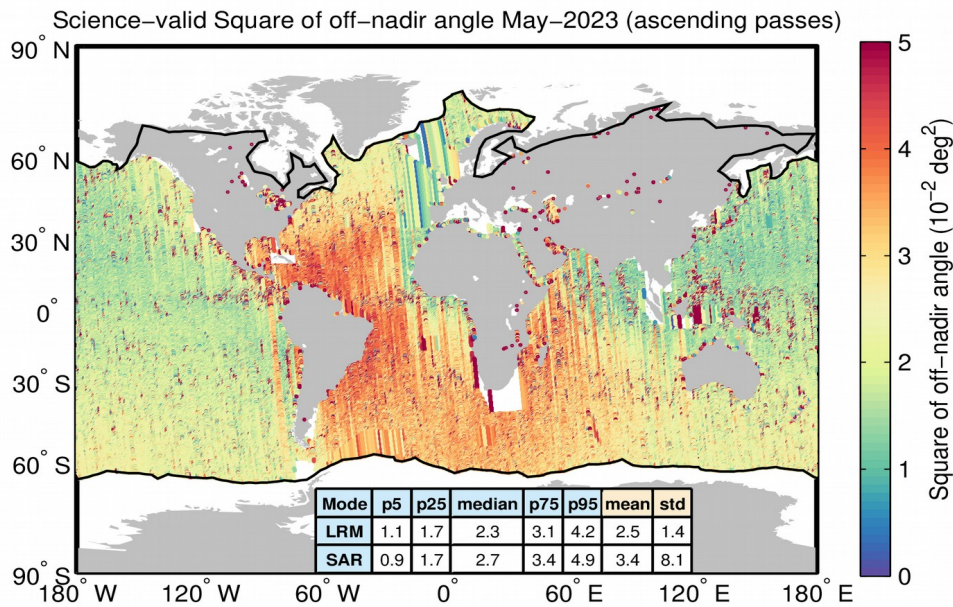


Figure 66. Percentage of science-valid IOP 1-Hz mispointing records over ocean and lakes relative to theory for each day in May 2023. The mean (μ) and standard deviation (σ) are also shown.



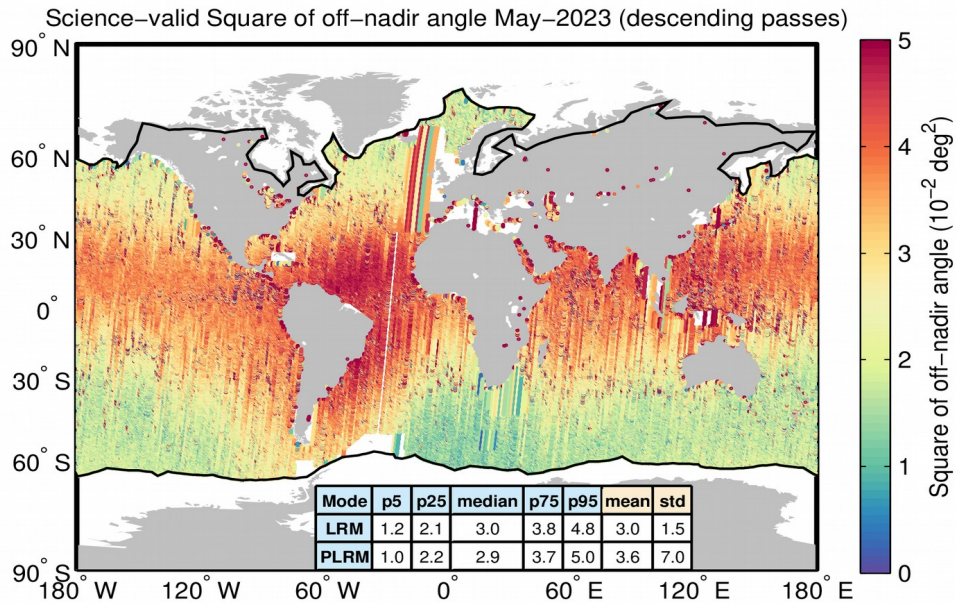


Figure 67. Geographical distribution of science-valid IOP mispointing data over oceans and lakes for ascending (top) and descending (bottom) passes for May 2023. The statistical values shown in the table refer to the wind in m and are calculated separately for LRM and SAR regions. Measurements taken over polar polygons have been excluded from the computation of the statistical values. The black lines mark the outer limit of the Arctic and Antarctic polar polygons.

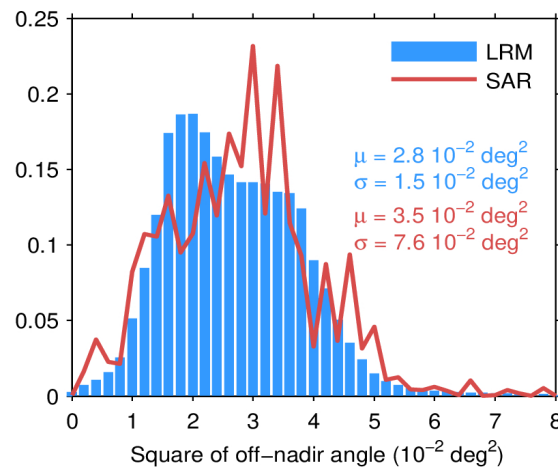


Figure 68. Histogram of science-valid IOP mispointing over oceans and lakes for LRM (blue) and SAR (red) for May 2023. The mean (μ) and standard deviation (σ) are also shown. Note that values larger than 12 m are excluded from the histogram for the sake of readability but not from the computation of μ and σ .

3 Quality control assessment for GOP

Note 3.1: unless otherwise stated, measurements taken over polar polygons have been excluded from the computation of all statistics shown in this section.

Note 3.2: most statistics shown in this section have been computed separately for the low resolution mode (LRM) and the pseudo low resolution mode (SAR).

Note 3.3: “flag-valid” refers to those records that have not been flagged as bad by either the average status flag or the measurement confidence flag.

Note 3.4: “science-valid” refers to flag-valid records (over oceans and lakes and excluding polar regions) that meet the editing criteria described in the Tables 12, 13, 14, 15.

3.1. Data used

Product: **GOP**

Date and time of the first record: **01 05 2023 00:00:00.189**

Date and time of the last record: **31 05 2023 23:59:59.906**

Range of complete orbits in present month: **69228 to 69676**

3.2. Data flow

Median latency [min max]: 28.5 days [26.5 - 32.3]

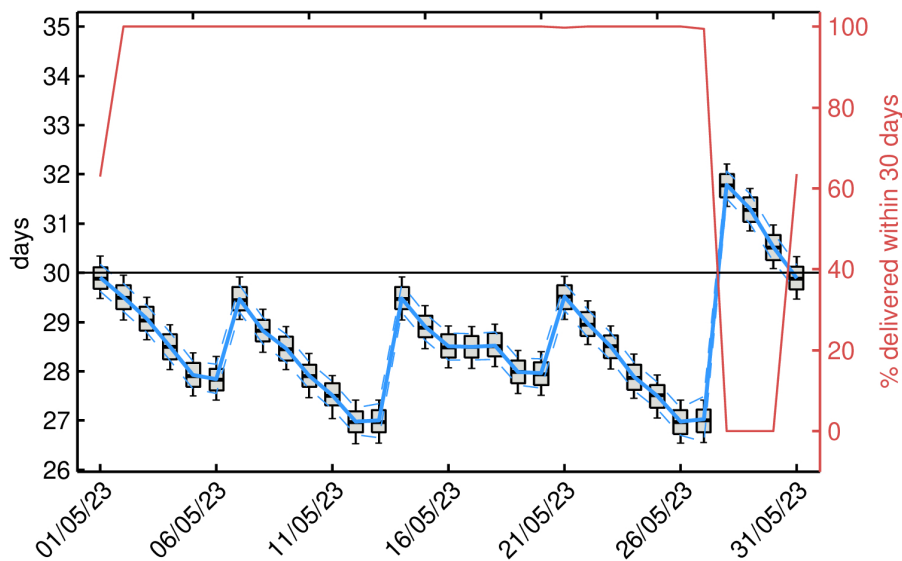


Figure 69. Box-and-whiskers plot for the GOP latency showing for each day in May 2023 the first and third quartiles (bottom and top of the box), the median (thick black), the 5% and 95% percentiles (lower and upper whiskers), the mean (blue) and the mean ± 1 standard deviation (blue dashed line). The percentage of records delivered within 3 days is also shown (red, right y-axis). The horizontal black line denotes the 30 days threshold.

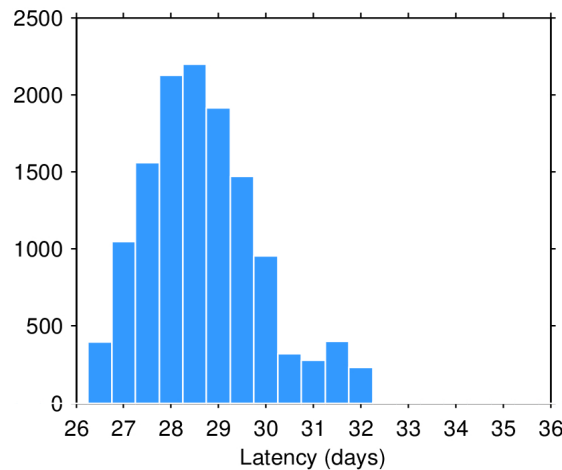


Figure 70. Histogram of the GOP data latency for May 2023. The y-axis denotes the number of files that are made available with a delay of x-hours with respect to the mean time of the records stored in the file.

3.3. Data coverage and completeness

| | Present in month | Theoretical max. | Percentage (%) |
|-------------------------|------------------|------------------|----------------|
| Total | 2665082 | 2716186 | 98.1 |
| Oceans and lakes | 1860112 | 1890524 | 98.4 |

Table 11. Number of total (land and ocean/lake) and only ocean/lake records (based on the surface_type flag) together with their percentage relative to the theoretically expected number of measurements from the orbits ground tracks for May 2023. Theoretical values are also shown.

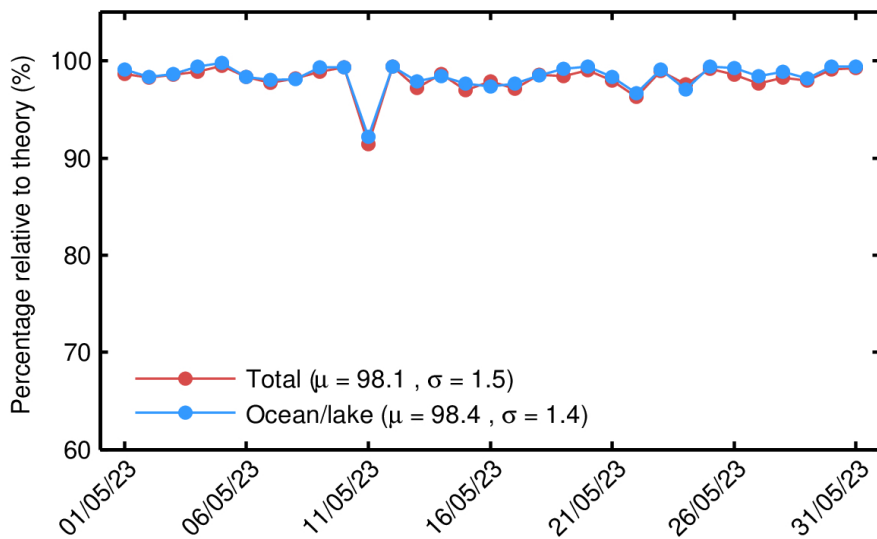


Figure 71. Percentage of GOP 1-Hz records over land and ocean/lake (red) and only over ocean/lake (blue) relative to the theoretically expected number from the orbits ground tracks for each day in May 2023.

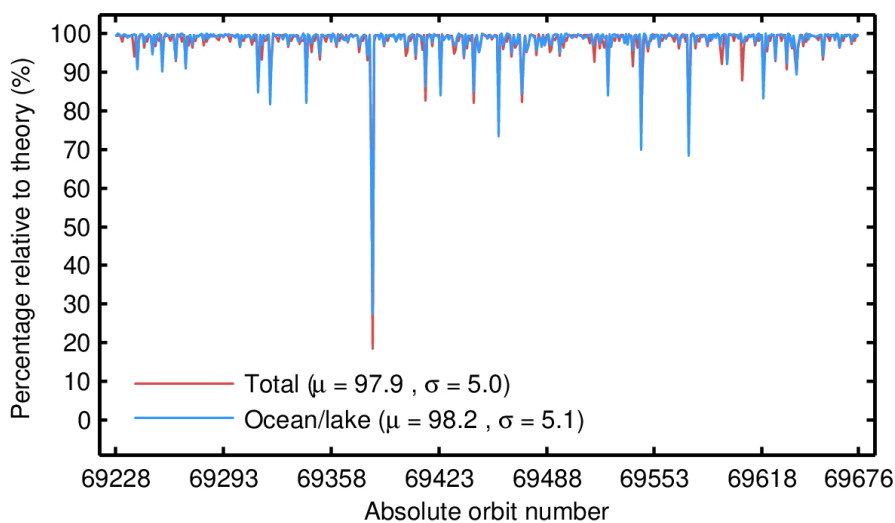


Figure 72. Percentage of GOP 1-Hz records over land and ocean/lake (red) and only over ocean/lake (blue) relative to the theoretically expected number from the orbits ground tracks for each orbit in May 2023. The mean (μ) and standard deviation (σ) are also shown.

3.4. SSH anomaly coverage and validity

| Parameter | Min | Max | Percentage |
|-----------|-----|-----|------------|
|-----------|-----|-----|------------|

| | threshold | threshold | edited |
|-----------------------------------|-----------|-----------|--------|
| Flagged as bad | - | - | 1.1% |
| Biased orbit | - | - | 20.5% |
| SSH anomaly | -3 m | 3 m | 0.1% |
| Standard deviation of SSH anomaly | 0 m | 0.20 m | 1.0% |
| Inverse barometer correction | -2 m | 2 m | 0.0% |
| Wet tropospheric correction | -0.5 m | -0.001 m | 0.0% |
| Dry tropospheric correction | -2.5 m | -1.9 m | 0.0% |
| Ionospheric correction | -0.4 m | 0.04 m | 0.0% |
| Sea state bias | -0.5 m | 0 m | 0.2% |
| Sigma0 | 7 dB | 30 dB | 0.2% |
| Standard deviation of sigma0 | 0 dB | 0.23 dB | 4.1% |
| All together | - | - | 24.2% |

Table 12. Editing criteria. The percentage of “flagged as bad” refers to records that have been flagged as bad by either the average status flag or the measurement confidence flag. Such percentage is computed only for records over oceans/lakes and outside polar regions. All other percentages refer to the percentage of flag-valid records that have been rejected by the corresponding criteria or by all criteria (“All together”). The biased orbit criteria in the table refers to the orbits highlighted in the 'Warnings' table at the beginning of this report as being suspicious of suffering from a significant orbit bias. For such orbits, all records are rejected.

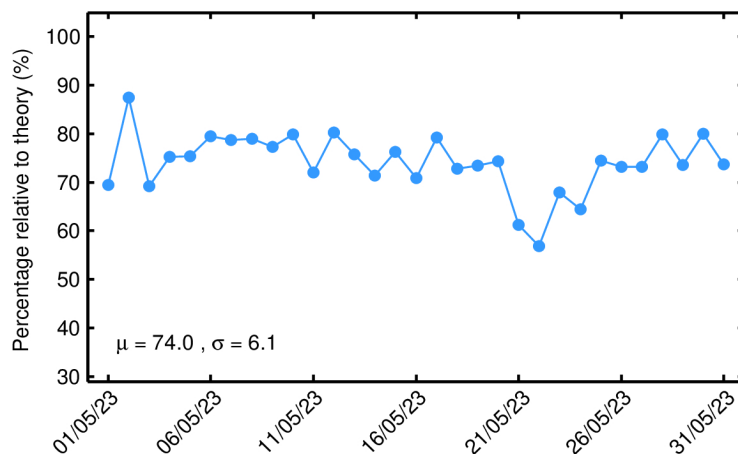


Figure 73. Percentage of science-valid GOP 1-Hz SSH records over ocean and lakes relative to theory for each day in May 2023. The mean (μ) and standard deviation (σ) are also shown.

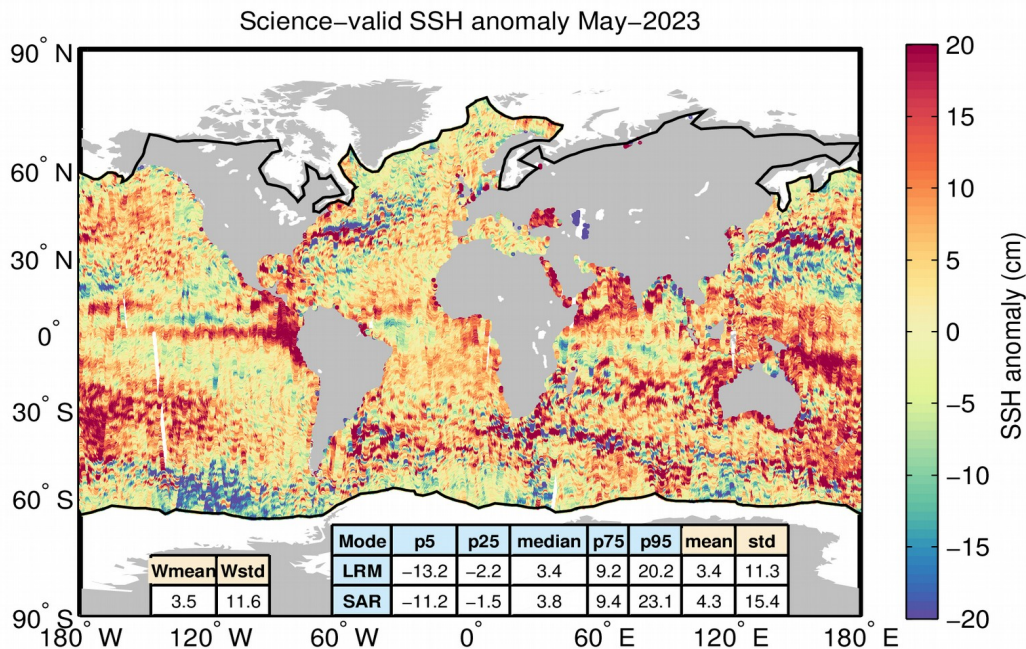


Figure 74. Geographical distribution of science-valid GOP 1-Hz SSH anomaly data over oceans and lakes for May 2023. The statistical values shown in the table refer to the SSH anomaly in cm and are calculated separately for LRM and SAR regions. Wmean and Wstd denote the spatial area-weighted average and its standard deviation. Measurements taken over polar polygons have been excluded from the computation of the statistical values. The black lines mark the outer limit of the Arctic and Antarctic polar polygons.

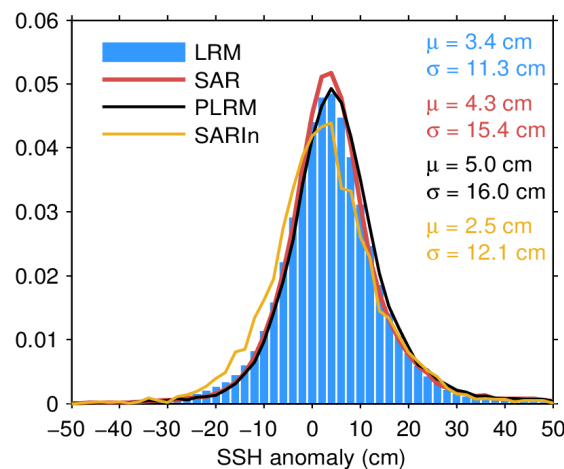


Figure 75. Histogram of science-valid GOP SSH anomaly over oceans and lakes for LRM (blue), SAR (red), PLRM (black) and SARIn (orange) for May 2023. The mean (μ) and

standard deviation (σ) are also shown. Values outside $[-50\ 50]$ cm are excluded from the histogram for the sake of readability but not from the computation of μ and σ .

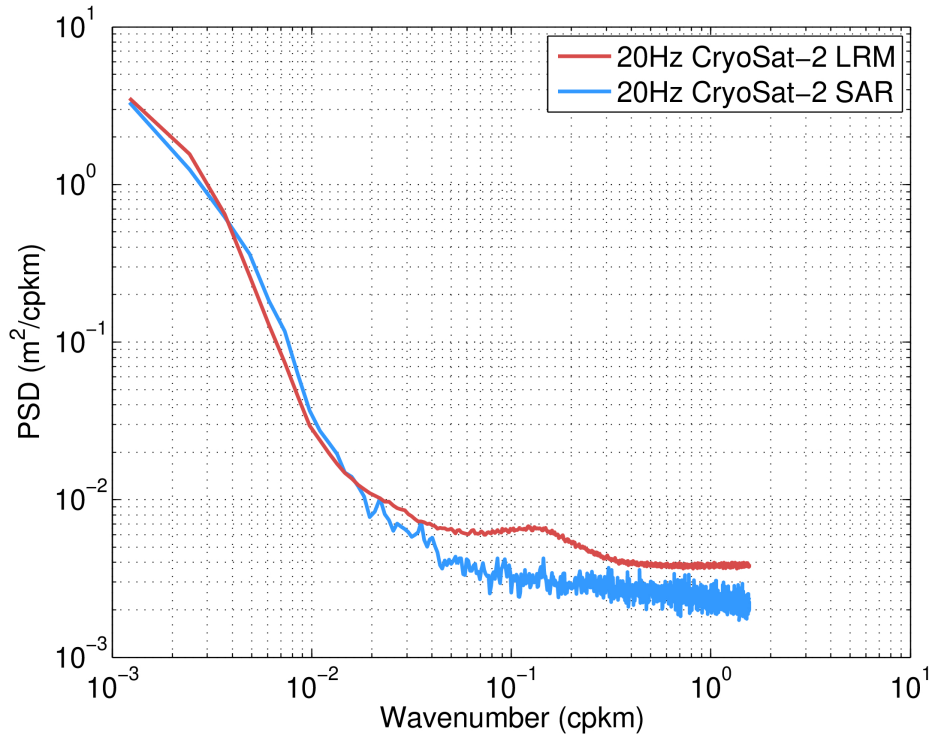
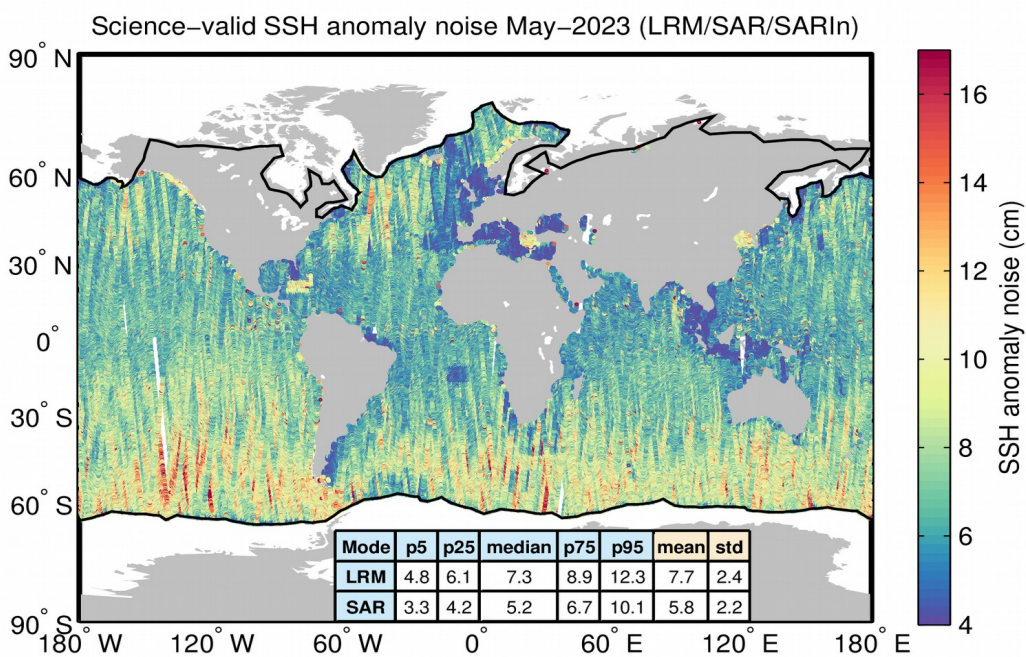


Figure 76. Along-track power spectrum density of the science-valid 20 Hz GOP SSH anomaly over oceans and lakes for LRM (red) and SAR (blue) for May 2023.



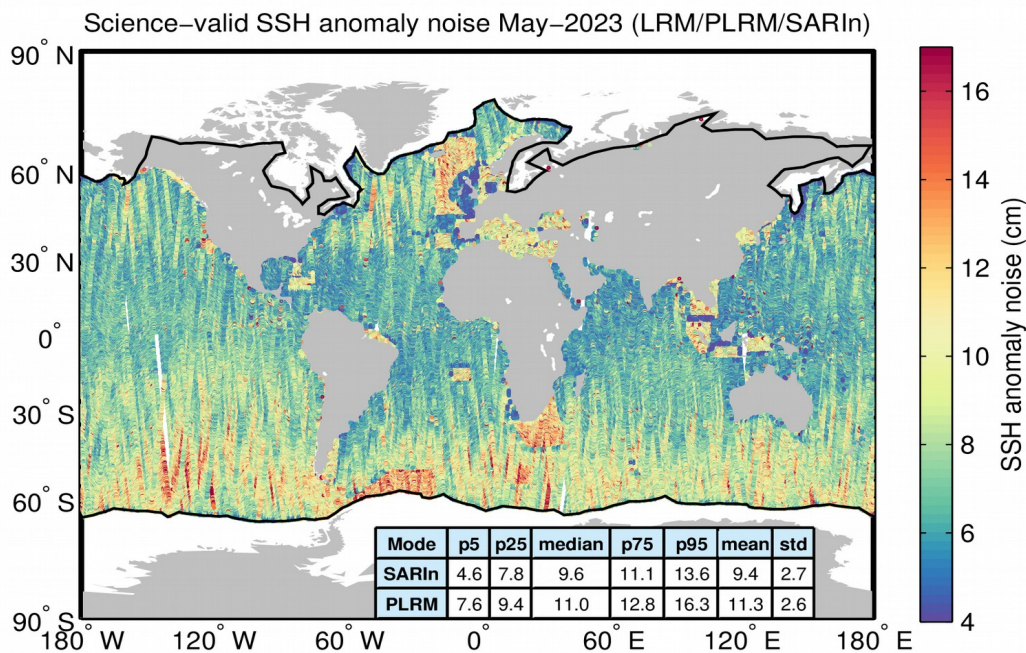


Figure 77. Geographical distribution of flag-valid 20-Hz SSH anomaly measurement noise over oceans and lakes for LRM/SAR/SARIn (top) and LRM/PLRM/SARIn (bottom) and for May 2023. The statistical values shown in the table refer to the SSH anomaly noise and are calculated separately for LRM, SAR/PLRM and SARIn regions. Measurements taken over polar polygons have been excluded from the computation of the statistical values. The black lines mark the outer limit of the Arctic and Antarctic polar polygons.

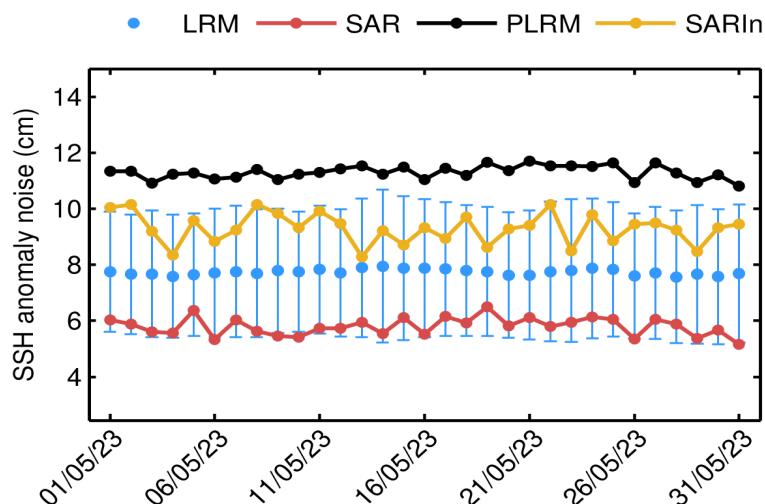


Figure 78. Mean science-valid GOP SSH anomaly noise for LRM (blue dot), SAR (red dot), PLRM (black dot) and SARIn (orange dot) for each day in May 2023. The corresponding standard deviation for LRM (blue error bar) is also shown.

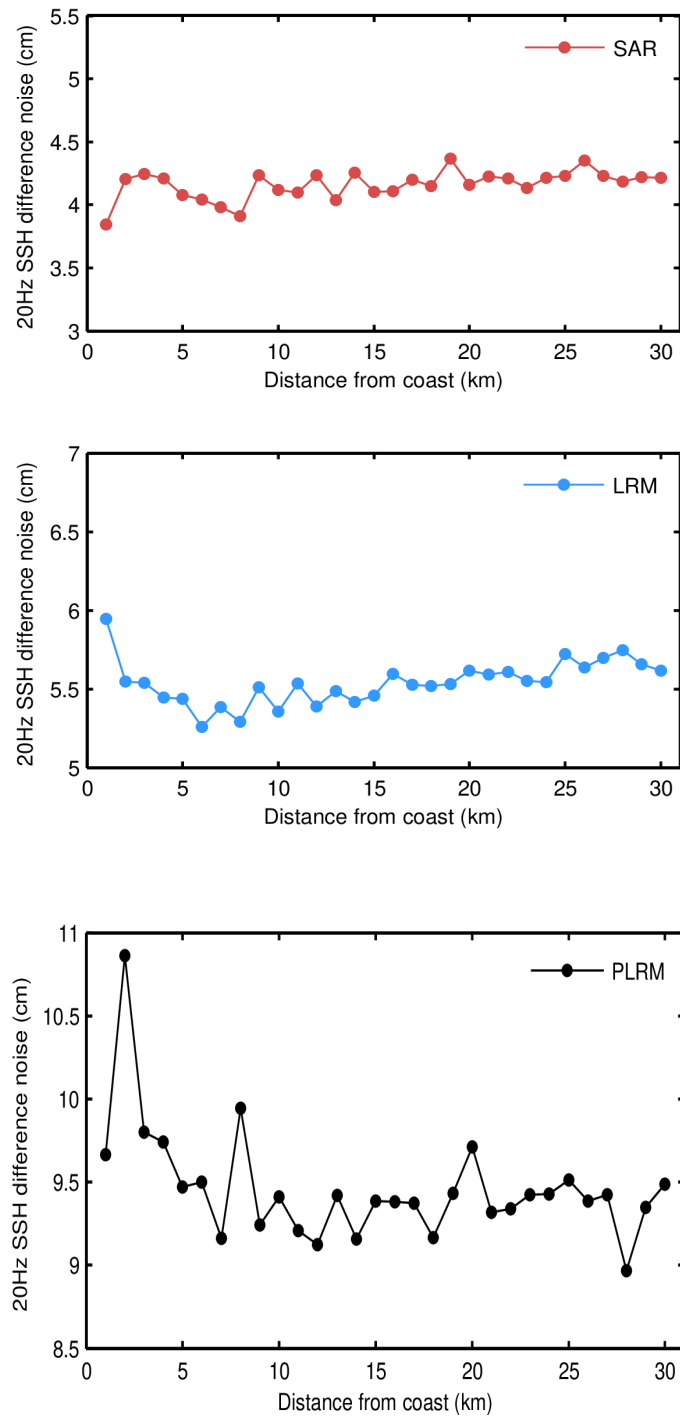
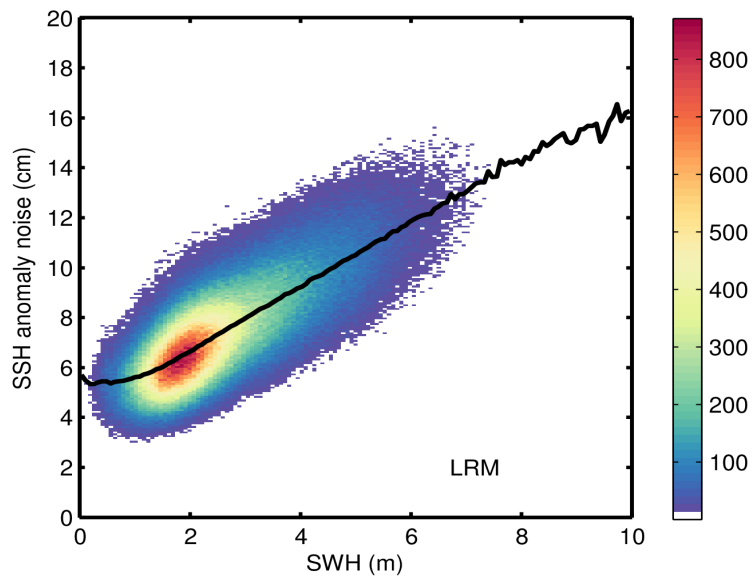
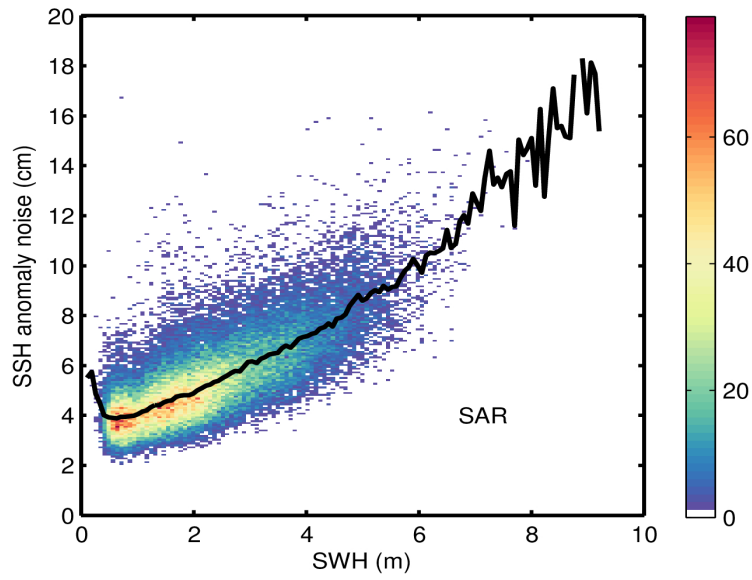


Figure 79. Science-valid GOP 20-Hz SSH anomaly noise as a function of distance from the coast for SAR (top panel), LRM (middle panel), and PLRM (bottom panel) for May 2023. Noise values have been calculated as the median of the absolute value of the difference between consecutive 20-Hz records.



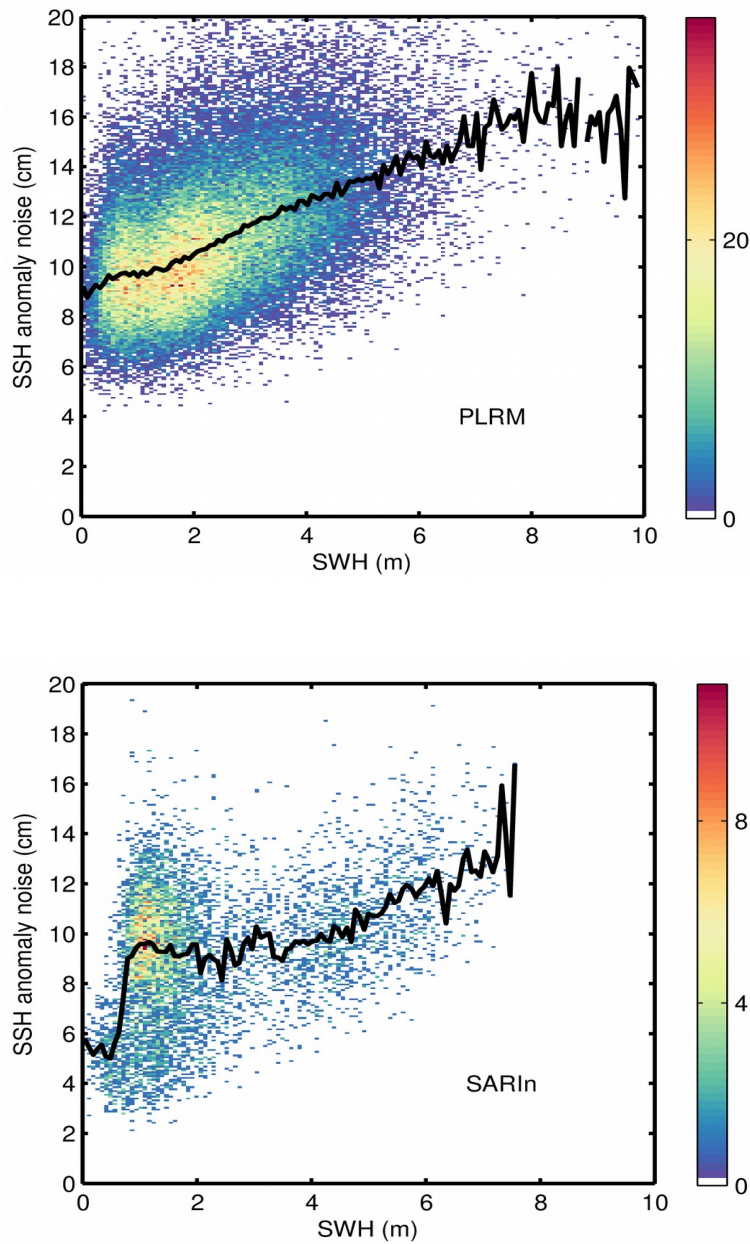


Figure 80. 2D histogram showing science-valid GOP SSH anomaly noise as a function of SWH for SAR, LRM, PLRM, and SARIn (from top to bottom) for May 2023. The black line denotes the median SSH anomaly noise as a function of SWH.

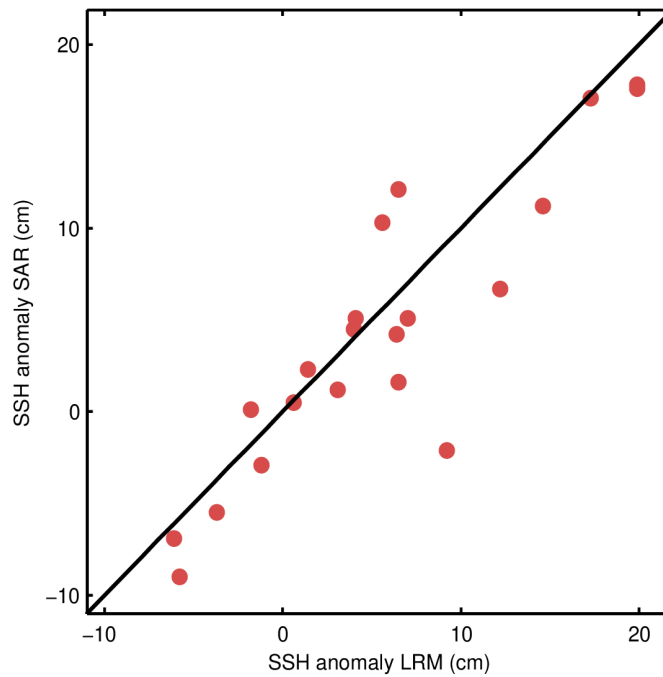


Figure 81. Scatter plot of the science-valid GOP SSH anomaly at the two nearest points outside (LRM, x-axis) and inside (SAR, y-axis) the Pacific SAR mode box for each pass. The RMS of the differences is 2.9 cm for the pairs shown in the figure as compared to a RMS of 4.4 cm for the differences between such outside points and their respective nearest neighbour also outside the box in the LRM region.

3.5. Crossover analysis

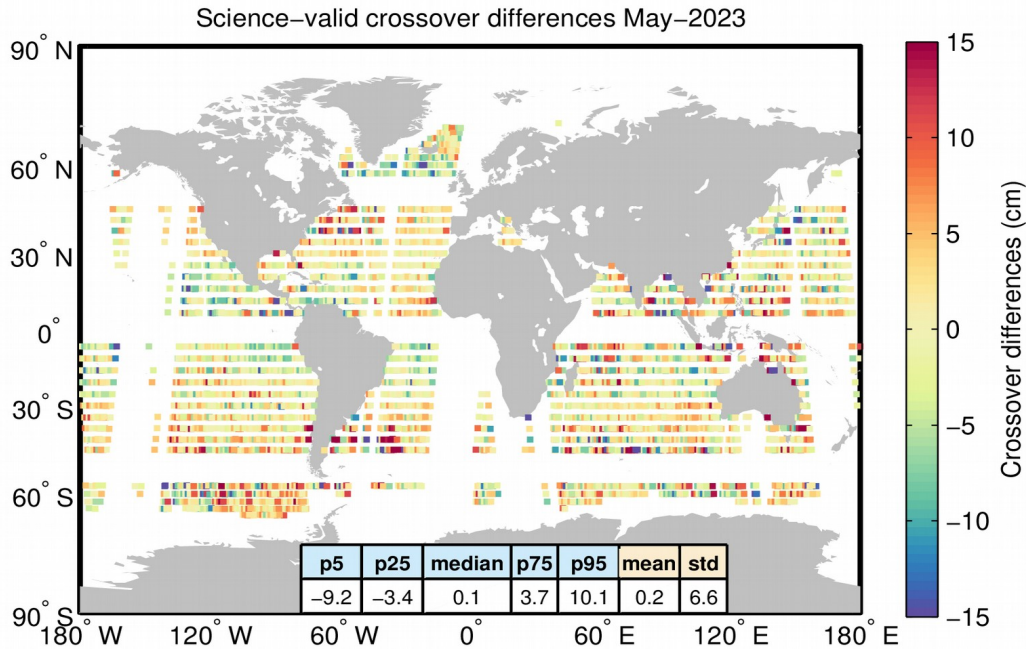


Figure 82. Crossover differences (absolute values) for the science-valid GOP SSH anomaly for May 2023. The difference at each crossover is computed as the difference between median values over 2-second windows centered about the crossover.

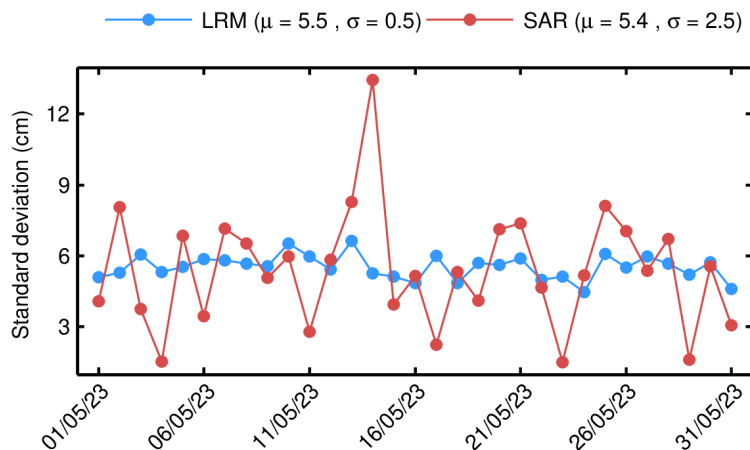


Figure 83. Standard deviation of differences at crossovers for GOP SSH anomaly for each day in May 2023. The values shown in this figure have been computed for the science-valid data further edited according to the following two additional criteria: 1) rejecting crossover differences larger than 20 cm; and 2) rejecting shallow waters (1000 m). The mean (μ) and standard deviation (σ) are also shown.

3.6. SWH coverage and validity

| Parameter | Min threshold | Max threshold | Percentage edited |
|--|---------------|---------------|-------------------|
| Flagged as bad | - | - | 1.1% |
| SWH | 0 m | 15 m | 0.0% |
| Standard deviation of SWH (1-Hz block) | 0 m | 1 m | 1.4% |
| All together | - | - | 1.4% |

Table 13. Editing criteria. The percentage of “flagged as bad” refers to records that have been flagged as bad by either the average status flag or the measurement confidence flag. Such percentage is computed only for records over oceans/lakes and outside polar regions. All other percentages refer to the percentage of flag-valid records that have been rejected by the corresponding criteria or by all criteria (“All together”).

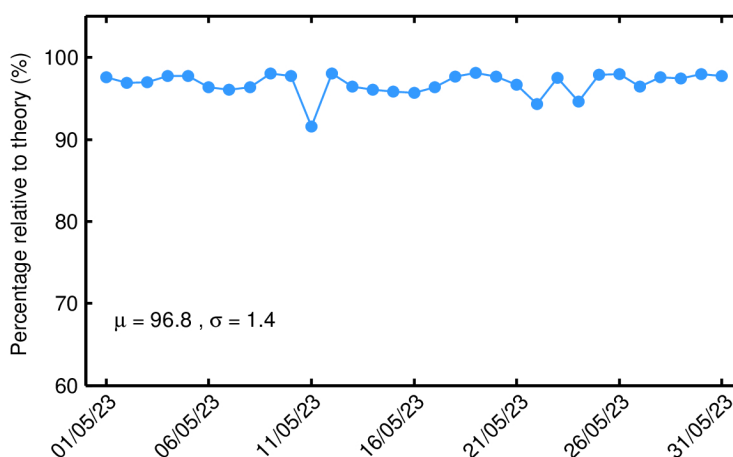


Figure 84. Percentage of science-valid GOP 1-Hz SWH records over ocean and lakes relative to theory for each day in May 2023. The mean (μ) and standard deviation (σ) are also shown.

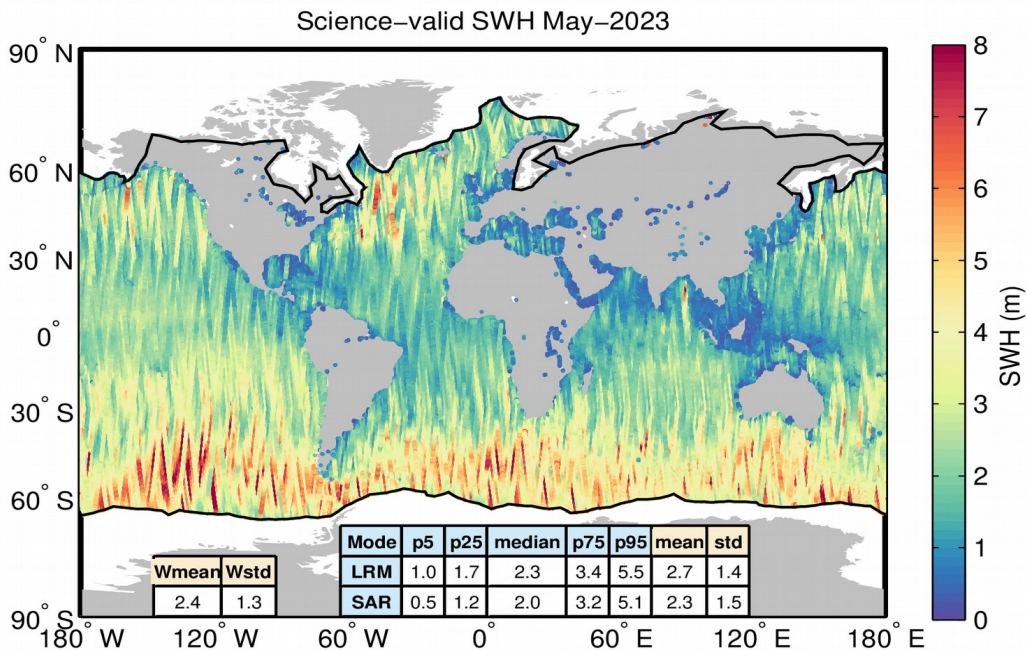


Figure 85. Geographical distribution of science-valid GOP SWH data over oceans and lakes for May 2023. The statistical values shown in the table refer to the SWH in m and are calculated separately for LRM and SAR regions. Wmean and Wstd denote the spatial area-weighted average and its standard deviation. Measurements taken over polar polygons have been excluded from the computation of the statistical values. The black lines mark the outer limit of the Arctic and Antarctic polar polygons.

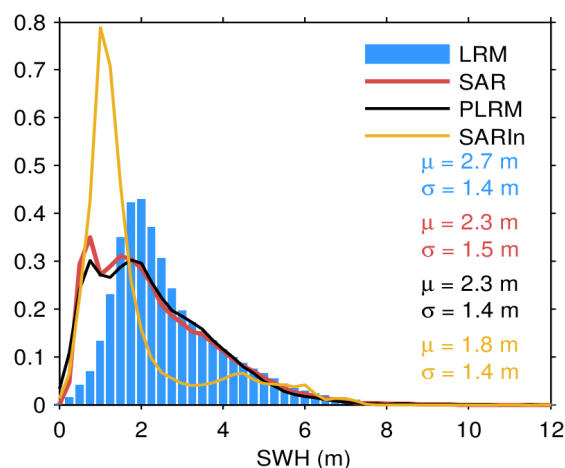


Figure 86. Histogram of science-valid GOP SWH over oceans and lakes for LRM (blue), SAR (red), PLRM (black) and SARIn (orange) and for May 2023. The mean (μ) and standard deviation (σ) are also shown. Values larger than 12 m are excluded from the histogram for the sake of readability but not from the computation of μ and σ .

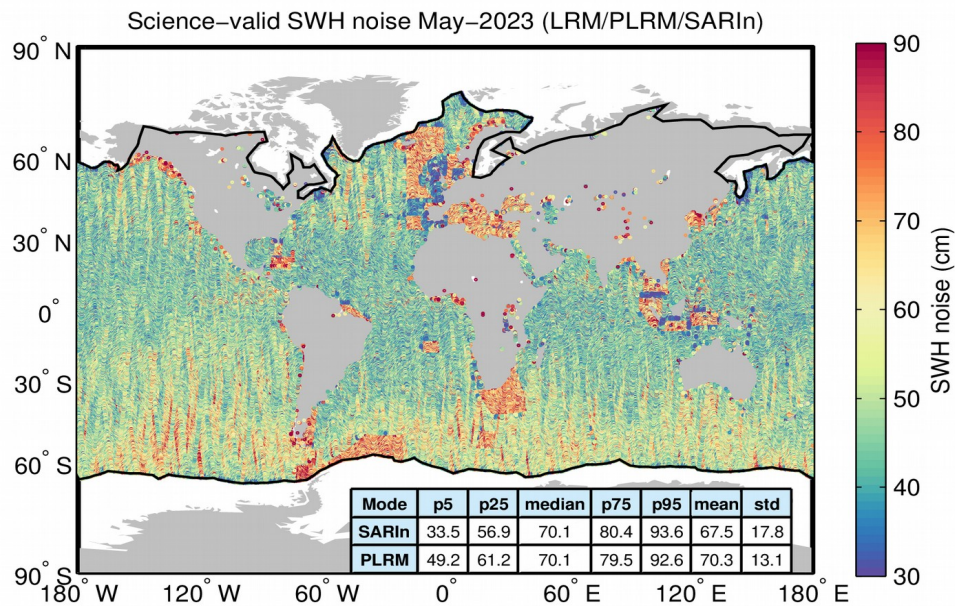
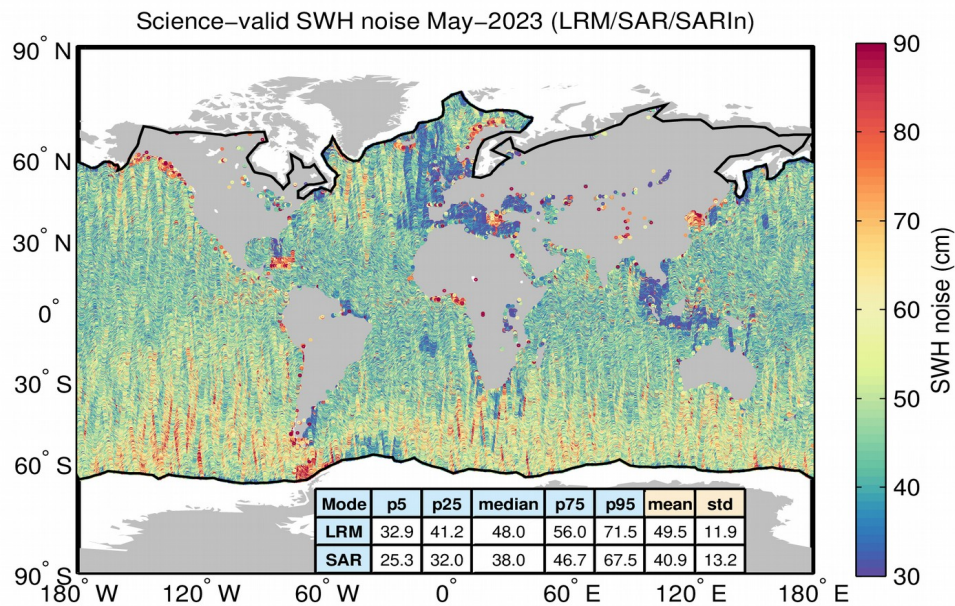


Figure 87. Geographical distribution of flag-valid 20-Hz SWH measurement noise over oceans and lakes for LRM/SAR/SARIn (top) and LRM/PLRM/SARIn (bottom) and for May 2023. The statistical values shown in the table refer to the SWH noise and are calculated separately for LRM, SAR/PLRM and SARIn regions. Measurements taken over polar polygons have been excluded from the computation of the statistical values. The black lines mark the outer limit of the Arctic and Antarctic polar polygons.

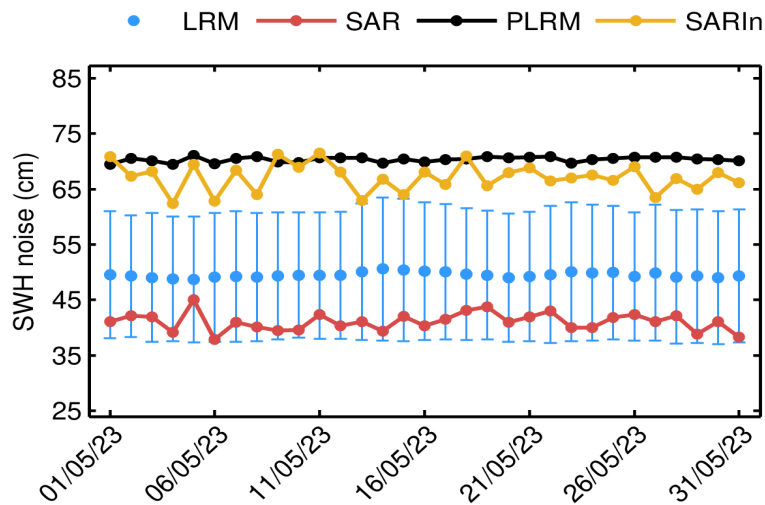
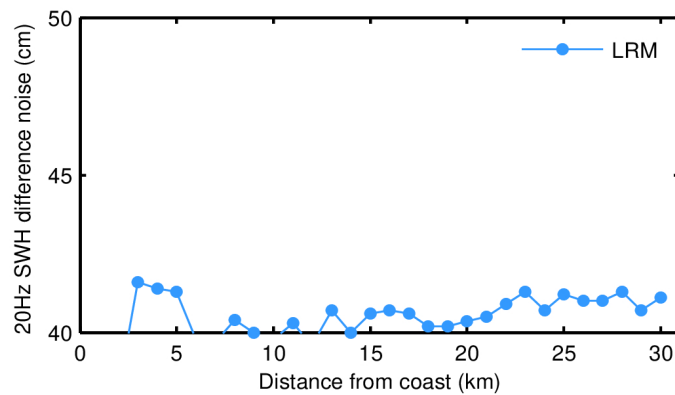
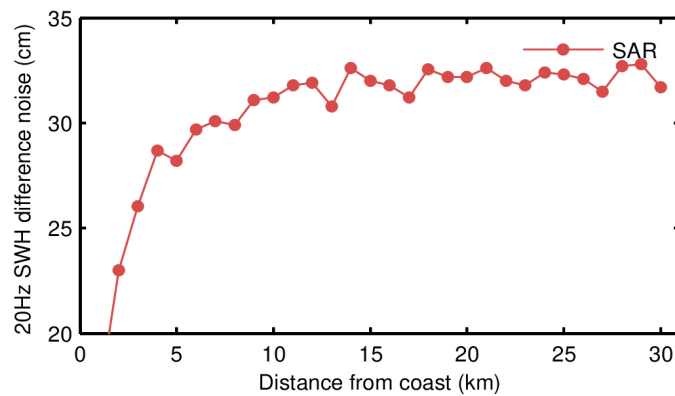


Figure 88. Mean science-valid GOP SWH noise for LRM (blue dot), SAR (red dot), PLRM (black dot) and SARIn (orange dot) for each day in May 2023. The corresponding standard deviation for LRM (blue error bar) is also shown.



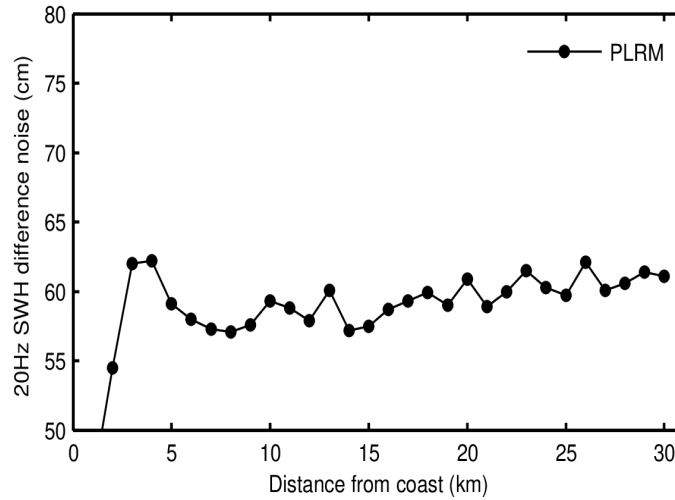


Figure 89. Science-valid GOP 20-Hz SWH noise as a function of distance from the coast for SAR (top panel), LRM (middle panel), and PLRM (bottom panel) for May 2023. Noise values have been calculated as the median of the absolute value of the difference between consecutive 20-Hz records.

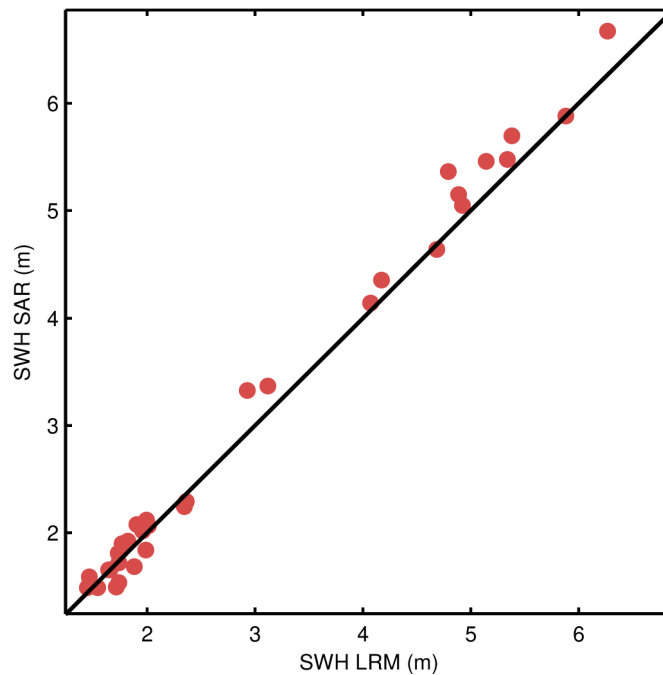


Figure 90. Scatter plot of the science-valid GOP SWH at the two nearest points outside (LRM, x-axis) and inside (SAR, y-axis) the Pacific SAR mode box for each pass. The RMS of the differences is 18.0 cm for the pairs shown in the figure as compared to a RMS of 15.8 cm for the differences between such outside points and their respective nearest neighbour also outside the box in the LRM region.

3.7. Sigma0 coverage and validity

| Parameter | Min threshold | Max threshold | Percentage edited |
|---|---------------|---------------|-------------------|
| Flagged as bad | - | - | 0.7% |
| Sigma0 | 7 dB | 30 dB | 0.2% |
| Standard deviation of Sigma0 (1-Hz block) | 0 dB | 0.23 dB | 4.4% |
| All together | - | - | 4.5% |

Table 14. Editing criteria. The percentage of “flagged as bad” refers to records that have been flagged as bad by either the average status flag or the measurement confidence flag. Such percentage is computed only for records over oceans/lakes and outside polar regions. All other percentages refer to the percentage of flag-valid records that have been rejected by the corresponding criteria or by all criteria (“All together”).

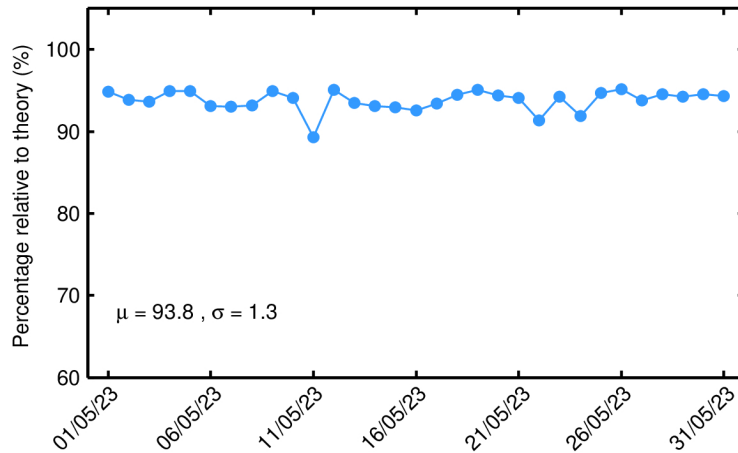


Figure 91. Percentage of science-valid GOP 1-Hz sigma0 records over ocean and lakes relative to theory for each day in May 2023. The mean (μ) and standard deviation (σ) are also shown.

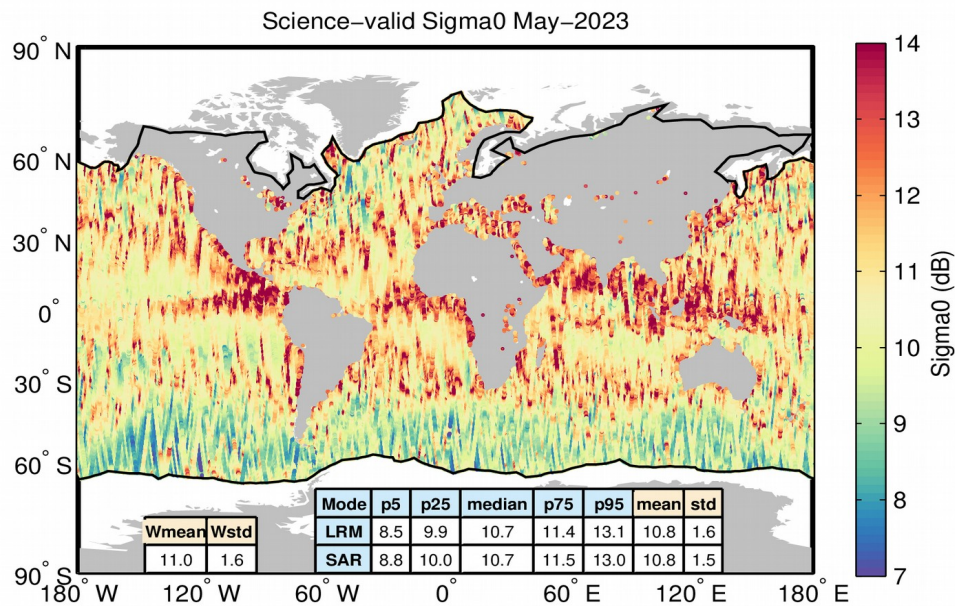


Figure 92. Geographical distribution of science-valid GOP sigma0 data over oceans and lakes for May 2023. The statistical values shown in the table refer to the sigma0 in m and are calculated separately for LRM and SAR regions. Wmean and Wstd denote the spatial area-weighted average and its standard deviation. Measurements taken over polar polygons have been excluded from the computation of the statistical values. The black lines mark the outer limit of the Arctic and Antarctic polar polygons.

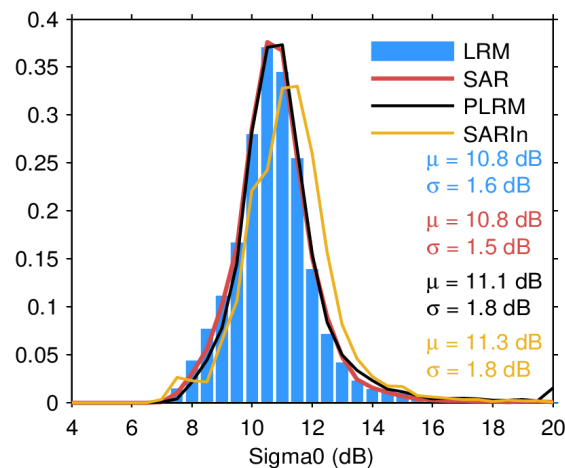


Figure 93. Histogram of science-valid GOP sigma0 over oceans and lakes for LRM (blue), SAR (red), PLRM (black) and SARIn (orange) and for May 2023. The mean (μ) and standard deviation (σ) are also shown. Values larger than 12 m are excluded from the histogram for the sake of readability but not from the computation of μ and σ .

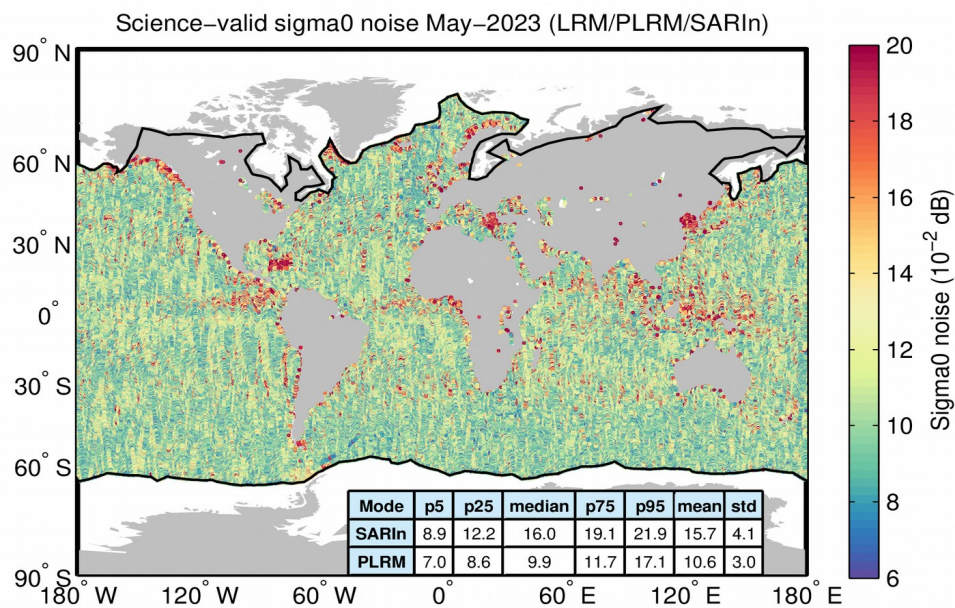
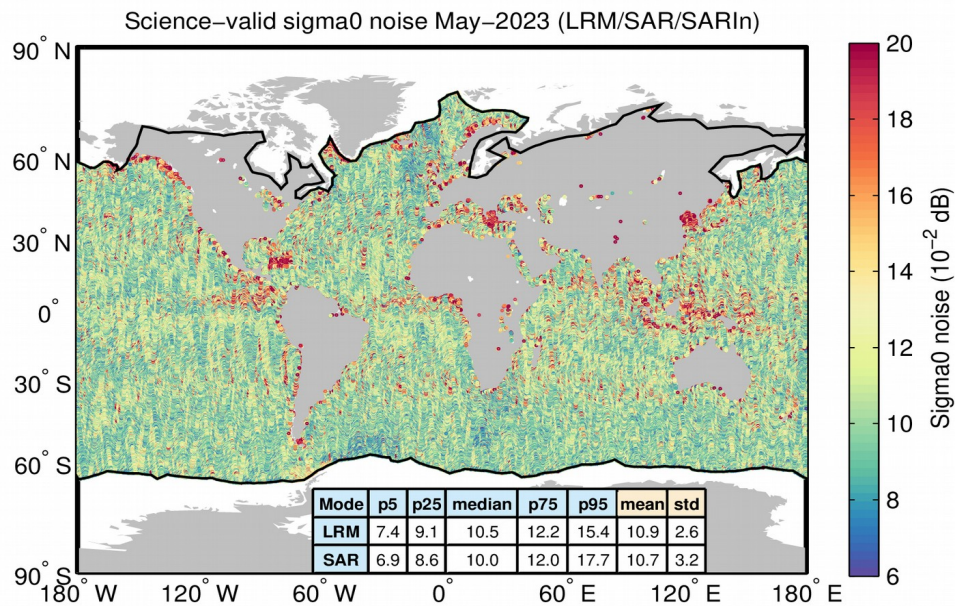


Figure 94. Geographical distribution of flag-valid 20-Hz sigma0 measurement noise over oceans and lakes for LRM/SAR/SARIn (top) and LRM/PLRM/SARIn (bottom) and for May 2023. The statistical values shown in the table refer to the sigma0 noise and are calculated separately for LRM, SAR/PLRM and SARIn regions. Measurements taken over polar polygons have been excluded from the computation of the statistical values. The black lines mark the outer limit of the Arctic and Antarctic polar polygons.

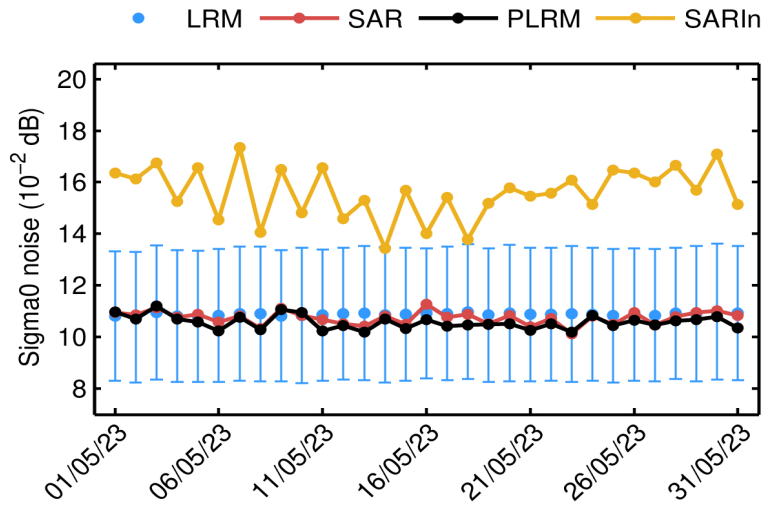
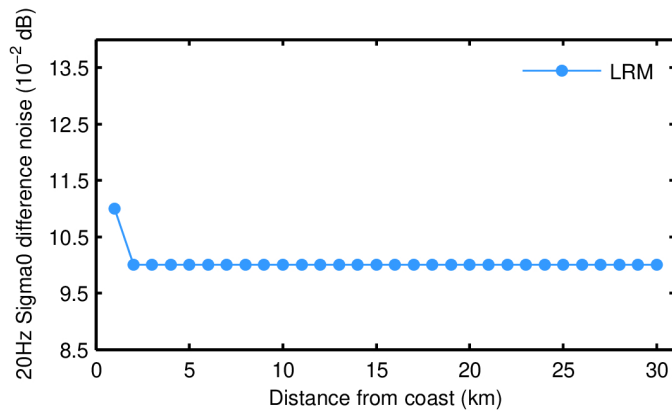
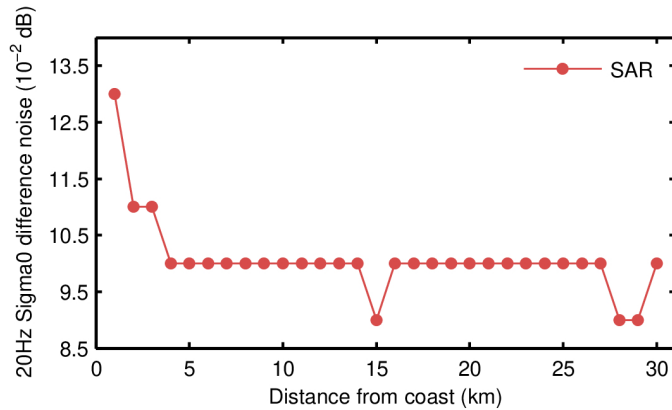


Figure 95. Mean science-valid GOP sigma0 noise for LRM (blue dot), SAR (red dot), PLRM (black dot) and SARIn (orange dot) for each day in May 2023. The corresponding standard deviation for LRM (blue error bar) is also shown.



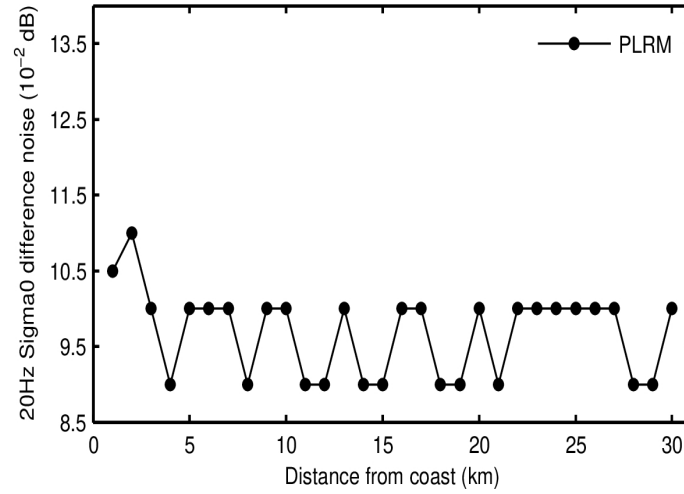


Figure 96. Science-valid GOP 20-Hz sigma0 noise as a function of distance from the coast for SAR (top panel), LRM (middle panel), and PLRM (bottom panel) for May 2023. Noise values have been calculated as the median of the absolute value of the difference between consecutive 20-Hz records.

3.8. Wind speed coverage and validity

| Parameter | Min threshold | Max threshold | Percentage edited |
|----------------------|---------------|---------------|-------------------|
| Flagged as bad | - | - | 0.7% |
| Altimeter wind speed | 0 m/s | 30 m/s | 0.0% |

Table 15. Editing criteria. The percentage of “flagged as bad” refers to records that have been flagged as bad by either the average status flag or the measurement confidence flag. Such percentage is computed only for records over oceans/lakes and outside polar regions. All other percentages refer to the percentage of flag-valid records that have been rejected by the corresponding criteria.

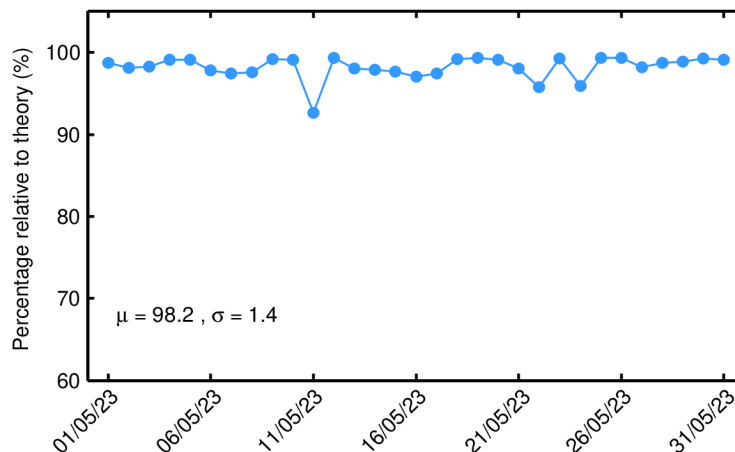


Figure 97. Percentage of science-valid GOP 1-Hz wind records over ocean and lakes relative to theory for each day in May 2023. The mean (μ) and standard deviation (σ) are also shown.

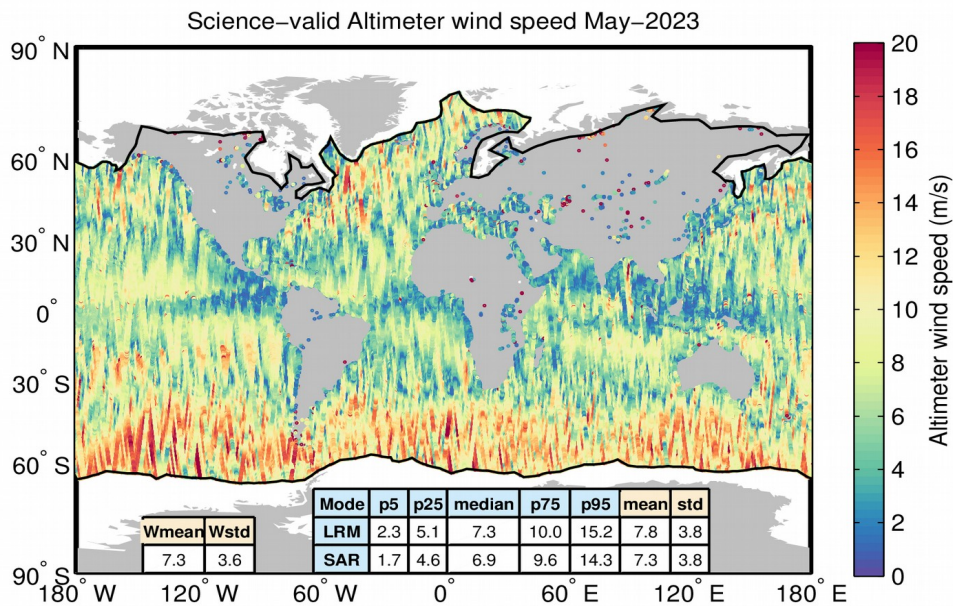


Figure 98. Geographical distribution of science-valid GOP wind data over oceans and lakes for May 2023. The statistical values shown in the table refer to the wind in m and are calculated separately for LRM and SAR regions. Wmean and Wstd denote the spatial area-weighted average and its standard deviation. Measurements taken over polar polygons have been excluded from the computation of the statistical values. The black lines mark the outer limit of the Arctic and Antarctic polar polygons.

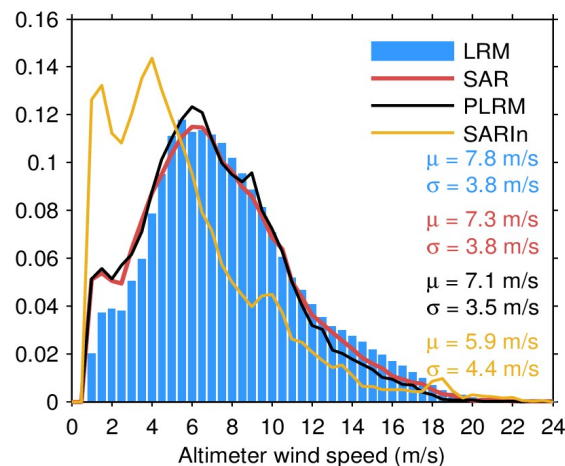


Figure 99. Histogram of science-valid GOP wind over oceans and lakes for LRM (blue), SAR (red), PLRM (black) and SARIn (orange) and for May 2023. The mean (μ) and standard deviation (σ) are also shown. Values larger than 12 m are excluded from the histogram for the sake of readability but not from the computation of μ and σ .

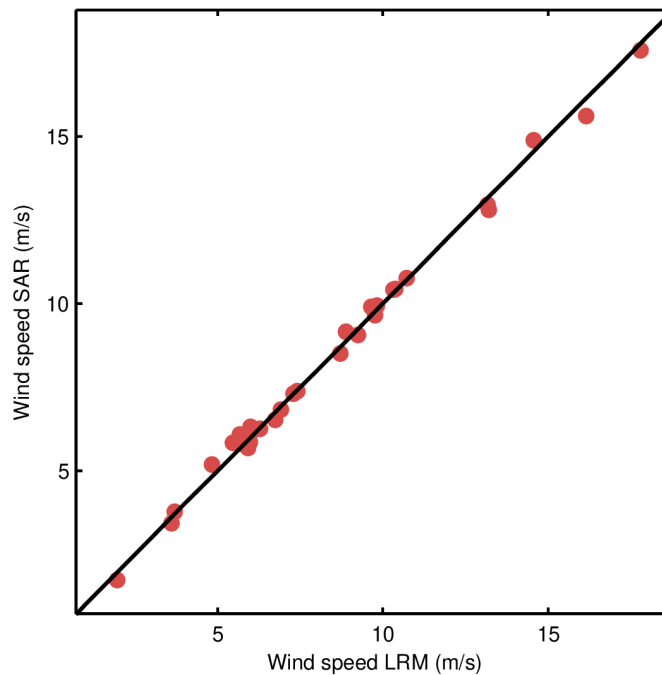


Figure 100. Scatter plot of the science-valid GOP wind speed at the two nearest points outside (LRM, x-axis) and inside (SAR, y-axis) the Pacific SAR mode box for each pass. The RMS of the differences is 23.3 cm/s for the pairs shown in the figure as compared to a RMS of 21.6 cm/s for the differences between such outside points and their respective nearest neighbour also outside the box in the LRM region.

3.9. Mispointing coverage and validity

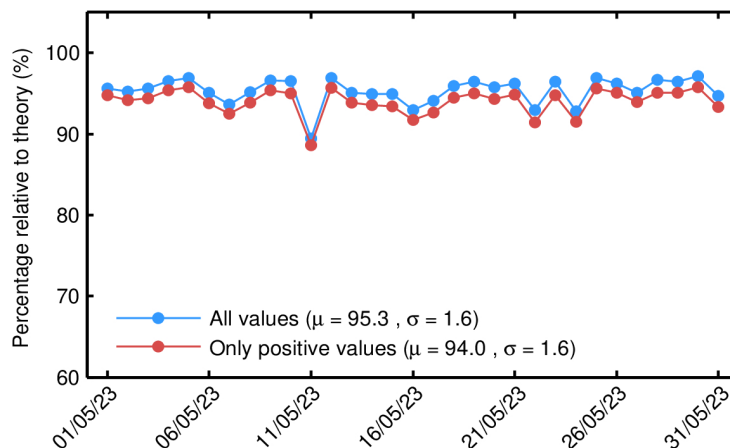


Figure 101. Percentage of science-valid GOP 1-Hz mispointing records over ocean and lakes relative to theory for each day in May 2023. The mean (μ) and standard deviation (σ) are also shown.

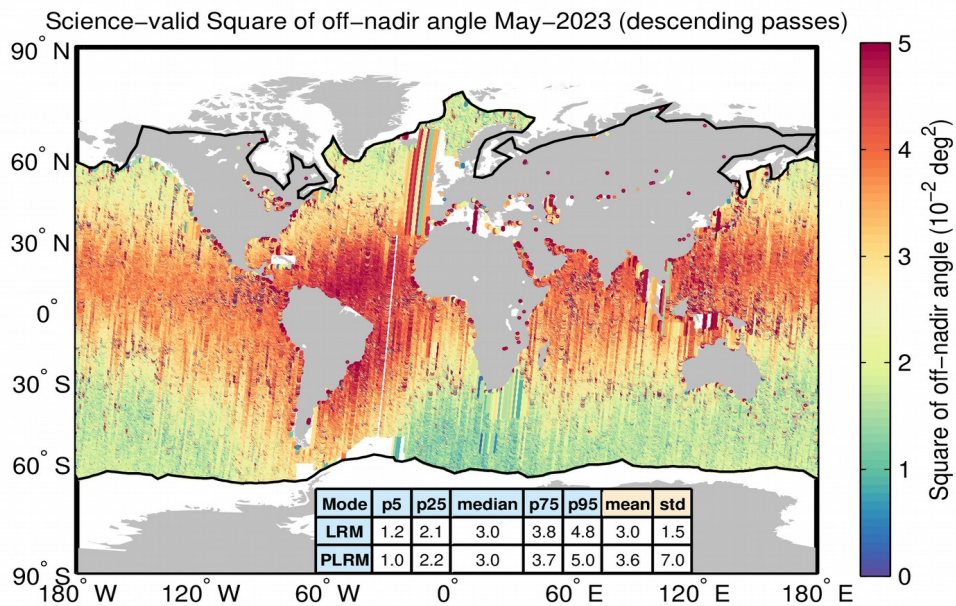
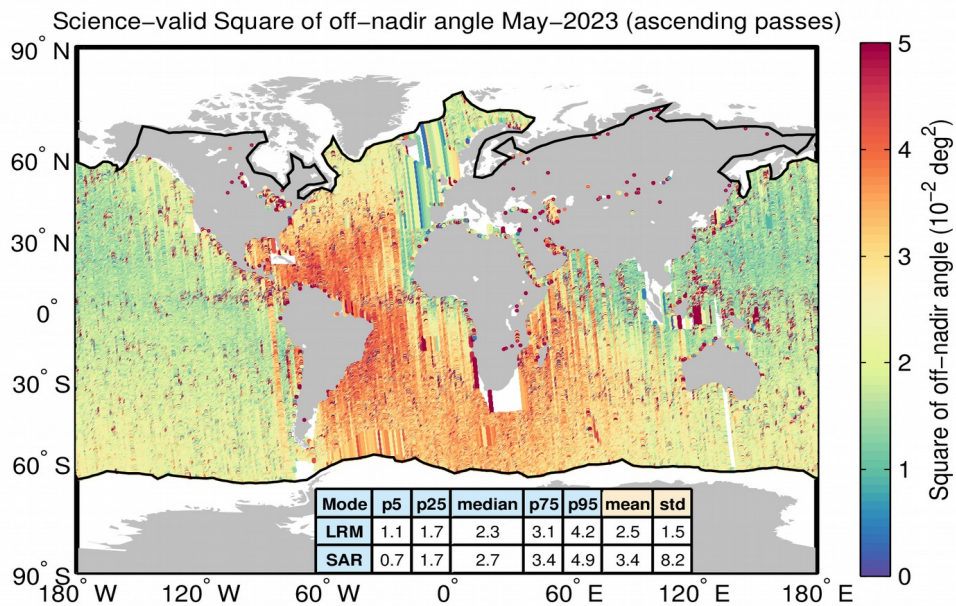


Figure 102. Geographical distribution of science-valid GOP mispointing data over oceans and lakes for ascending (top) and descending (bottom) passes for May 2023. The statistical values shown in the table refer to the wind in m and are calculated separately for LRM and SAR regions. Measurements taken over polar polygons have been excluded from the computation of the statistical values. The black lines mark the outer limit of the Arctic and Antarctic polar polygons.

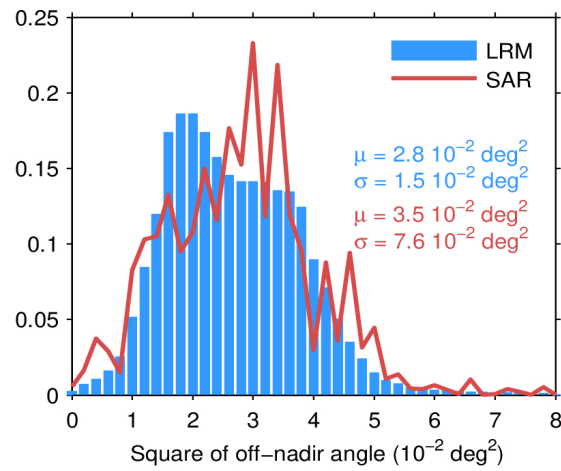


Figure 103. Histogram of science-valid GOP mispointing over oceans and lakes for LRM (blue) and SAR (red) for May 2023. The mean (μ) and standard deviation (σ) are also shown. Note that values larger than 12 m are excluded from the histogram for the sake of readability but not from the computation of μ and σ .

4 GOP validation

4.1. Validation against in situ measurements and models

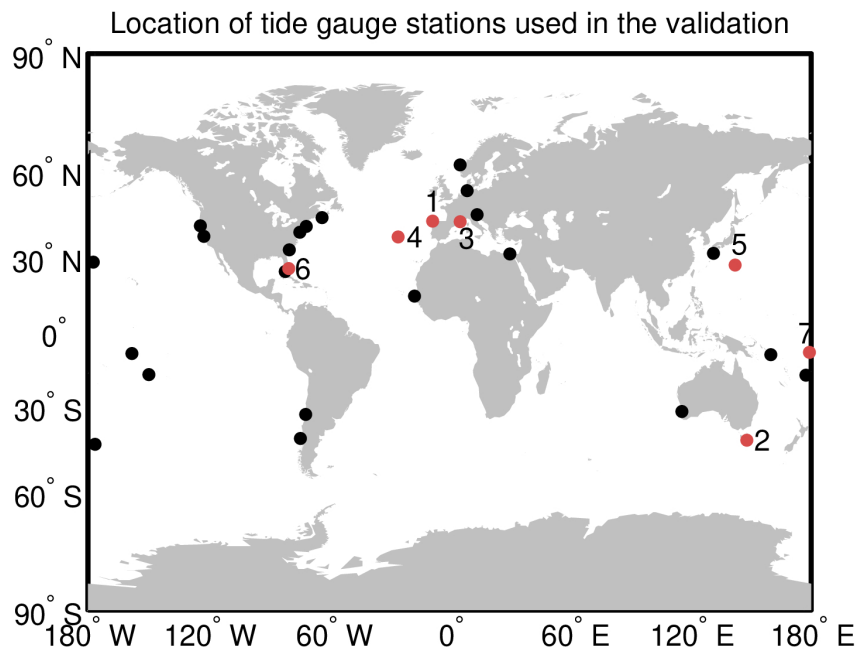


Figure 104. Location of the tide gauge stations used in the validation of GOP SSH. Red dots denote stations that have good ties with a nearby GPS stations and have been used in the absolute validation (numbers are used as labels to identify such tide gauges).

4.1.1. Absolute validation of GOP SSH against selected tide gauges

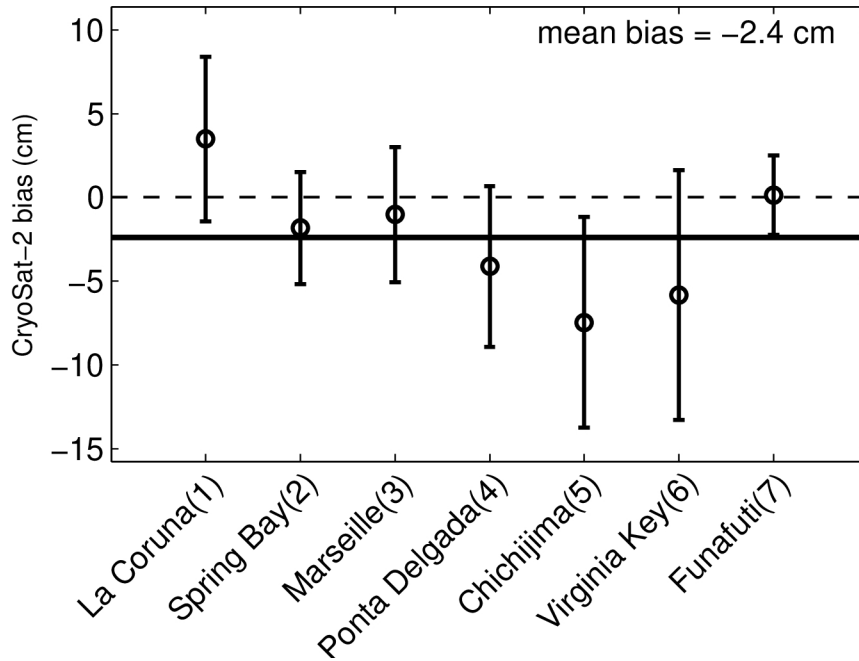


Figure 105. Mean difference in cm between the GOP SSH from CryoSat-2 and the ellipsoidal heights at 9 tide gauge stations (La Coruña, Spring Bay, Marseille, Ponta Delgada, Chichijima, Virginia Key, and Funafuti) over the period April 2014 to May 2023. The numbers correspond to those used in Figure 104 to identify the tide gauge stations.

4.1.2. Validation of GOP SSH anomaly against tide gauges

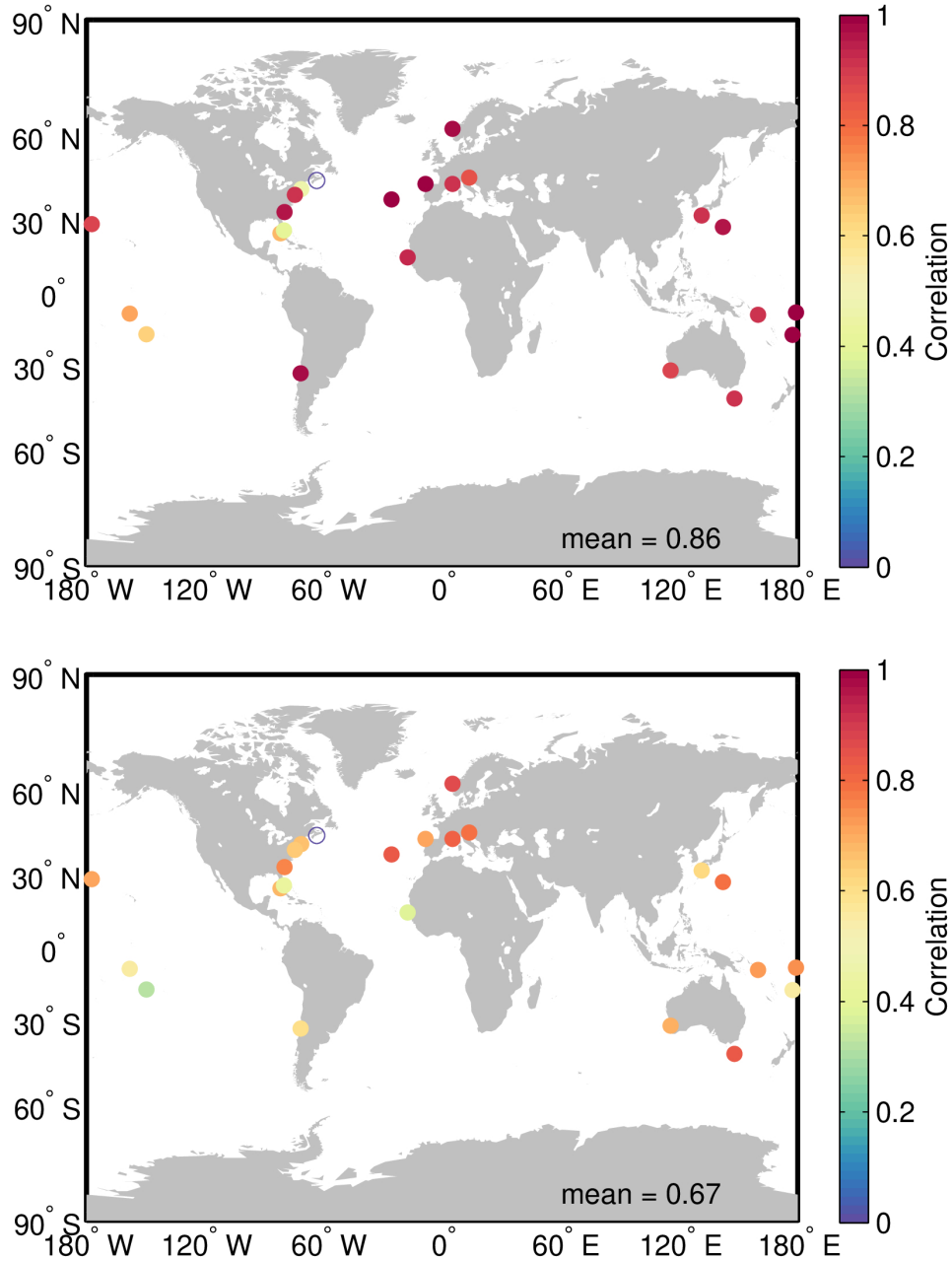


Figure 106. Map showing the correlation between the GOP SSH anomaly and the sea level from tide gauge records over the period June 2021 to May 2023 for the cases with (top) and without (bottom) the tidal component. For this comparison the atmospheric component has not been subtracted. Empty dots denote statistically non-significant correlation.

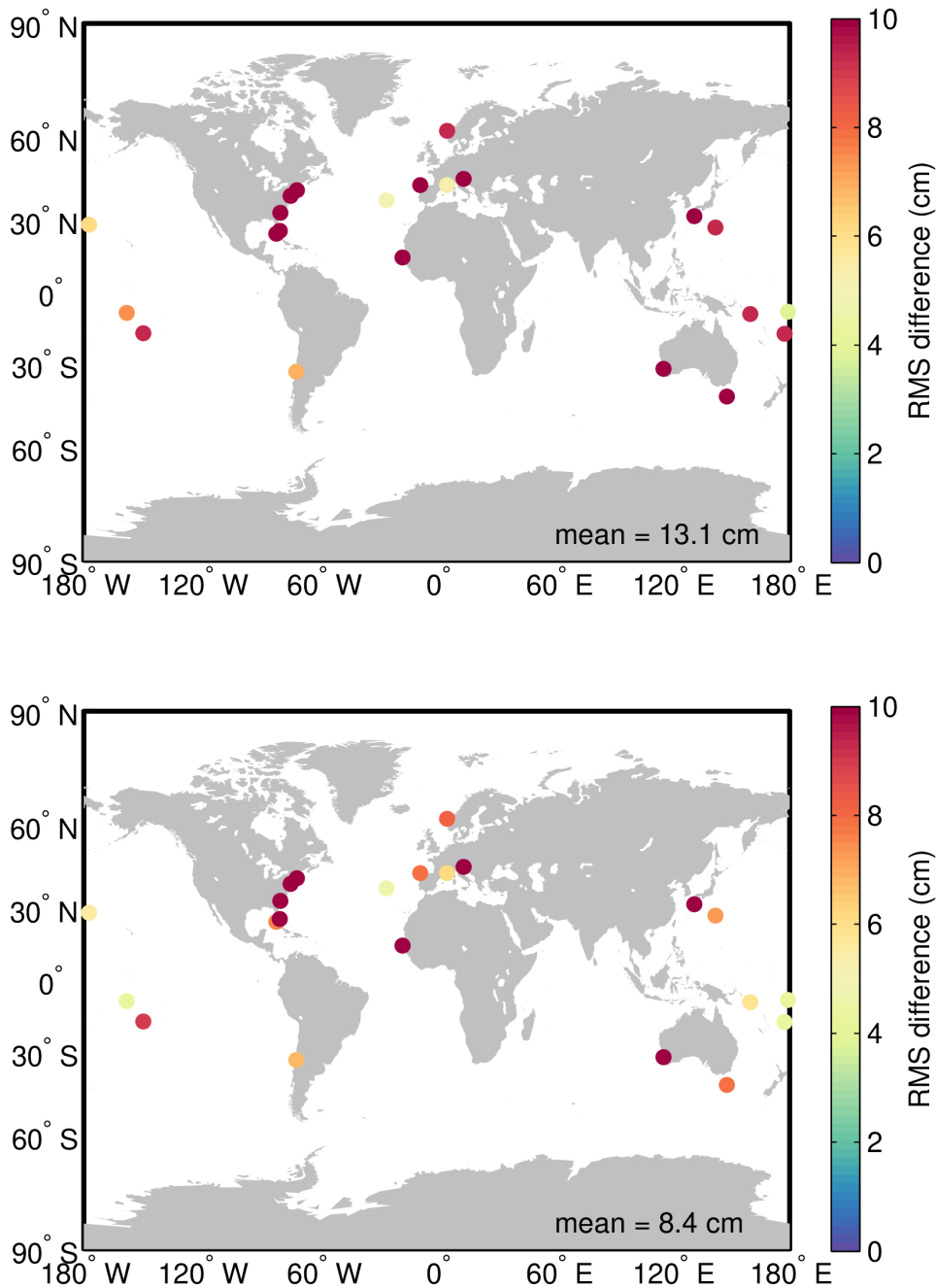


Figure 107. Map showing the RMS difference between the GOP SSH anomaly and the sea level from tide gauge records over the period June 2021 to May 2023 for the cases with (top) and without (bottom) the tidal component. For this comparison the atmospheric component has not been subtracted.

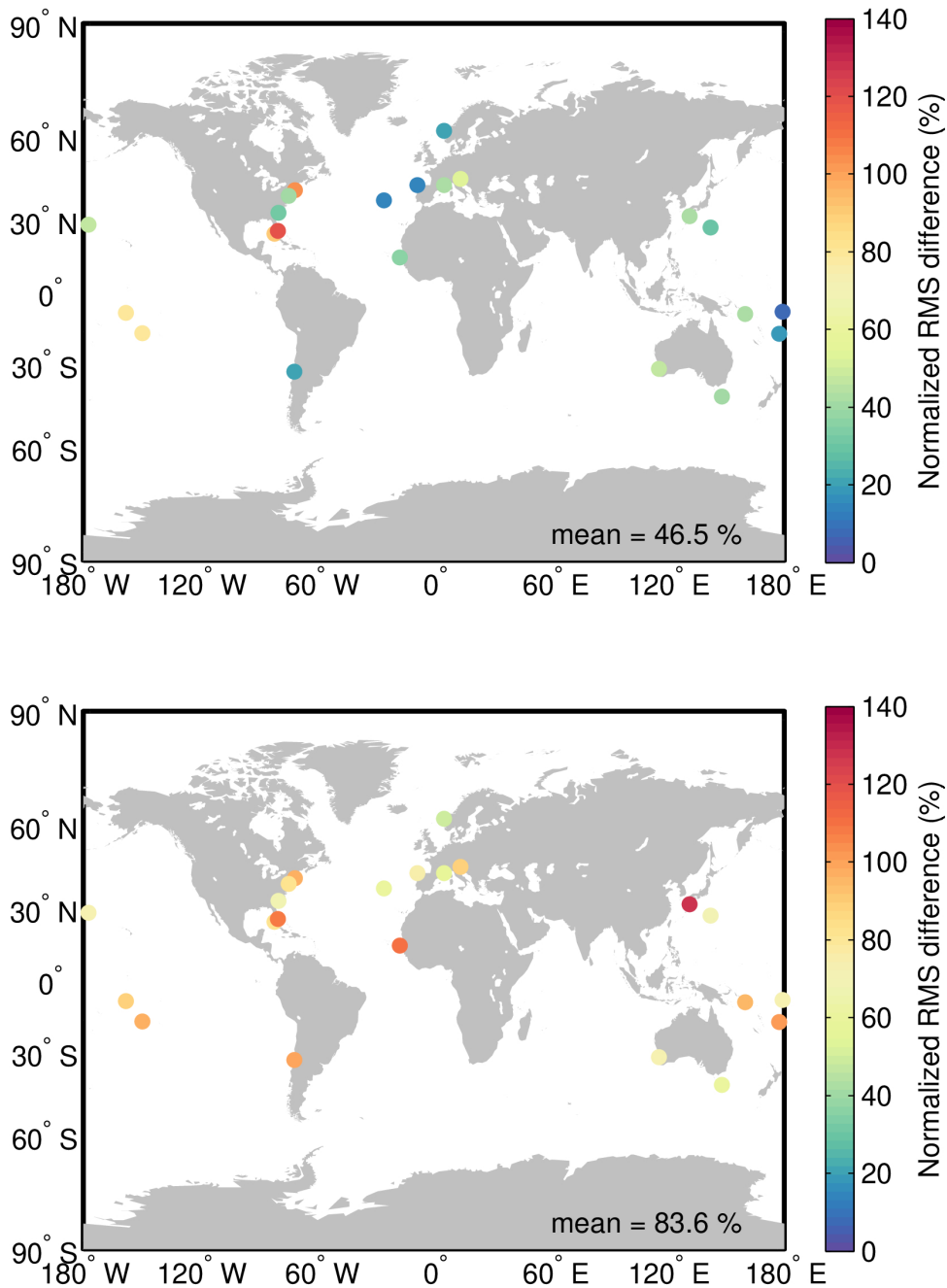


Figure 108. Map showing the normalized RMS difference (i.e., the RMS divided by the standard deviation of the tide gauge record) between the GOP SSH anomaly and the sea level from tide gauge records over the period June 2021 to May 2023 for the cases with (top) and without (bottom) the tidal component. For this comparison the atmospheric component has not been subtracted.

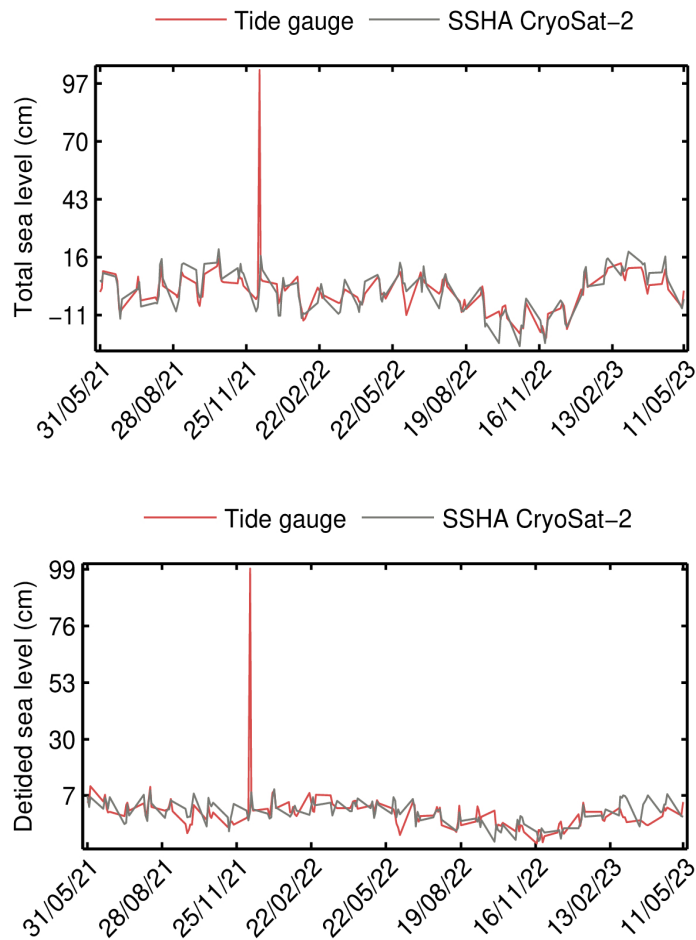
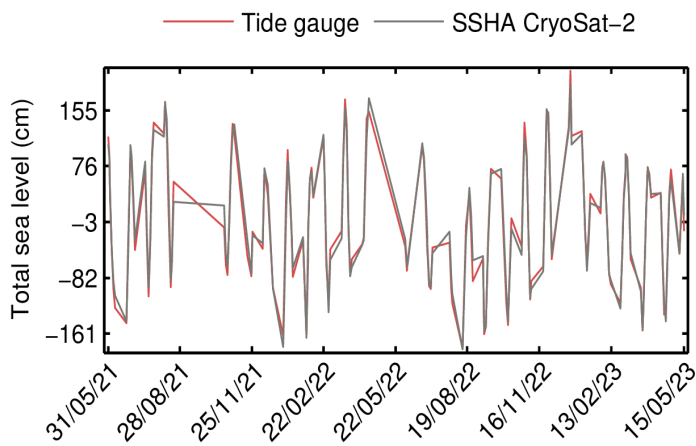


Figure 109. Comparison of the GOP SSH anomaly and the sea level at the Papeete tide gauge for the cases with (top) and without (bottom) the tidal component. For this comparison the atmospheric component has not been subtracted



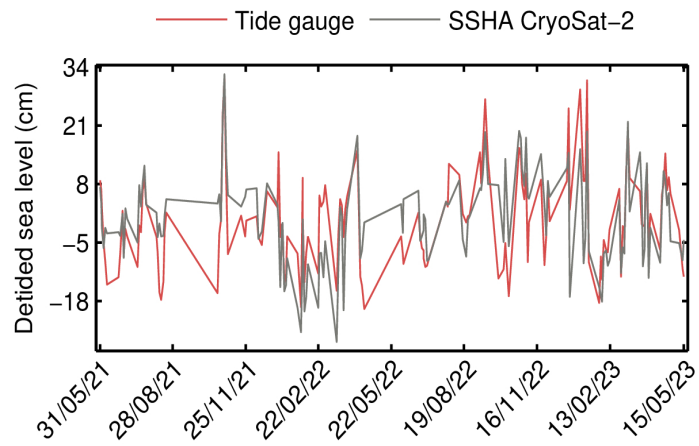


Figure 110. Comparison of the GOP SSH anomaly and the sea level at the La Coruña tide gauge for the cases with (top) and without (bottom) the tidal component. For this comparison the atmospheric component has not been subtracted

4.1.3. Validation of GOP SWH and wind speed against buoy data

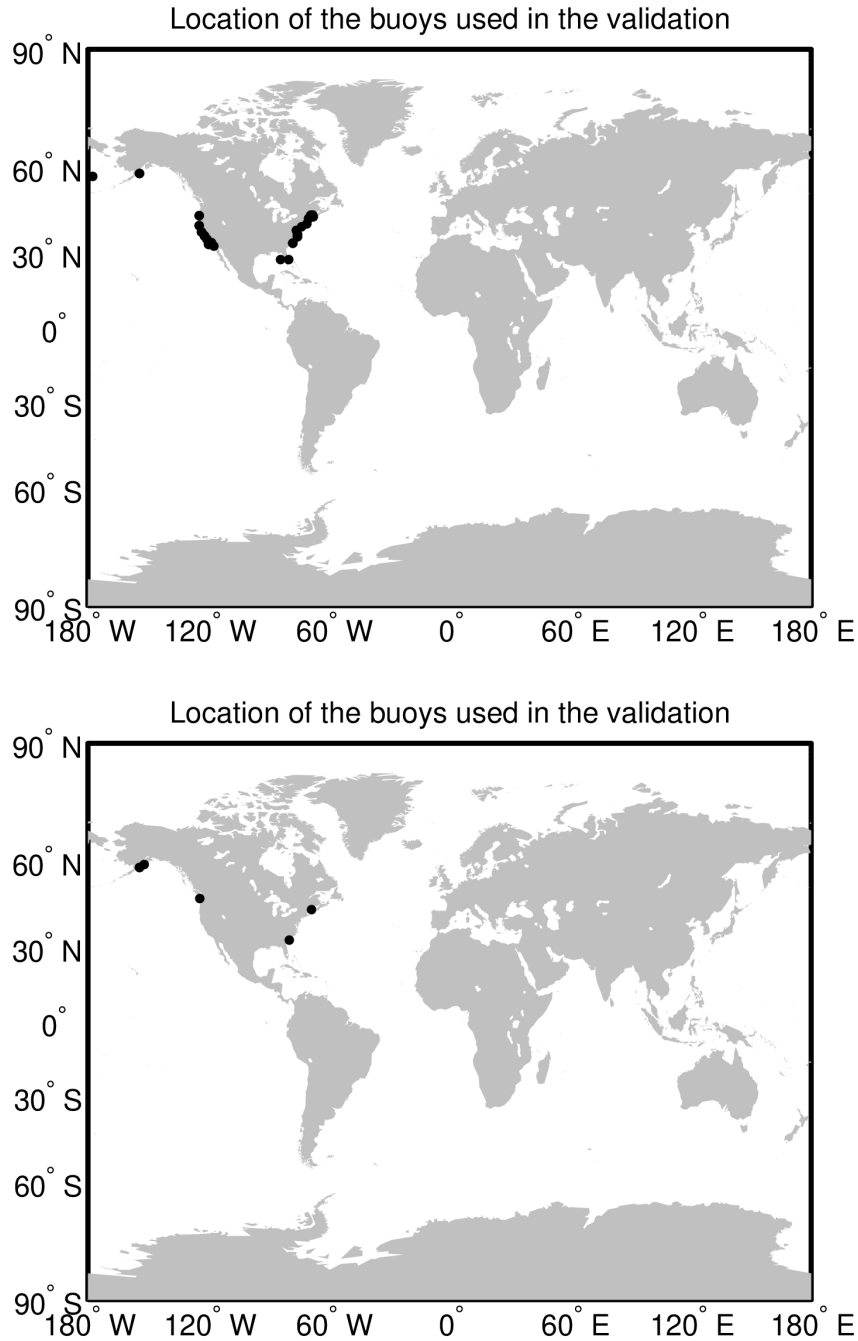


Figure 111. Location of the buoys used in the validation of GOP SWH (top) and wind speed (bottom).

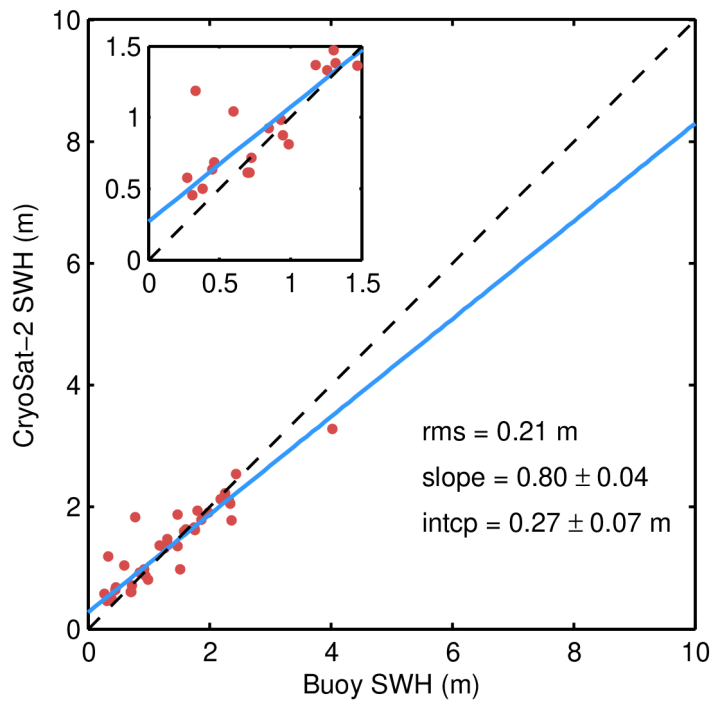


Figure 112. Scatter plot showing a comparison of GOP SWH with SWH from NDBC buoy data for May 2023. The inset plot shows a zoomed-in for SWH < 1.5 m.

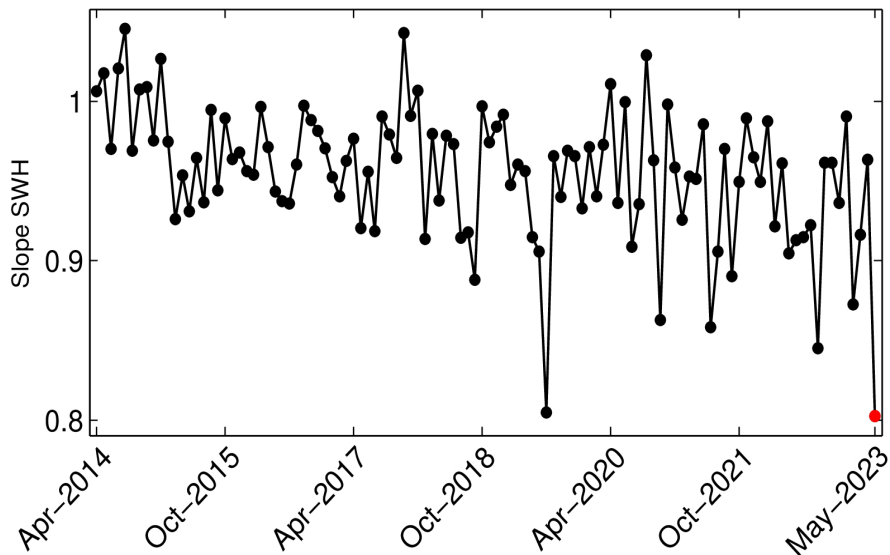


Figure 113. Regression slope of GOP SWH on SWH from NDBC buoy data over time. The red dot highlights the value for the month analysed in this report.

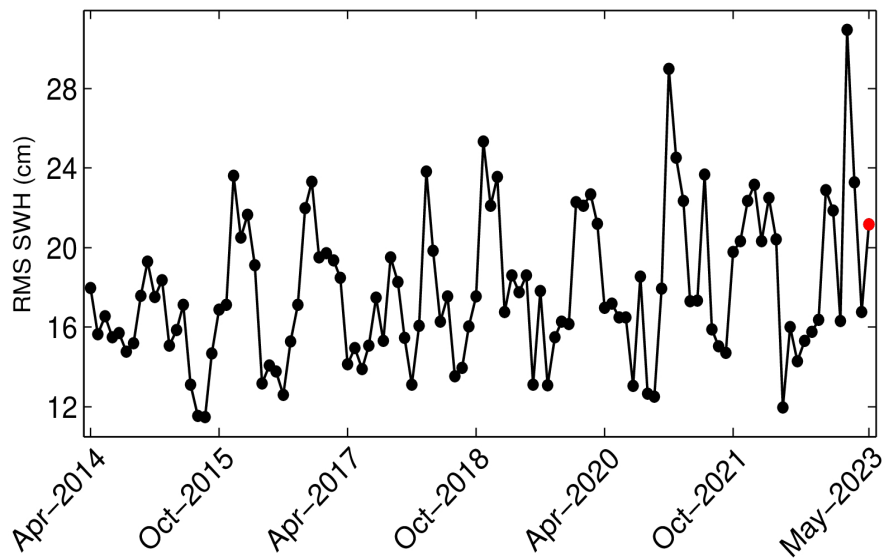


Figure 114. RMS difference between GOP SWH and SWH from NDBC buoy data over time. The red dot highlights the value for the month analysed in this report.

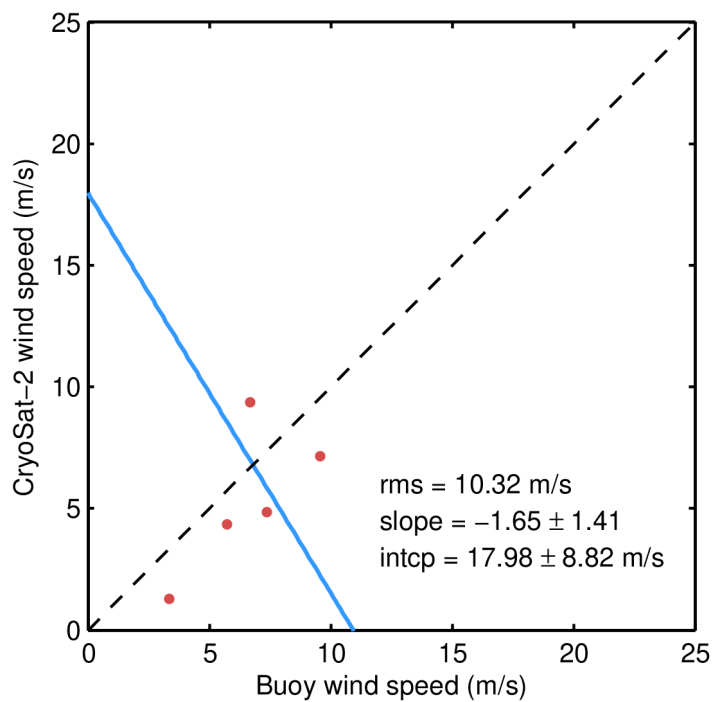


Figure 115. Scatter plot showing a comparison of GOP wind speed with wind speed from NDBC buoy data for May 2023.

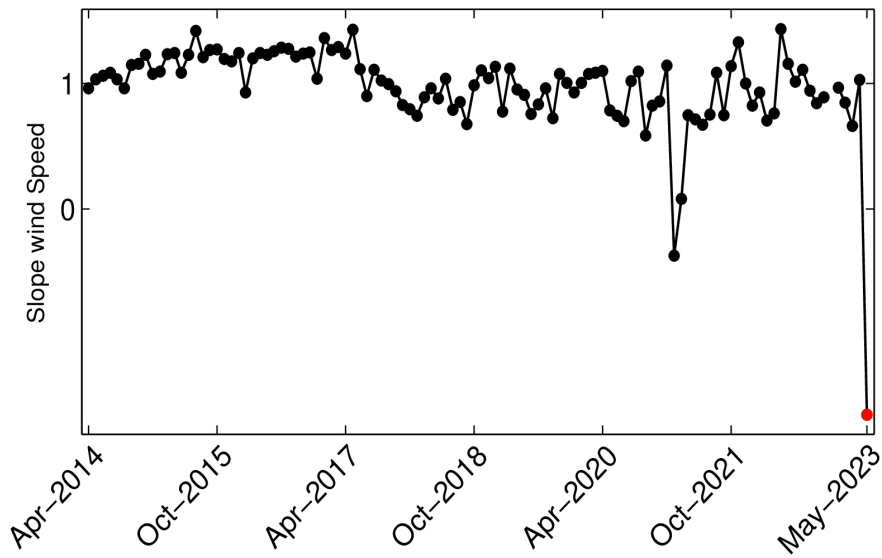


Figure 116. Regression slope of GOP wind speed on wind speed from NDBC buoy data over time. The red dot highlights the value for the month analysed in this report.

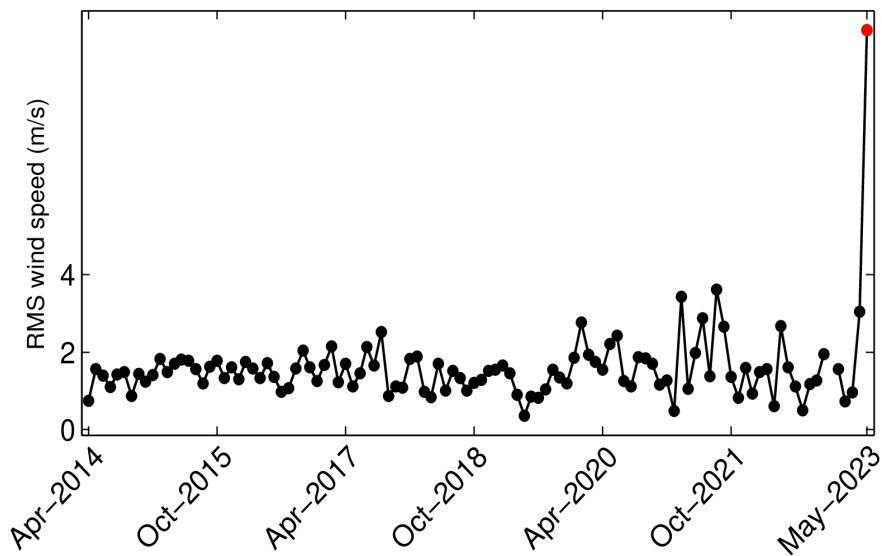


Figure 117. RMS difference between GOP wind speed and wind speed from NDBC buoy data over time. The red dot highlights the value for the month analysed in this report.

4.1.4. Validation of GOP SWH against Wavewatch III model data

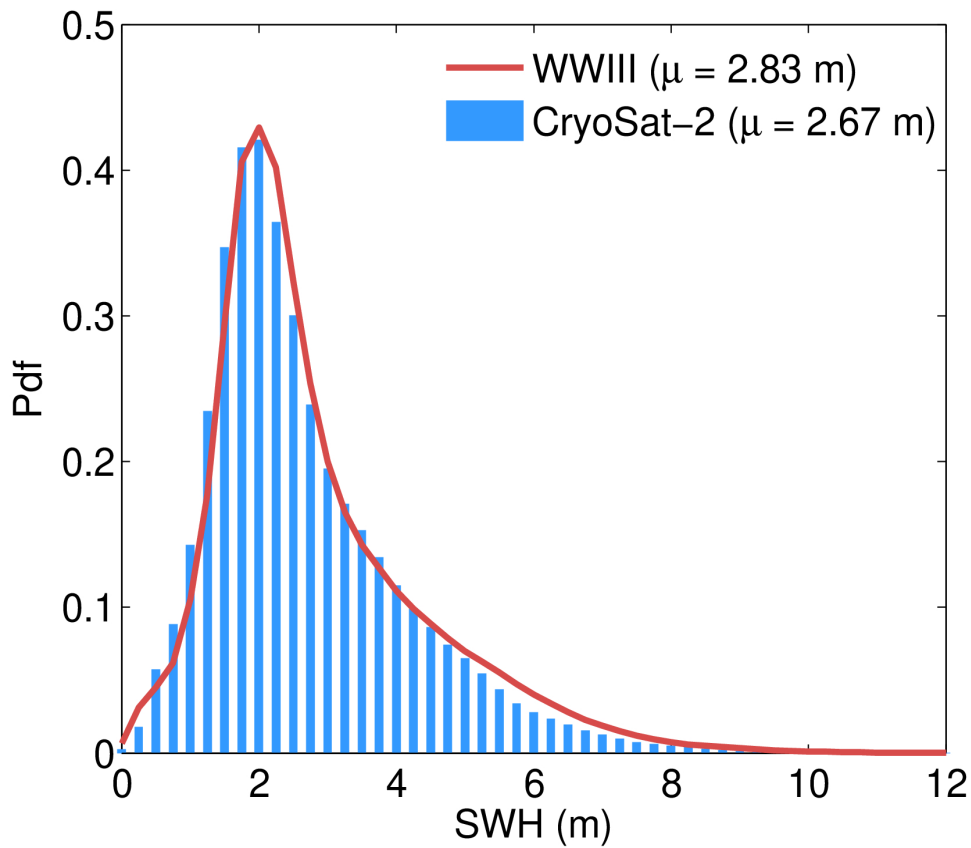


Figure 118. Histograms (normalized to have a total area of 1) of the GOP SWH (blue bars) and the SWH from the Wavewatch III model (red line) for May 2023.

4.1.5. Validation of GOP derived geostrophic velocities

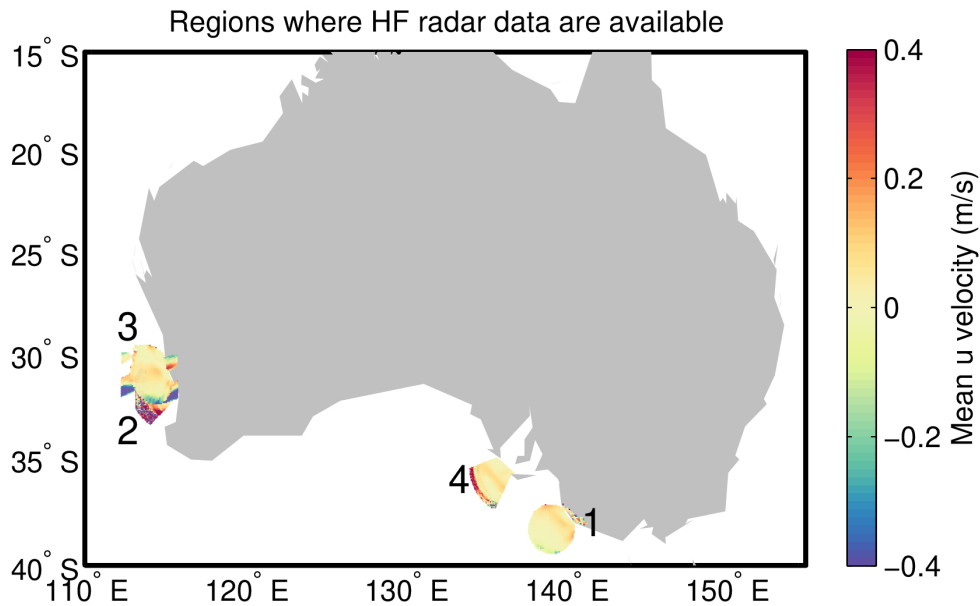


Figure 119. Map showing the regions in Australia where HF radar velocities are available and thus where the validation of GOP geostrophic velocities is performed. Each region is identified by a number.

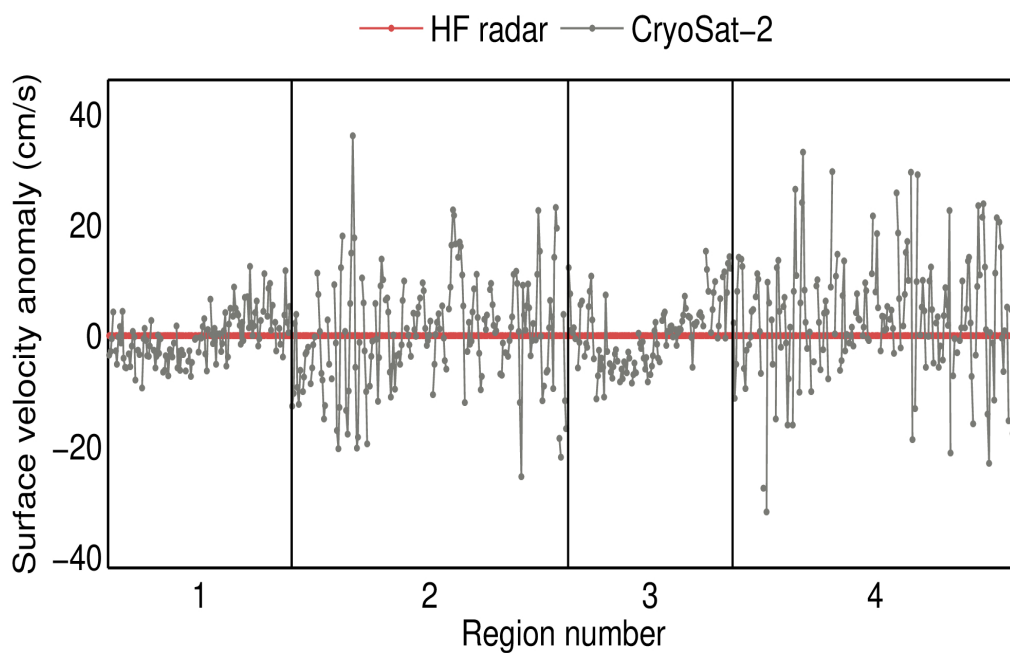
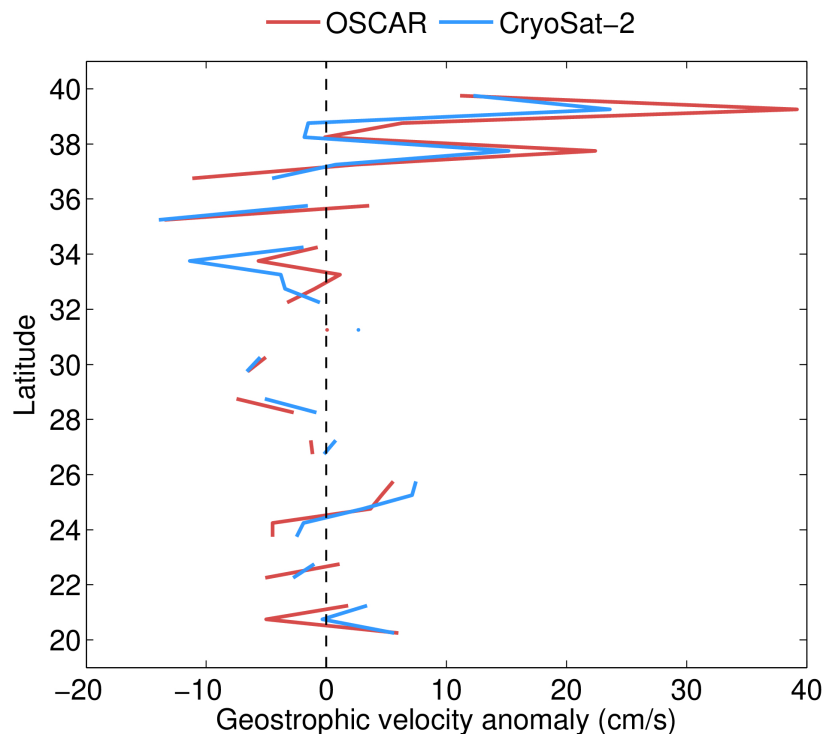


Figure 120. Comparison of the GOP geostrophic velocity anomalies with HF radar velocity anomalies perpendicular to the altimetry tracks in the regions shown in Figure 119 over the period November 2022 to May 2023. The numbers on the x-axis correspond to those used to identify each region in Figure 119. HF radar velocity anomalies have been obtained by subtracting the mean velocity over the period 2010-2014 from the observed velocities. GOP geostrophic velocities have been computed using the optimal difference operator by Powell and Leben (2004). Each dot represents a comparison at a particular location (hence different dots correspond to different points in space). Dots joined by a continuous line correspond to single altimeter passes.



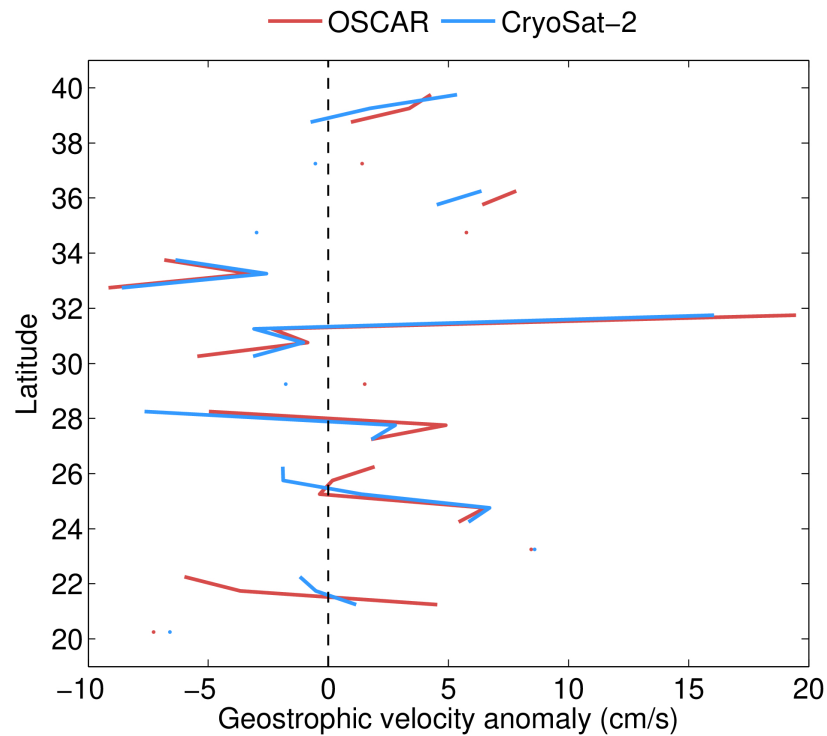


Figure 121. Comparison of the GOP geostrophic velocity anomalies with geostrophic velocities anomalies from the Ocean Surface Current Analyses – Real time (OSCAR) for May 2023 in the Atlantic (top, 20°N – 40°N, 315°E – 325°E) and Pacific (bottom, 20°N – 40°N, 220°E – 230°E) boxes as a function of latitude (i.e., for each latitude the geostrophic velocities have been averaged over the longitudes within the box). GOP geostrophic velocities have been computed using the optimal difference operator by Powell and Leben (2004).

4.1.6. Comparison of GOP SSH anomaly with steric heights derived from temperature and salinity ARGO profiles.

Note 4.1: *To be consistent with the GOP SSH anomalies, the steric height anomalies at each Argo float were obtained by subtracting a mean steric height computed over the period 1993-2009 (same as the base period for DTU10 MSS) from the absolute (i.e., referred to 1000m) steric height. The steric height is the dynamic height at the surface scaled by gravitational acceleration.*

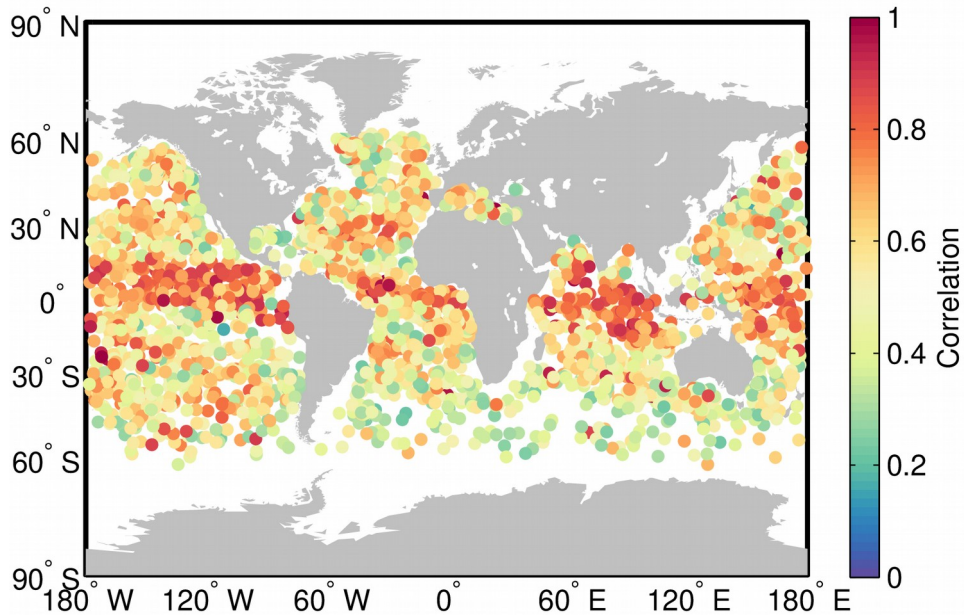


Figure 122. Map showing the correlation between the GOP SSH anomaly and the steric height anomaly (referred to 1000 m) derived from the temperature and salinity provided by Argo floats over the period June 2021 to May 2023. Each dot in the map represents the mean position of each Argo float used in the validation.

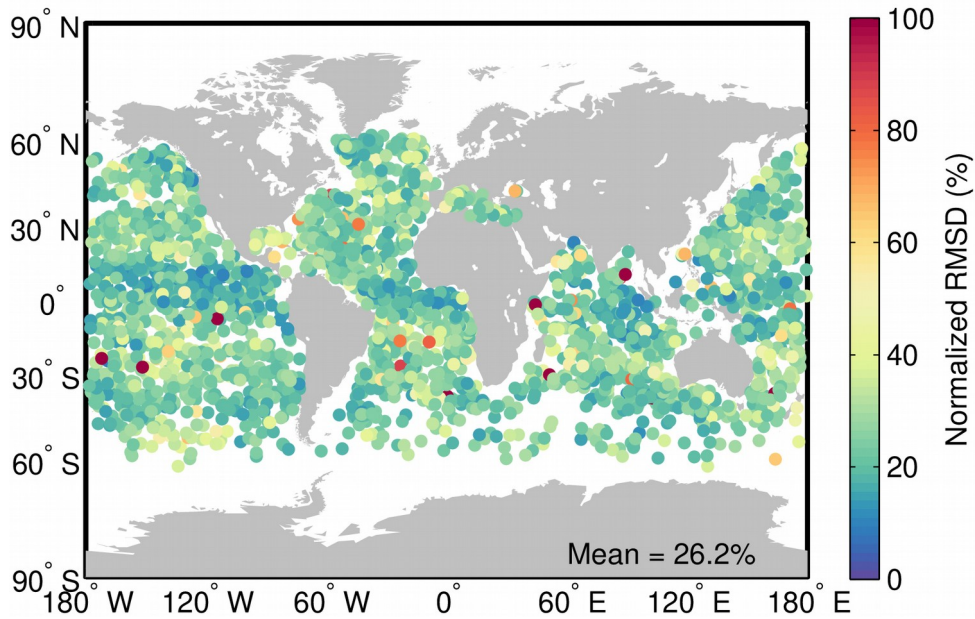


Figure 123. Map showing the normalized RMS difference between the GOP SSH anomaly and the steric height anomaly (referred to 1000 m) derived from the temperature and salinity provided by Argo floats over the period June 2021 to May 2023. Each dot in the map represents the mean position of each Argo float used in the validation.

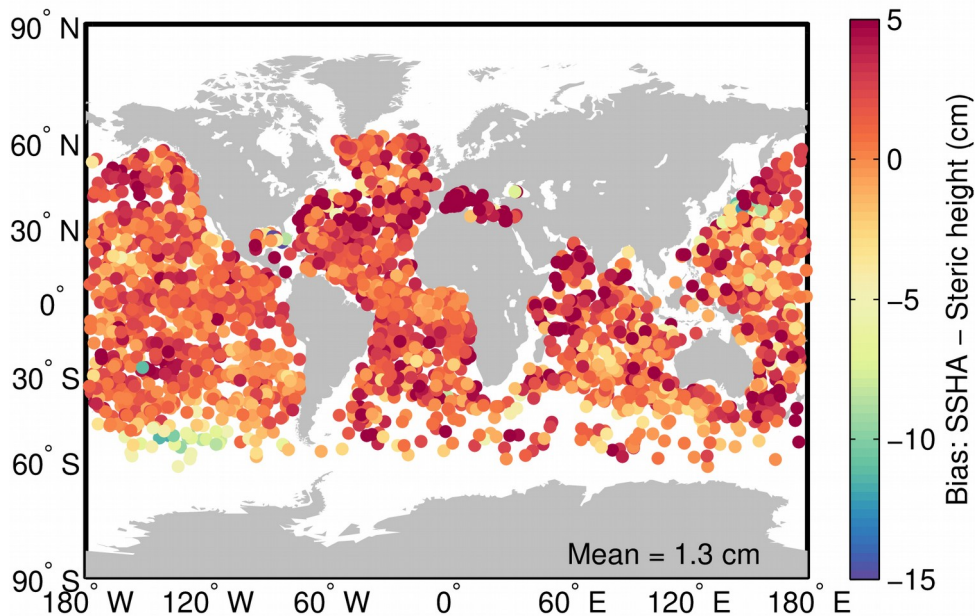


Figure 124. Map showing the mean difference (bias) between the GOP SSH anomaly and the steric height anomaly (referred to 1000 m) derived from the temperature and salinity provided by Argo floats over the period June 2021 to May 2023. Each dot in the map represents the mean position of each Argo float used in the validation.

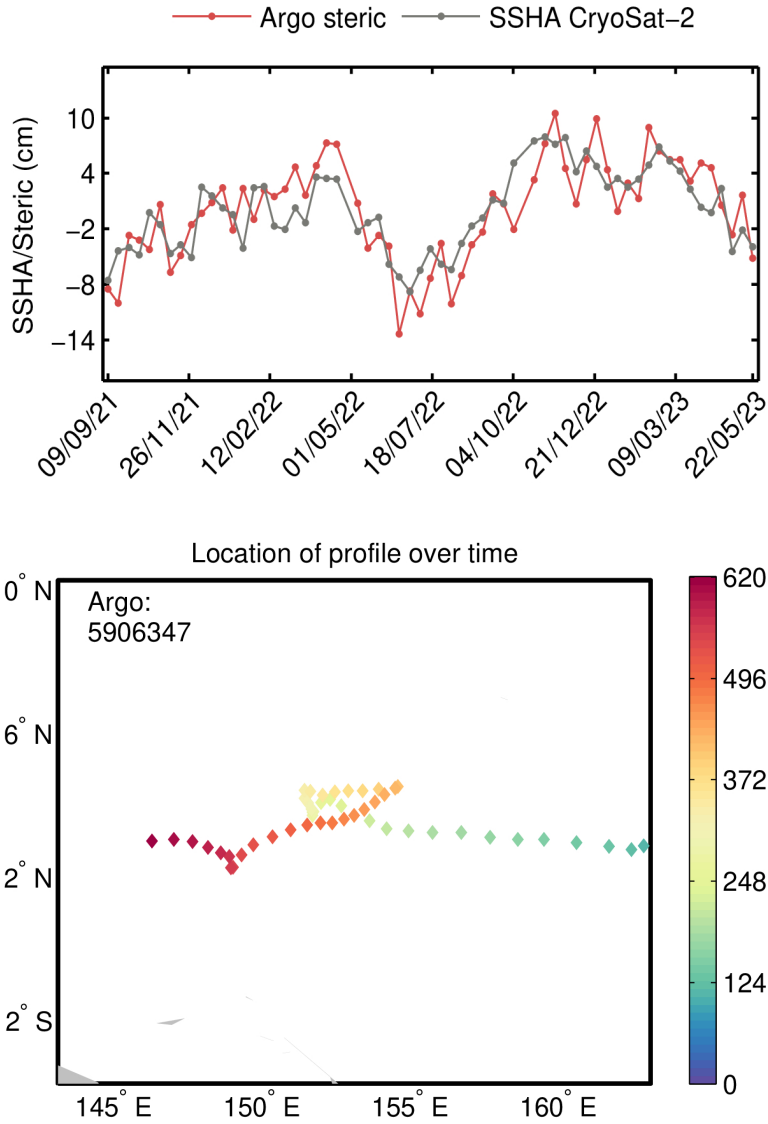


Figure 125. Comparison of the GOP SSH anomaly and the steric height anomaly (referred to 1000 m) for one particular Argo float (top). The location of the Argo float over time is also shown (bottom).

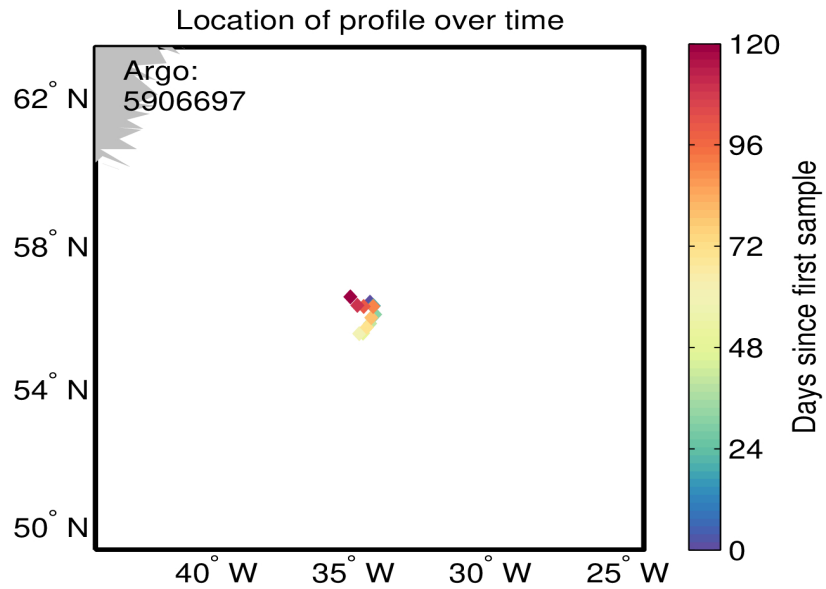
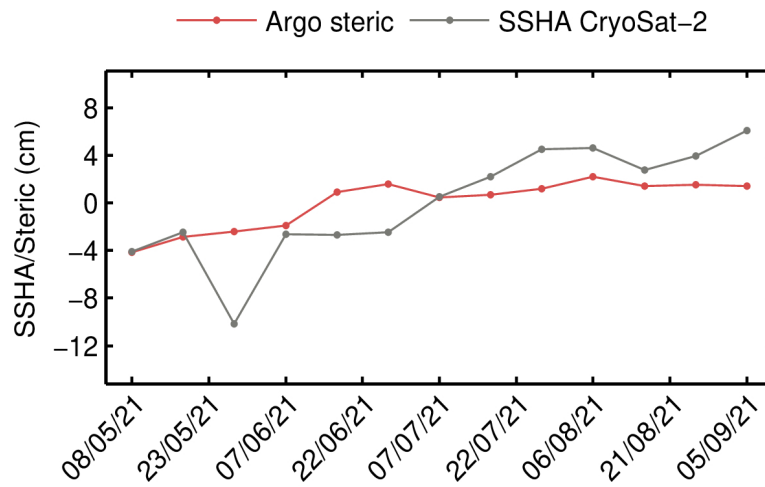


Figure 126. Comparison of the GOP SSH anomaly and the steric height anomaly (referred to 1000 m) for one particular Argo float (top). The location of the Argo float over time is also shown (bottom).

4.2. Validation against reference mission (Jason/Sentinel-6a)

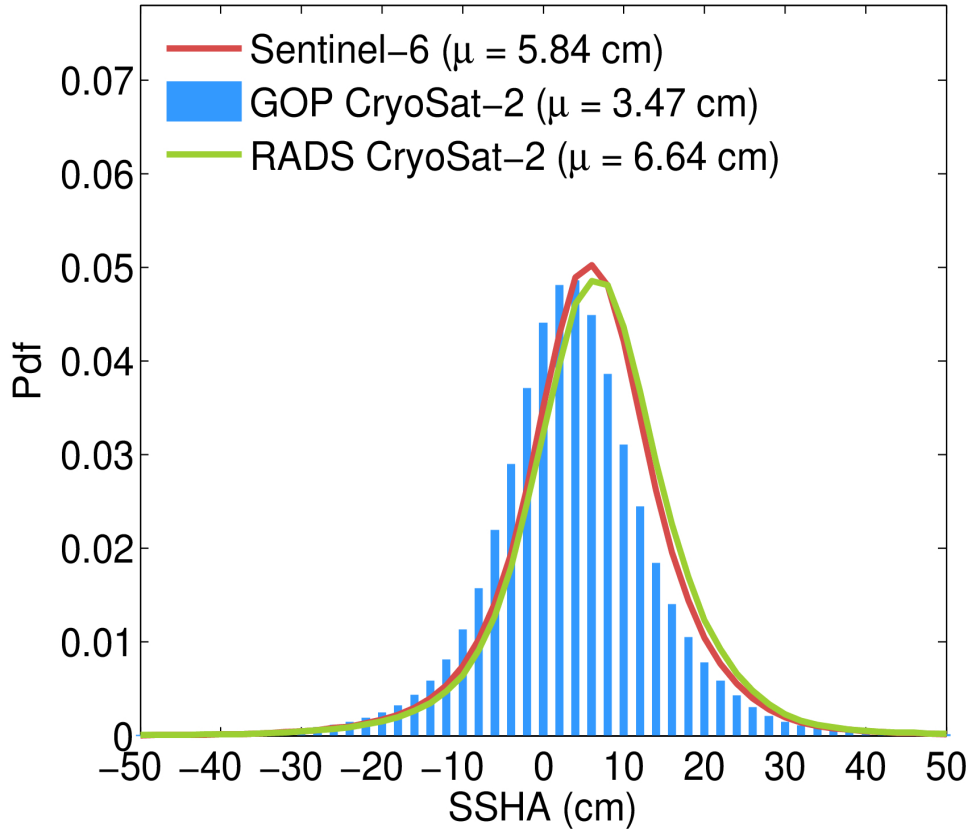


Figure 127. Histograms (normalized to have a total area of 1) of the SSH anomaly from GOP (blue bars), reference mission (red line) and RADS CryoSat-2 (green) for May 2023.

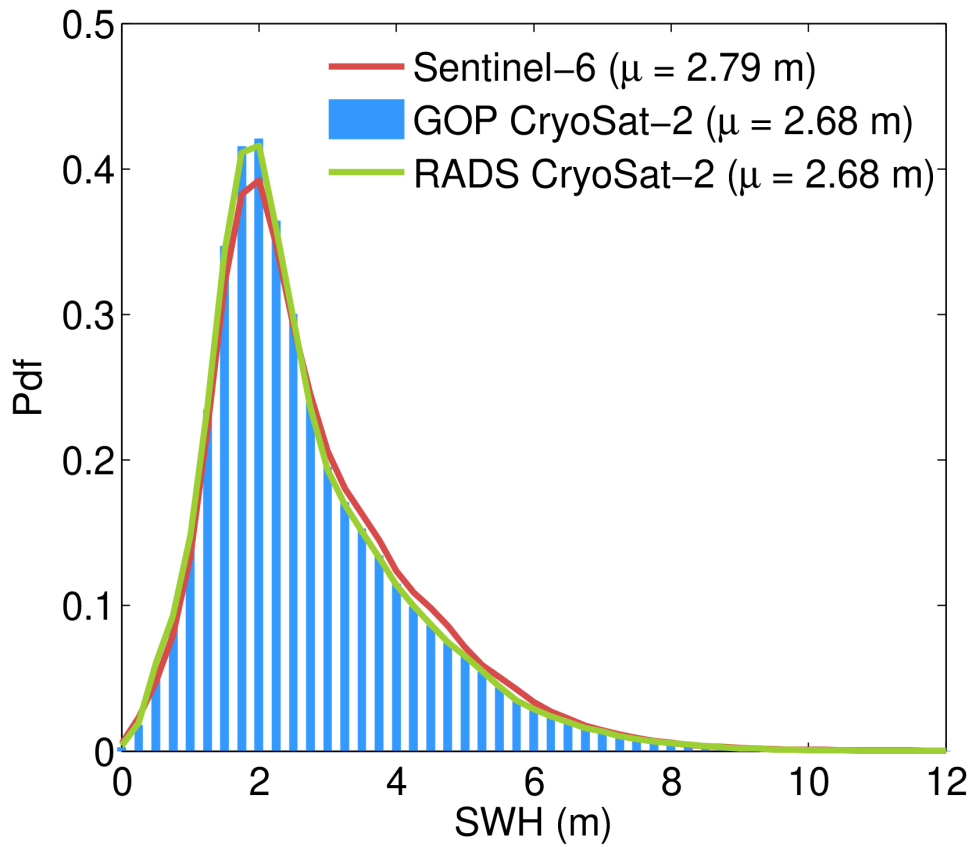


Figure 128. Histograms (normalized to have a total area of 1) of the SWH from GOP (blue bars), reference mission (red line) and RADS CryoSat-2 (green) for May 2023.

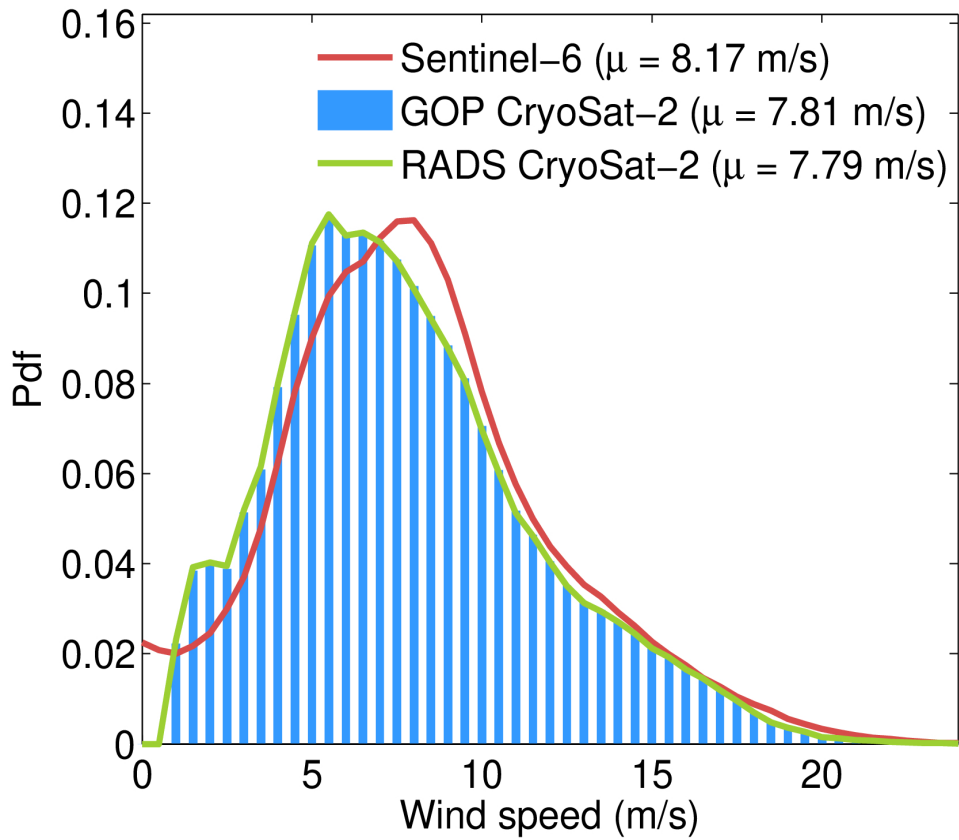


Figure 129. Histograms (normalized to have a total area of 1) of the wind speed from GOP (blue bars), reference mission (red line) and RADS CryoSat-2 (green) for May 2023.

4.3. Global mean sea level time series

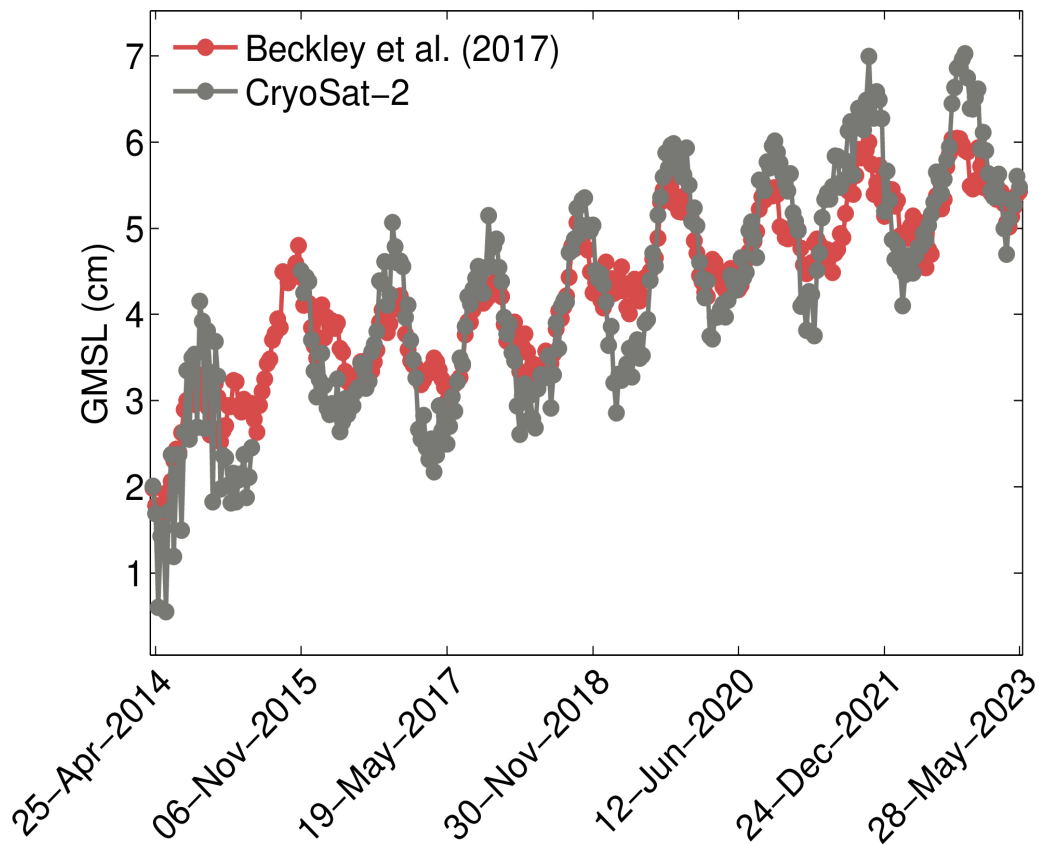


Figure 130. Global mean sea level (latitude < 65°) from GOP CryoSat-2 (grey) together with that derived from OSTM/Jason at the University of Colorado (red). The shift in 2017 in the time series from CryoSat-2 reflects the transition from Baseline B to Baseline C and is due to an offset in the SSHA between the two Baselines.

Annex

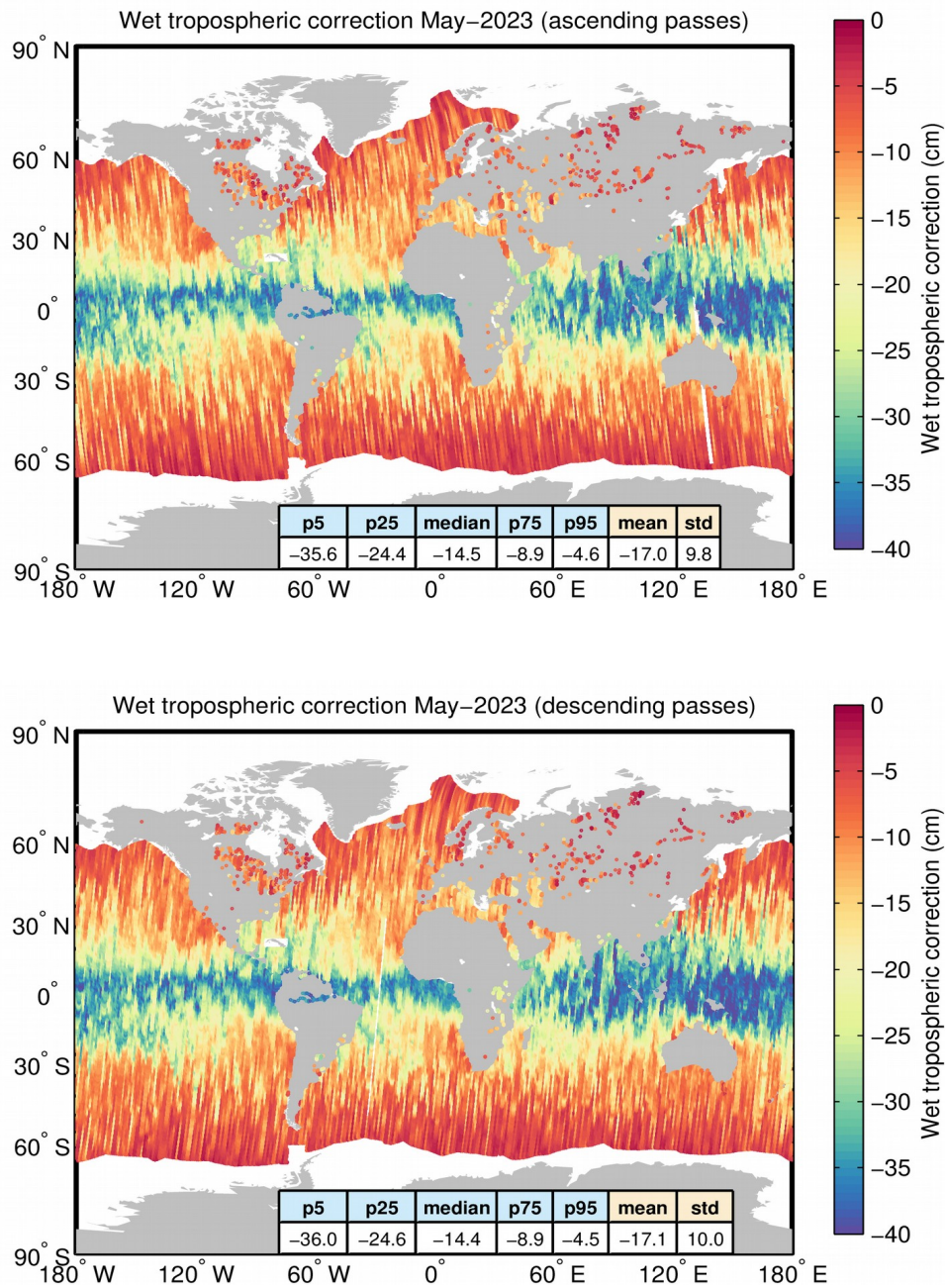


Figure A1. Geographical distribution of the wet tropospheric correction over oceans and lakes for ascending (top) and descending (bottom) passes for May 2023. The statistical values shown in the table refer refer to the wet tropospheric correction in cm. Measurements taken over polar polygons have been excluded from the computation of the statistical values. The black lines mark the outer limit of the Arctic and Antarctic polar polygons.

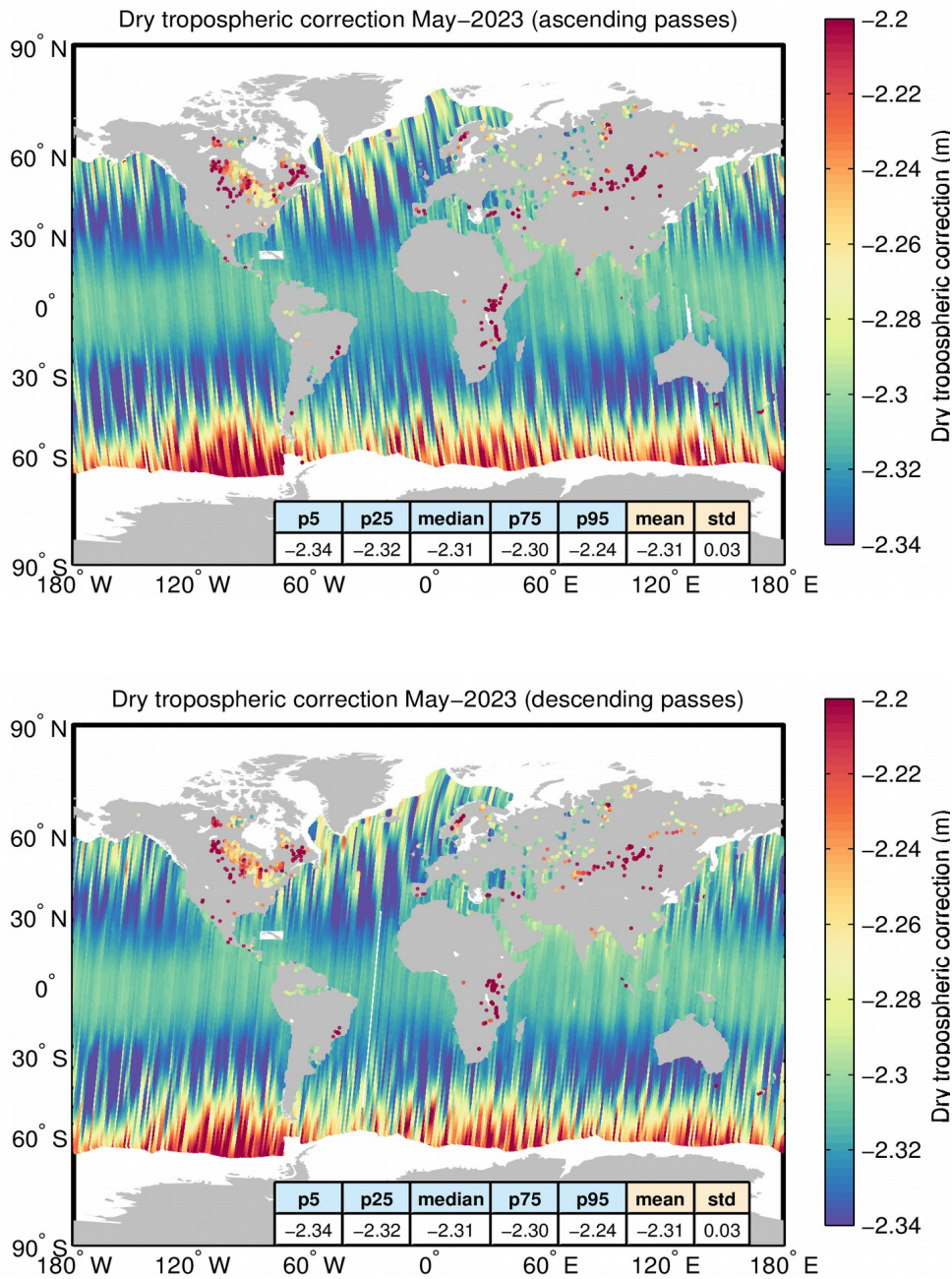


Figure A2. Geographical distribution of the dry tropospheric correction over oceans and lakes for ascending (top) and descending (bottom) passes for May 2023. The statistical values shown in the table refer refer to the dry tropospheric correction in m. Measurements taken over polar polygons have been excluded from the computation of the statistical values. The black lines mark the outer limit of the Arctic and Antarctic polar polygons.

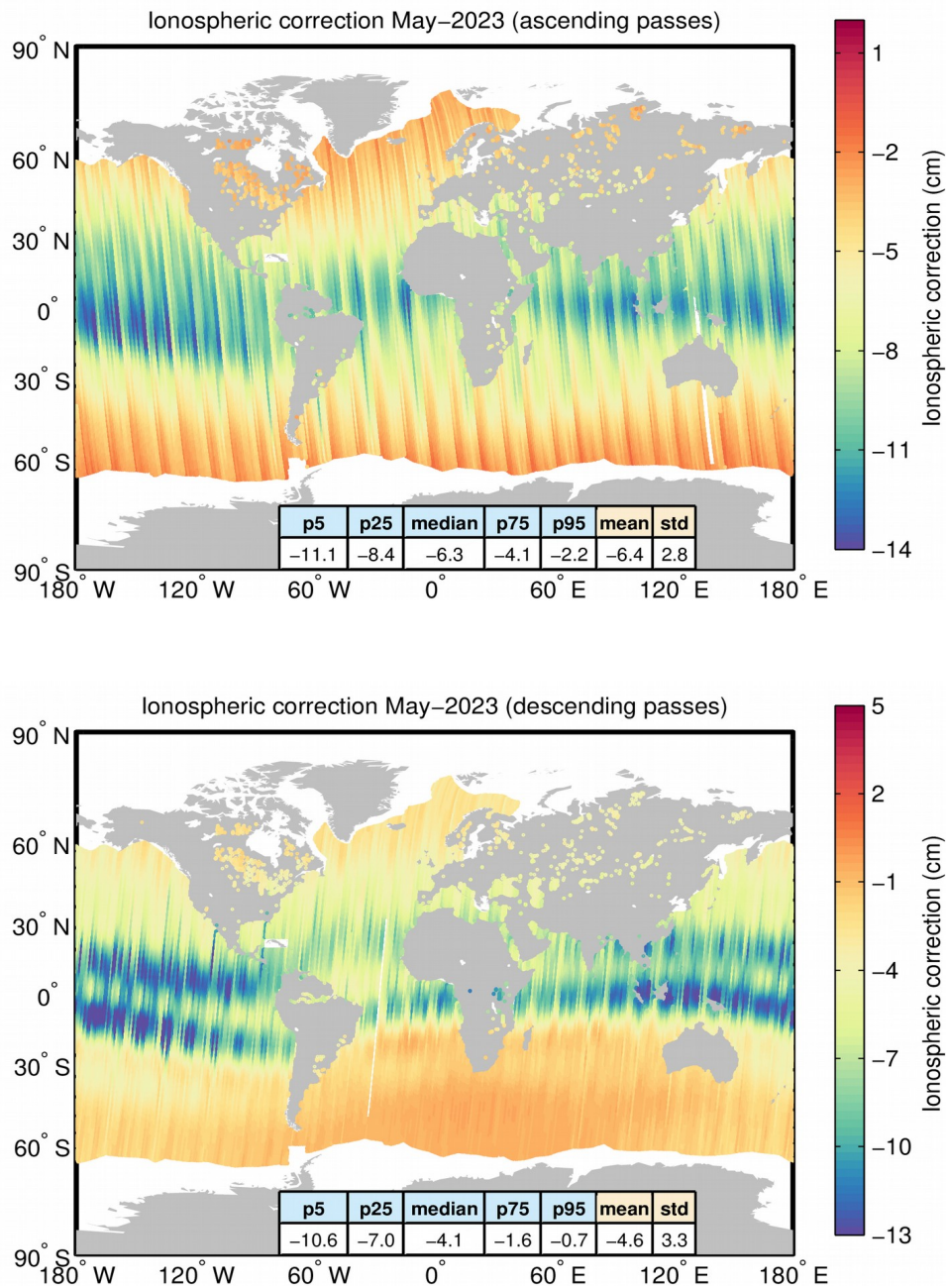


Figure A3. Geographical distribution of the Ionospheric correction over oceans and lakes for ascending (top) and descending (bottom) passes for May 2023. The statistical values shown in the table refer refer to the Ionospheric correction in cm. Measurements taken over polar polygons have been excluded from the computation of the statistical values. The black lines mark the outer limit of the Arctic and Antarctic polar polygons.

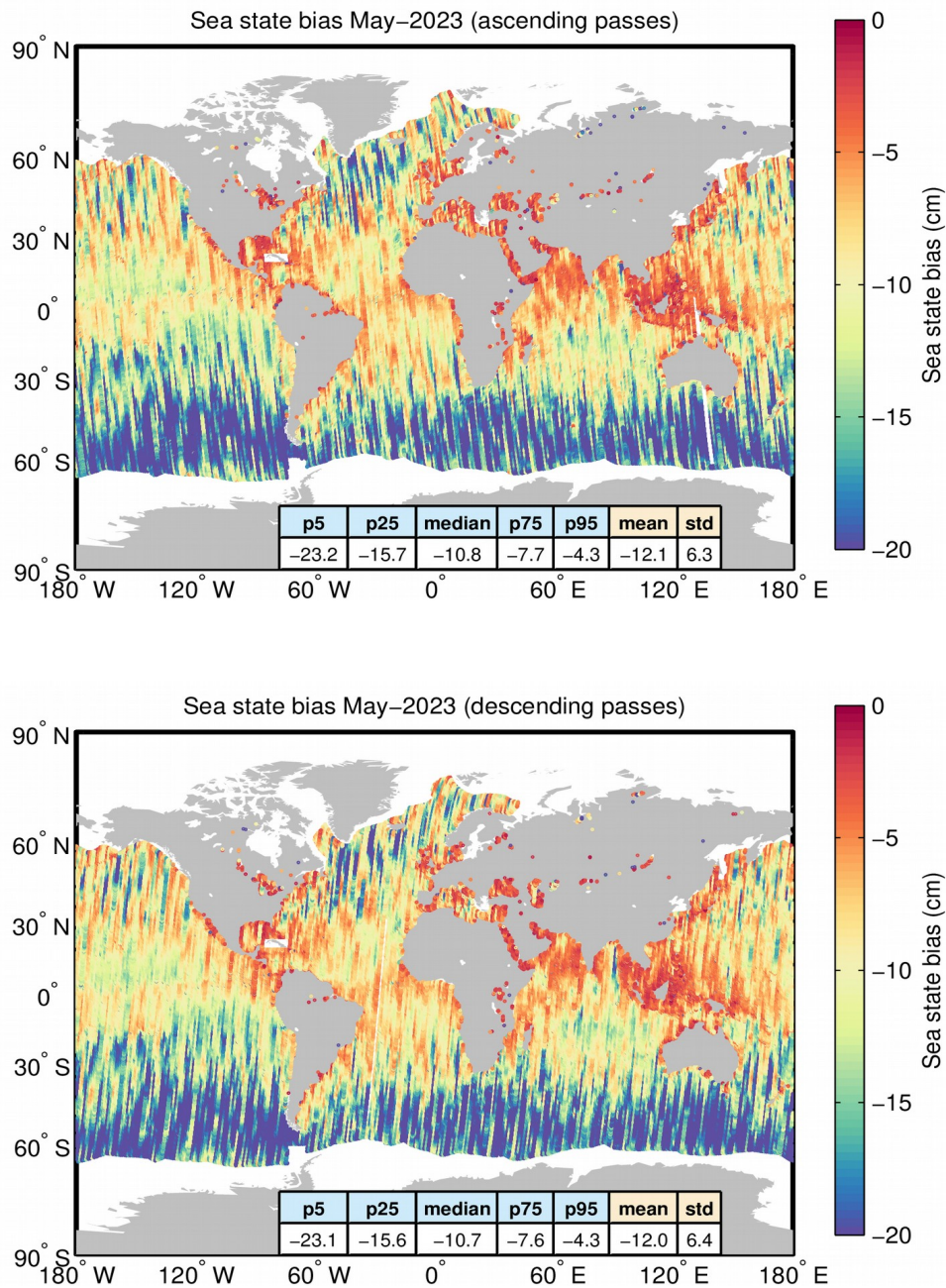


Figure A4. Geographical distribution of the sea state bias over oceans and lakes for ascending (top) and descending (bottom) passes for May 2023. The statistical values shown in the table refer refer to the sea state bias in cm. Measurements taken over polar polygons have been excluded from the computation of the statistical values. The black lines mark the outer limit of the Arctic and Antarctic polar polygons.

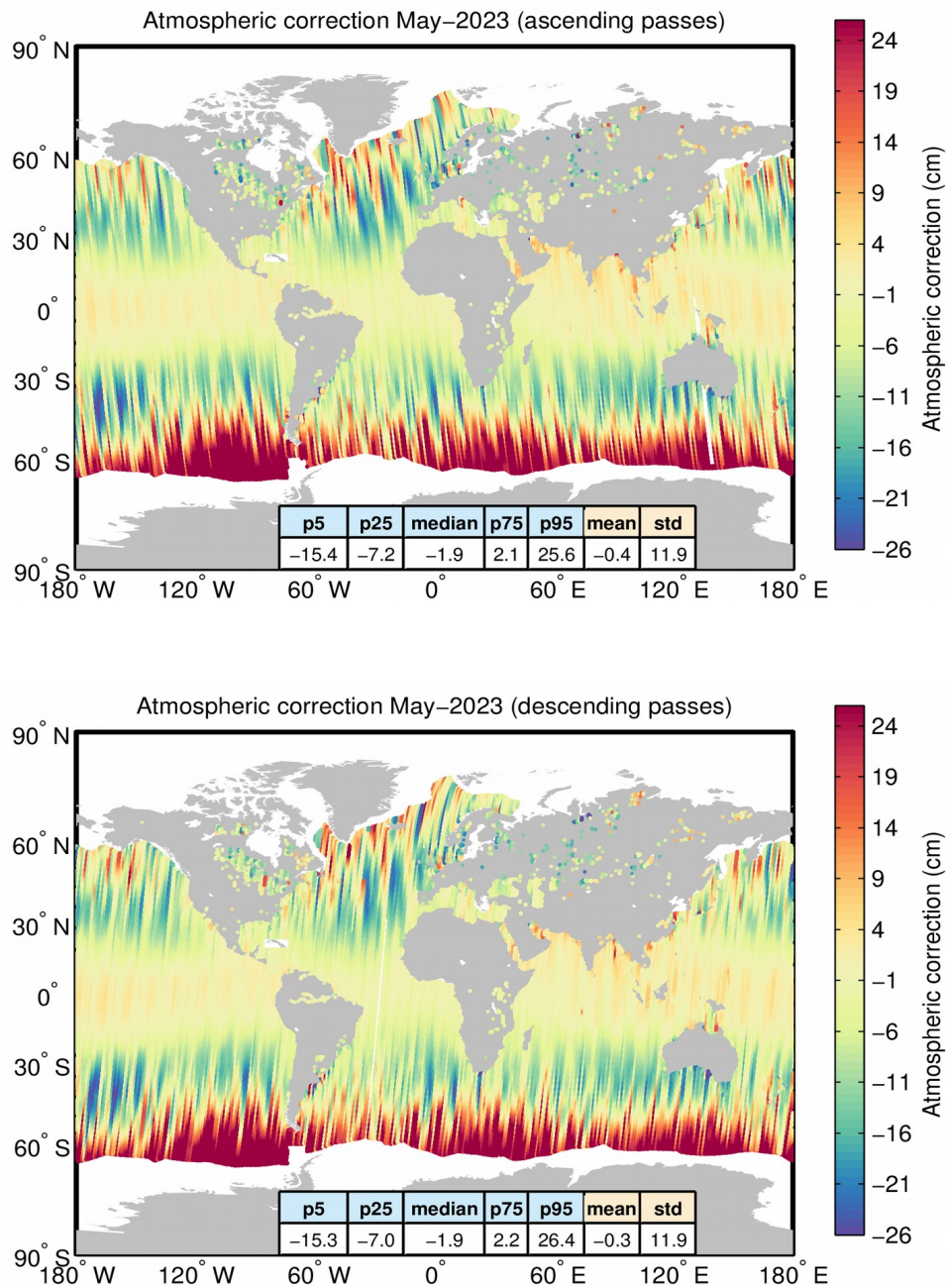


Figure A5. Geographical distribution of the atmospheric correction over oceans and lakes for ascending (top) and descending (bottom) passes for May 2023. The statistical values shown in the table refer refer to the atmospheric correction in cm. Measurements taken over polar polygons have been excluded from the computation of the statistical values. The black lines mark the outer limit of the Arctic and Antarctic polar polygons.

(end of Document)